R-11-12

Rock stress orientation measurements using induced thermal spalling in slim boreholes

Eva Hakami, Geosigma AB

May 2011

Svensk Kärnbränslehantering AB
Swedish Nuclear Fuel
and Waste Management Co

Box 250, SE-101 24 Stockholm
Phone +46 8 459 84 00

ISSN 1402-3091
SKB R-11-12

Rock stress orientation measurements using induced thermal spalling in slim boreholes

Eva Hakami, Geosigma AB

May 2011

This report concerns a study which was conducted for SKB. The conclusions and viewpoints presented in the report are those of the author. SKB may draw modified conclusions, based on additional literature sources and/or expert opinions.

A pdf version of this document can be downloaded from www.skb.se.

Abstract

In the planning and design of a future underground storage for nuclear waste based on the KBS-3 method, one of the aims is to optimize the layout of deposition tunnels such that the rock stresses on the boundaries of deposition holes are minimized. Previous experiences from heating of larger scale boreholes at the Äspö Hard Rock Laboratory (ÄHRL) gave rise to the idea that induced borehole breakouts using thermal loading in smaller diameter boreholes, could be a possible way of determining the stress orientation. Two pilot experiments were performed, one at the Äspö Hard Rock Laboratory and one at ONKALO research site in Finland.

An acoustic televiewer logger was used to measure the detailed geometrical condition of the borehole before and after heating periods. The acoustic televiewer gives a value for each 0.7 mm large pixel size around the borehole periphery. The results from the loggers are presented as images of the borehole wall, and as curves for the maximum, mean and minimum values at each depth. Any changes in the borehole wall geometry may thus be easily detected by comparisons of the logging result images. In addition, using an optical borehole televiewer a good and detailed realistic colour picture of the borehole wall is obtained. From these images the character of the spalls identified may be evaluated further.

The heating was performed in a 4 m long section, using a heating cable centred in an 8 m deep vertical borehole, drilled from the floor of the tunnels. For the borehole in the Q-tunnel of ÄHRL the results from the loggings of the borehole before the heating revealed that breakouts existed even before this pilot test due to previous heating experiments at the site (CAPS). Quite consistent orientation and the typical shape of small breakouts were observed. After the heating the spalling increased slightly at the same locations and a new spalling location also developed at a deeper location in the borehole. At ONKALO three very small changes in the borehole wall, having the same orientation, was found when comparing images before and after the heating. The main differences between sites were that the rock types were quite different and the borehole diameter was 76 mm at ÄHRL and 101 mm in ONKALO. The amount of induced spalls by the heating was small at both sites, and less than what was expected based on an empirical spalling strength criterion for tunnels. This may be an indication of different spalling strength for different borehole sizes due to the fact that the induced spalling is in the scale of the mineral grains. The interpreted principal stress orientations agree with the orientations estimated based on other measurement methods, both at the Q-tunnel in Äspö Hard Rock Laboratory and the POSE site in ONKALO.

It is recommended that in future efforts using this methodology to determine stress orientation, the heater effect be higher to increase the thermal load and amount of spalling, and also decrease the heating time needed. Procedures for faster identification of the small breakouts from the logger results may also be developed. Further, it is suggested that fragments induced are simultaneously collected below the heater in the borehole, such that the point of time when spalling occur may be easily detected. If the heating procedures are standardized for small diameter boreholes there will as well be a possibility to use the method to directly quantify the spalling sensitivity for the rock type around the borehole.

Sammanfattning

Vid planering och design för ett framtida slutförvar för använt kärnbränsle enligt KBS-3-metoden är ett av målen att optimera layouten hos deponeringstunnlarna så att bergspänningarna på ränderna av deponeringshålen minimeras. Tidigare erfarenheter från värmning i borrhål med stor diameter vid Äspölaboratoriet låg till grund för idén att inducera spjälkning i borrhål genom termisk belastning i klena borrhål, som en metod att bestämma orienteringen på bergspänningen. Två pilotförsök har utförts, ett på Äspölaboratoriet och ett i ONKALO underjordsanläggning i Finland.

En akustisk televiewer-logger användes för att mäta upp den exakta geometrin hos borrhålet före och efter värmningsperioderna. En akustisk televiewer ger ett värde för varje 0.7 mm stor pixel längs borrhålets periferi. Resultatet från loggningen presenteras som bilder av borrhålsväggen, och som kurvor för max, medel och minimum värde på radien för varje djup längs hålet. Varje förändring i borrhålsväggens geometri kan således enkelt detekteras genom en jämförelse av bilder som presenterar mätresultaten. Därutöver kan en optisk borrhålslogg användas för att ge en detaljerad realistisk färgbild av borrhålsväggen. Från dessa bilder kan utseendet hos det spjälkande berget som hittats studeras närmare.

Värmningen gjordes i en 4 m lång sektion med hjälp av en elektrisk värmare som placeras centrerat i ett 8 m djupt vertikalt borrhål, borrat från tunnelbotten. För borrhålet i Q-tunneln i ÄHRL visade resultatet från loggningen före värmning att spjälkning existerade redan innan värmningen från detta försök gjordes på grund av de värmningar som sedan tidigare gjorts i försöksområdet (CAPS). En tämligen konstant orientering och en typisk form på spjälkningarna kunde noteras. Efter värmningen ökade spjälkningen något dessa punkter och spjälkning uppstod i en ny punkt på en djupare nivå i borrhålet. I ONKALO noterades tre mycket små förändringar i borrhålsväggen, alla med samma orientering, vid en jämförelse bilder från loggningar före respektive efter värmning. Den väsentligaste skillnaden mellan de två försöksplatserna var att bergarterna har skilda egenskaper och att borrhålets diameter var 76 mm i Äspö och 101 mm i ONKALO. Mängden inducerade spjälkningarna var mycket liten vid båda platserna, mindre än vad som förväntats baserats på ett empiriskt kriterium för spjälkningsstabilitet i tunnlar. Detta kan vara en indikation på att det finns skaleffekter i spjälkningshållfasthet för borrhål, på grund av att den spjälkning som induceras är av samma storleksordning som kornstorleken hos mineralen. Den tolkade orienteringen hos huvudspänningen samstämmer väl med den orientering som man kan förvänta baserat på mätningar med andra metoder, både vid Q-tunneln i Äspö och i försöksplatsen i ONAKLO (POSE).

I framtida försök att använda denna metod att bestämma spänningsorientering rekommenderas det att värmeeffekten är högre, för att få en högre termisk last och mera spjälkning, och samtidigt minska den värmningstid som krävs. Man kan också utveckla procedurerna för att snabbare identifiera de små spjälkningarna i resultaten från loggningen. Därutöver föreslå att fragment som spjälkat under värmningen samlas upp under värmares så att den tidpunkt när spjälkning sker kan detekteras på ett enkelt sätt. Om värmningsproceduren standardiserades för klena borrhål skulle det även innebära en möjlighet att använda metoden för att direkt kvantifiera spjälkningsbenägenheten i bergarten omkring borrhålet.

Contents

1 Background 7

2 Objective and scope 11

3 Field test in Äspö Hard Rock Laboratory 13
3.1 Geological conditions and previous testing at the site 13
3.2 Equipment 20
3.2.1 Borehole heating equipment 20
3.2.2 Temperature measurements 20
3.2.3 Acoustic televiewer 21
3.2.4 Optical logger 22
3.2.5 Ground water flow conditions 23
3.2.6 Borehole brushing and fragment collection 23
3.3 Temperature results 24
3.4 Acoustic and optical logger results 27
3.5 Collected fragments and alsphaltite 33
3.6 Determination of in situ stress orientation 37
3.6.1 Stress orientation at the SLITS borehole 37
3.6.2 Calculation of influence on stress field from CAPS boreholes 39
3.6.3 Comparisons with previous observations at site and in the region 40

4 Field test at ONKALO 43
4.1 Geological conditions at the site 43
4.2 Equipment 45
4.2.1 Borehole heating equipment 45
4.2.2 Temperature measurements 45
4.2.3 Acoustic televiewer 45
4.3 Temperature results 45
4.4 Logging results 46
4.5 Stress orientation results 47
4.6 Comparisons with previous measurements at site. 47

5 Conclusions and recommendations 49

6 References 51

Appendix A Optical loggings in KQ0048G01 53

Appendix B Acoustic televiewer loggings in KQ0048G01 Amplitude measurements 57

Appendix C Acoustic televiewer loggings in KQ0048G01 Radii measurement comparison between stages 61

Appendix D Logging results from all three methods after last heating in KQ0048G01 65

Appendix E Acoustic televiewer loggings in ONK-PP259 71

1 Background

One of the rock mechanics factors that are considered in the design of the future final storage for nuclear waste is how the repository tunnels should be oriented. Because the orientation of the repository tunnels, with respect to the in situ stresses, will influence the risk for stress related stability problems, there is a need for good determination of in situ stress orientation (Figure 1-1).

During the work performed within the descriptive modelling for the potential future sites, Forsmark and Laxemar, different techniques were used to determine the in situ stress orientation (Hakami et al. 2008, Glamheden et al. 2008, Martin 2007). Direct measurements were made with overcoring and hydraulic methods and in addition the breakouts observed in the ordinary core drilled investigation boreholes were used to evaluate stresses. This approach was based on several previous studies in literature, e.g. Ask and Ask (2007). It was concluded from the studies at the investigated sites that, even if the amount of breakouts in the boreholes was limited, the directions of the breakouts were consistent and unambiguous, and could be used as a determination of primary stress field orientation (see Figure 1-2).

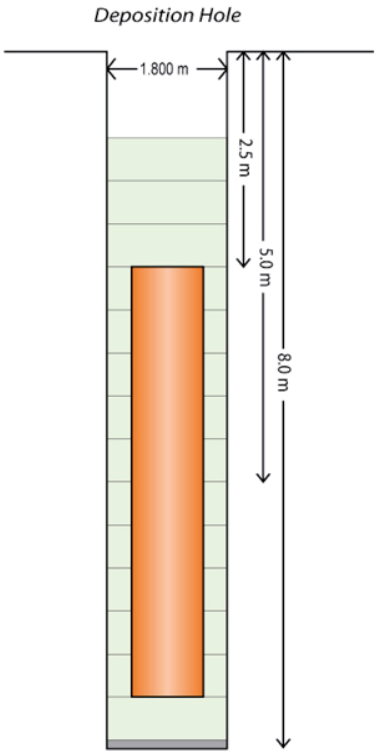

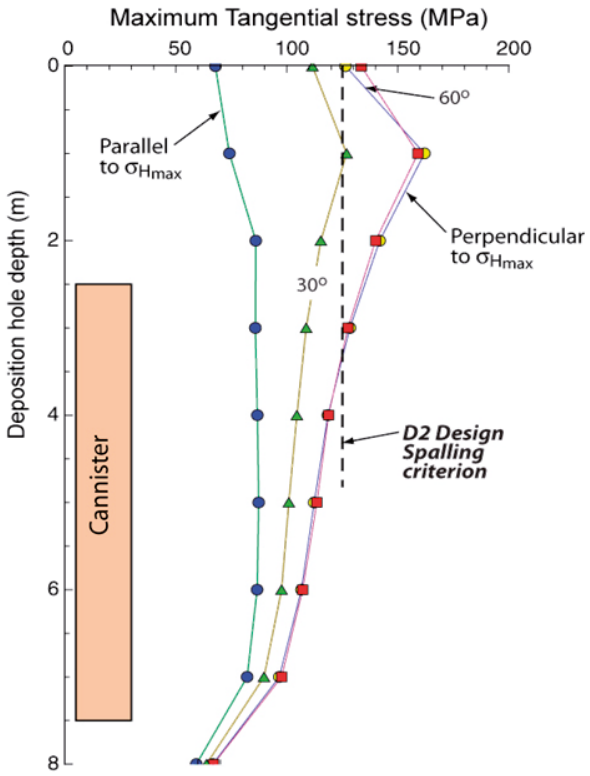

Figure 1-1. *The preliminary design for a future final disposal using the KBS3 concept. The stresses around the deposition borehole and the orientation of the tunnels with respect to the orientation of the in situ stress field will determine the risk for spalling occurring at the wall of the deposition holes. The diagram shows calculated tangential stress in the deposition borehole wall for different cases in terms of the angle between the maximum in situ stress and the orientation of deposition tunnel. A tunnel direction parallel to the maximum horizontal stress is the most beneficial (SKB 2009).*

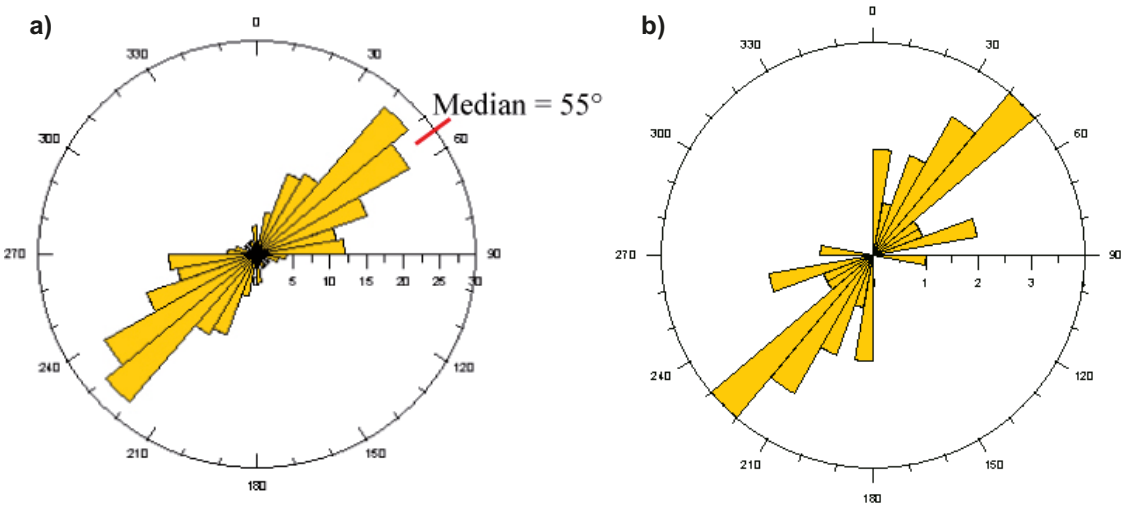

Figure 1-2. *Rose diagram of the orientation interpreted from borehole breakouts observed at a) the Forsmark site (Glamheden et al. 2008) and b) the Laxemar site (Hakami et al. 2008). The results are from the breakouts that are not associated with structures or fractures and they are compiled from several boreholes. The orientation of the breakouts is expected to be in the direction of the minimum principal stress and the maximum principal stress is thus expected in the perpendicular NW-SE direction.*

Field research regarding the thermal spalling phenomenon have been carried out at the Äspö Hard Rock Laboratory in two major projects, the APSE project (Andersson 2007) where heating was performed at full scale deposition boreholes and the CAPS project (Glamheden et al. 2010) where borehole of 485 mm diameter were heated. As a result of these two studies it was clear that breakouts, i.e. "thermal spalling", could be induced in large diameter holes using applied heating at the boreholes (see example of induced spalling in Figure 1-3).

Figure 1-3. *Photograph taken from below of chips forming at 3.7 m depth in the 1.75 m diameter vertical borehole of the Äspö Pillar Stability Experiment (APSE) site. Note the fairly consistent orientation of the centre, deepest points, of the wedge shaped spalls in the borehole periphery. This spalling was induced by heating in the pillar next to the large diameter borehole. From Andersson (2007).*

These two experiences was the starting point to the idea to try and develop a simple and robust technique to measure stress orientation in ordinary slim (76 mm diameter) boreholes, based on an applied heat load inside the boreholes. The method, or the development project, has been named SLITS (SLIm borehole Thermal Spalling). Foreseen advantages of this method were that it could be applied in existing borehole and already existing techniques would be primary components. The cost for observation at several points in the same borehole was expected to be relatively low compared to existing stress measurement techniques and a fairly high certainty in the determination of the orientation was expected, in particular in high stress magnitude domains.

2 Objective and scope

The overall objective of the field tests was to evaluate if the method has potential to be used in the future detailed site investigation and, if so, to give a basis for planning of further developments and testing. The specific objective of the pilot field tests was to assess the potential of the SLITS method, by performing tests where the stress orientation already was known through other measurements. The aim was further that the tests should be performed with existing heater tools and in short vertical existing boreholes, to reduce costs in the pilot stage.

The test strategy of both pilot field test was simply to measure the borehole geometry in detail before heating, apply a heat load in the centre of the hole for a certain period of time, and then to repeat the detailed geometry measurements afterwards. In this way any changes in geometry would be revealed. By analysing the location of induced spalls (changes) the orientation of stress would be determined.

The first field test, performed in May 2010, was at the ONKALO underground research excavations in western Finland, at an existing experimental site (the POSE site). This test is presented in Chapter 4 of this report.

The second field test was performed in August 2010 at the Äspö Hard Rock Laboratory (ÄHRL), in the same tunnel (Q-tunnel) as the earlier APSE and CAPS experiments have been carried out. This choice implied that the test had to be performed in a time frame of three weeks since the tunnel was only available for this period, and the pilot test activities were adjusted to comply with this requirement. The pilot test at ÄHRL is presented in Chapter 3.

The main uncertainty foreseen in the planning stage of the SLITS pilot test was the unknown scale effects on the spalling behaviour. The earlier induced thermal spalling at the ÄHRL was observed in much larger boreholes (0.485 m and 1.2 m in diameter), while the SLITS method is meant for slim boreholes used in site investigations. The two pilot tests were carried out in 101 mm and 76 mm diameter boreholes, respectively. The aim was that pilot field tests in slim boreholes would reveal if this possible scale factor would prevent the use of the SLITS method.

A secondary issue that we wanted to address in the pilot study was the question of whether induced temperature gradients had any influence on the amount of spalling. Of this reason the heating in the first period was increased stepwise and in second period applied with at highest effects directly from start. As the time available for pilot tests was limited, and the results showed that only the highest possible effect with the equipment produced additional spalling, the study of temperature gradient could not be pursued as initially planned.

3 Field test in Äspö Hard Rock Laboratory

3.1 Geological conditions and previous testing at the site

For the field test an already existing borehole at Äspö Hard Rock Laboratory (ÄHRL) was used, KQ0048G01. This 8 m deep, 76 mm diameter, borehole is drilled vertically from the tunnel floor and located at the same site as another field experiment called CAPS (Counterforce Applied to Prevent Spalling) (Glamheden et al. 2010), see Figure 3-1, Figure 3-2 and Figure 3-3.

The rock type in the Q-tunnel where the CAPS and SLITS pilot test were performed includes Äspö diorite, Pegmatite and mylonite (Figure 3-4). The mylonite is associated with a shear zone that is crossing through the tunnel floor area where CAPS experiments were carried out (Figure 3-5).

The Äspö diorite is a quartz monzodiorite to granodiorite. The grain size is medium to coarse and the rock has a faint to weak foliation. There is a varying degree of oxidation in the rock, from weak to medium, in particular in the uppermost parts. Laboratory test results from this rock and similar rock in the region has shown that the oxidation may be accompanied by a slight weakening of the rock (Hakami et al. 2008). No laboratory tests were performed on drill cores from the particular borehole tested in the SLITS pilot test (Figure 3-6), but since the distance is so small to the already tested sample location in the tunnel there is no reason to expect much different rock properties. However, an important experience from the results of previous tests in the tunnel is that the variation in rock type composition and rock oxidation does have an influence on the rock strength and spalling behaviour (Glamheden et al. 2010, Andersson 2007, Staub et al. 2004).

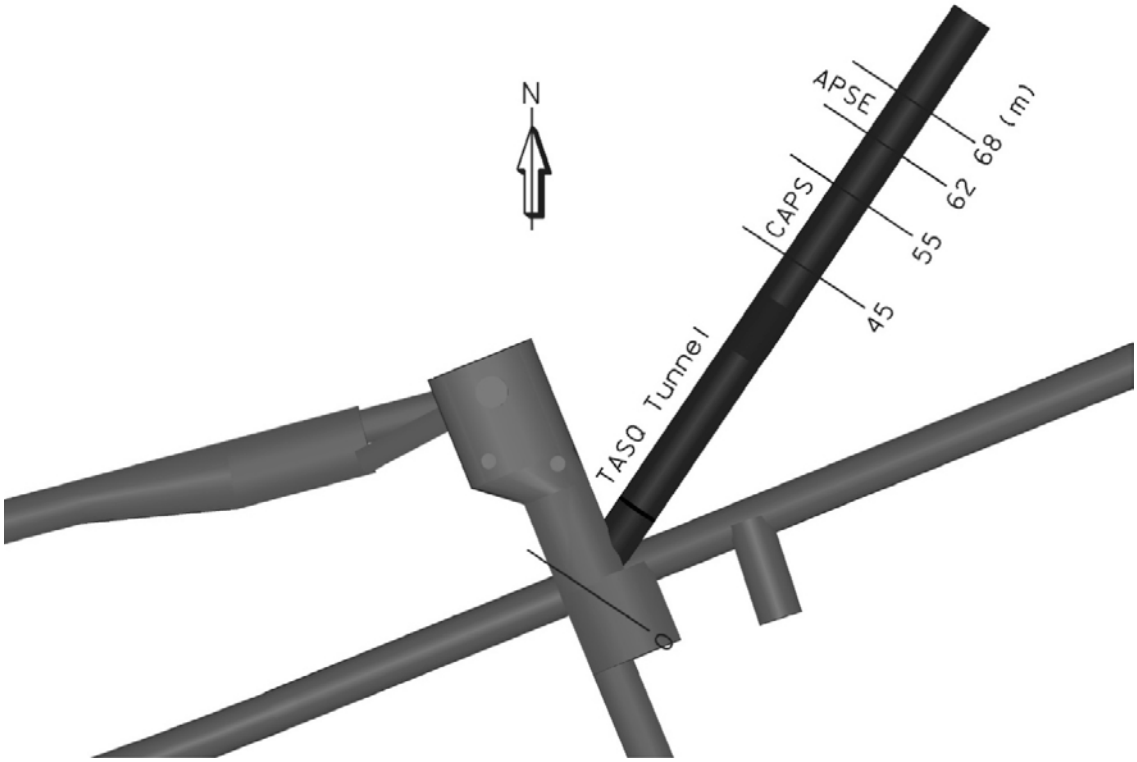

Figure 3-1. *Location of the CAPS and APSE field test in the TASQ Tunnel of the Äspö Hard Rock Laboratory. The SLITS pilot test was performed in a borehole located inside the CAPS site at length measurement 48. From Glamheden et al. (2010).*

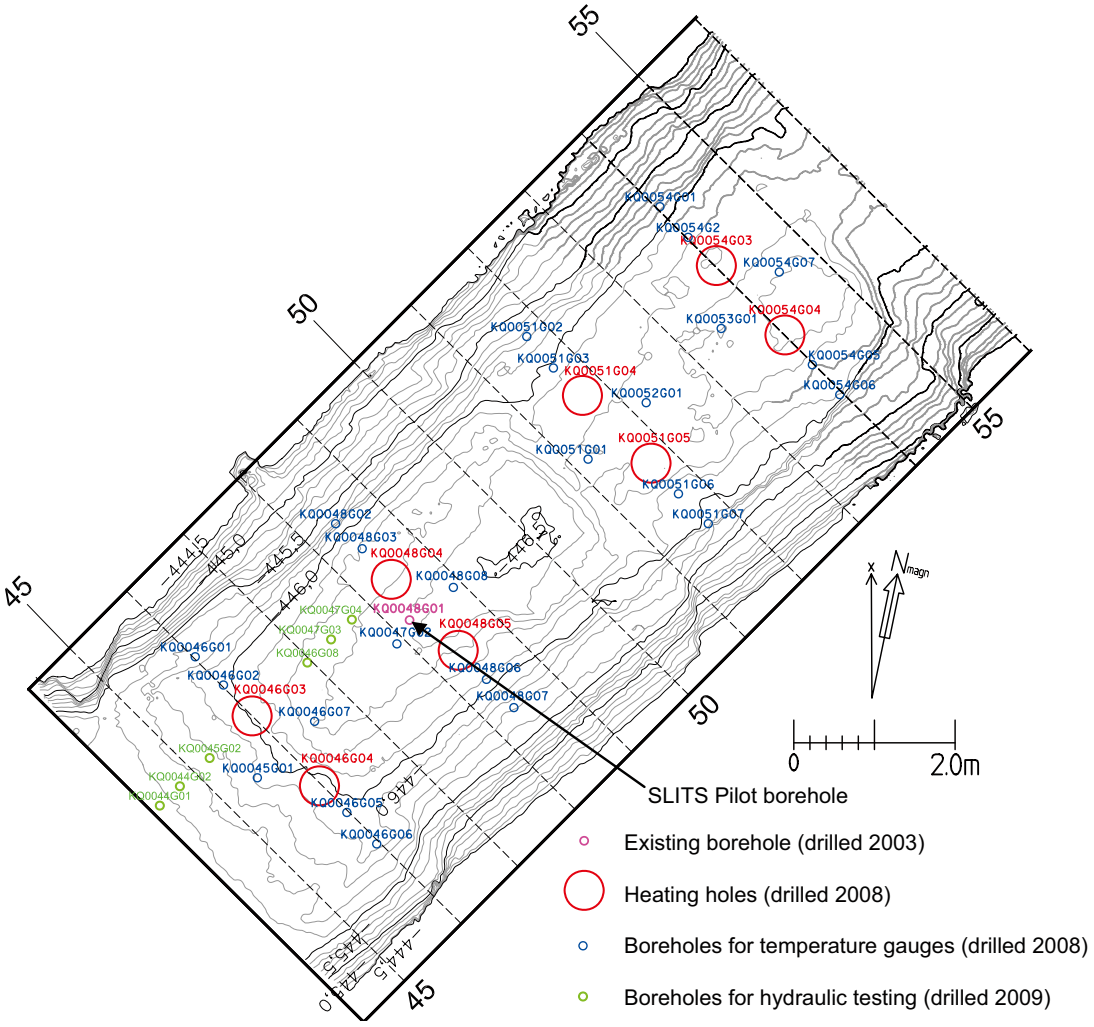

Figure 3-2. *The configuration and labels of boreholes in the CAPS experiment. The borehole used for the SLITS pilot test is KQ0048G01 located at about a distance of 0.4 m to the wall of the CAPS heating borehole KQ0048G04. From Glamheden et al. (2010).*

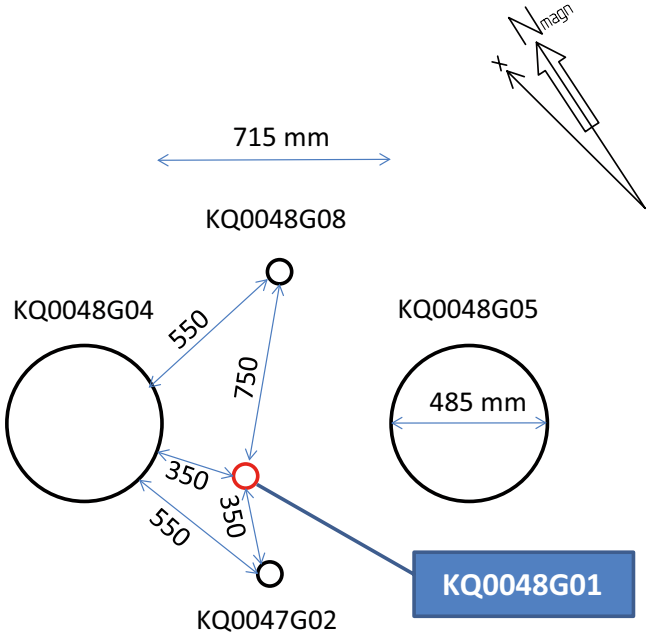

Figure 3-3. *Location of the borehole used for the pilot SLITS experiment, in relation to the other boreholes in the CAPS area. The diameter of KQ0048G01 is 76 mm.*

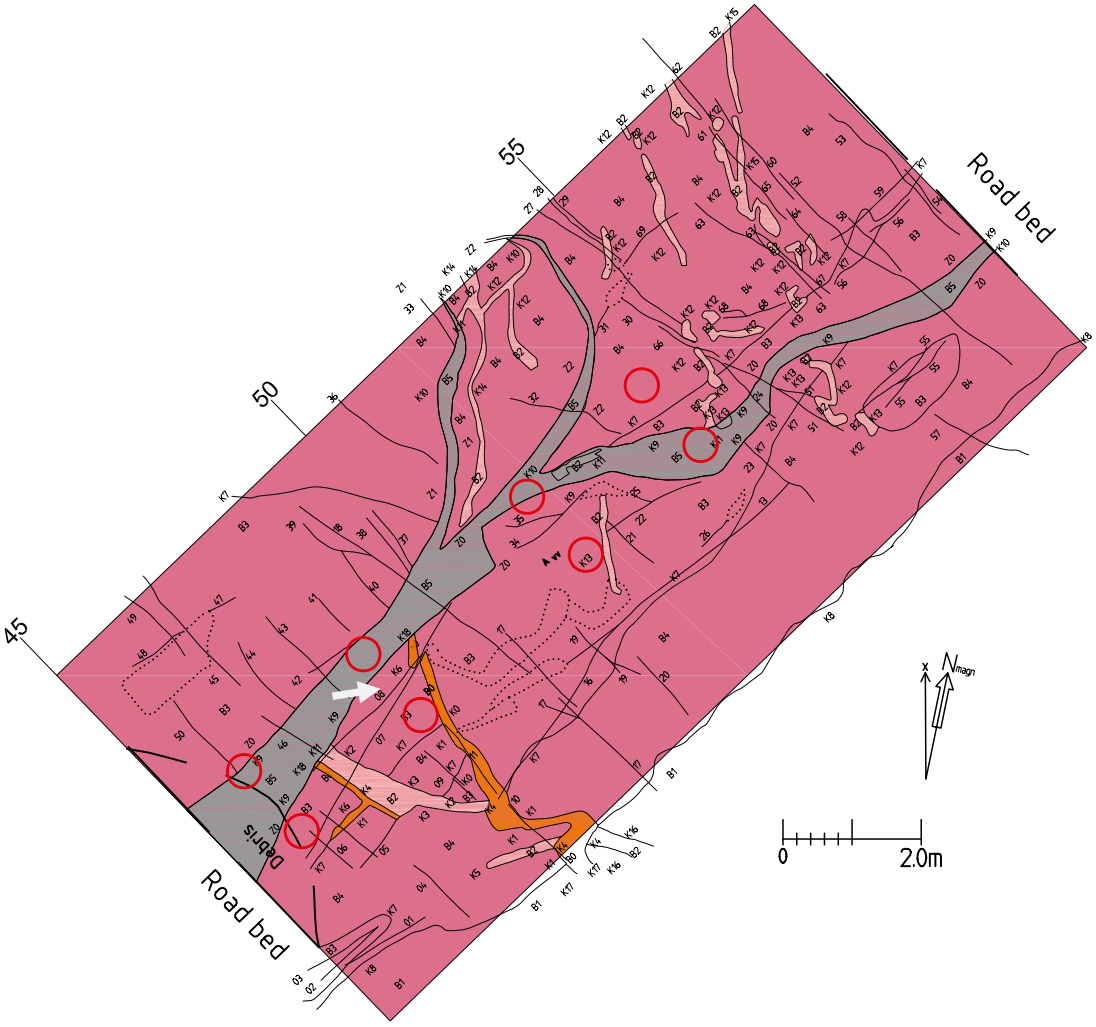

Figure 3-4. *Map of the rock types of the CAPS site (cf. Figure 3-2). Äspö diorite – Dark pink; Pegmatite – orange; Mylonite – grey. From Glamheden et al. (2010). The location of the SLITS borehole KQ0048G01 is at the arrow.*

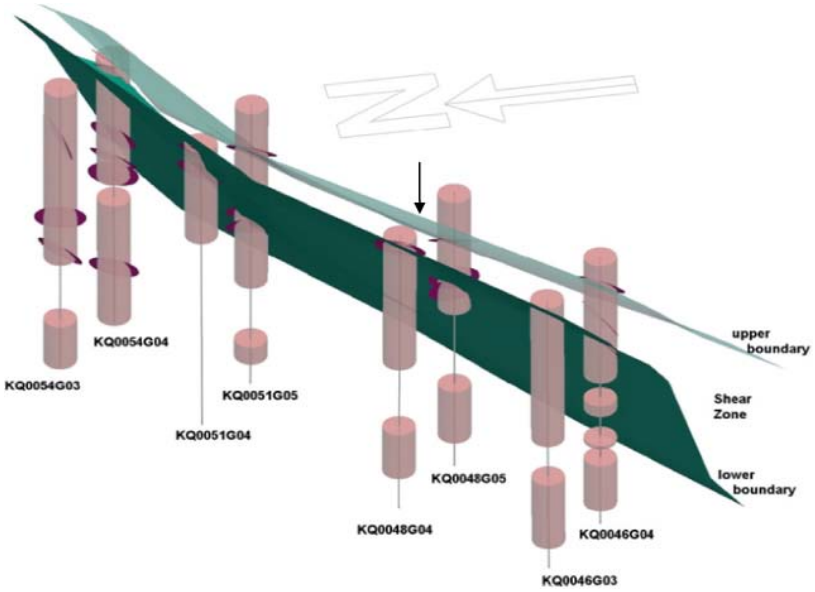

Figure 3-5. *Borehole sections logged with oxidation (pink cylinders) and shear zone boundaries (purple disks). The boundaries of the shear zone intersect also the borehole in which the SLITS method was tested. The location of KQ0048G01 is indicated with an arrow. The 4 m heated part of the borehole is located below the shear zone.*

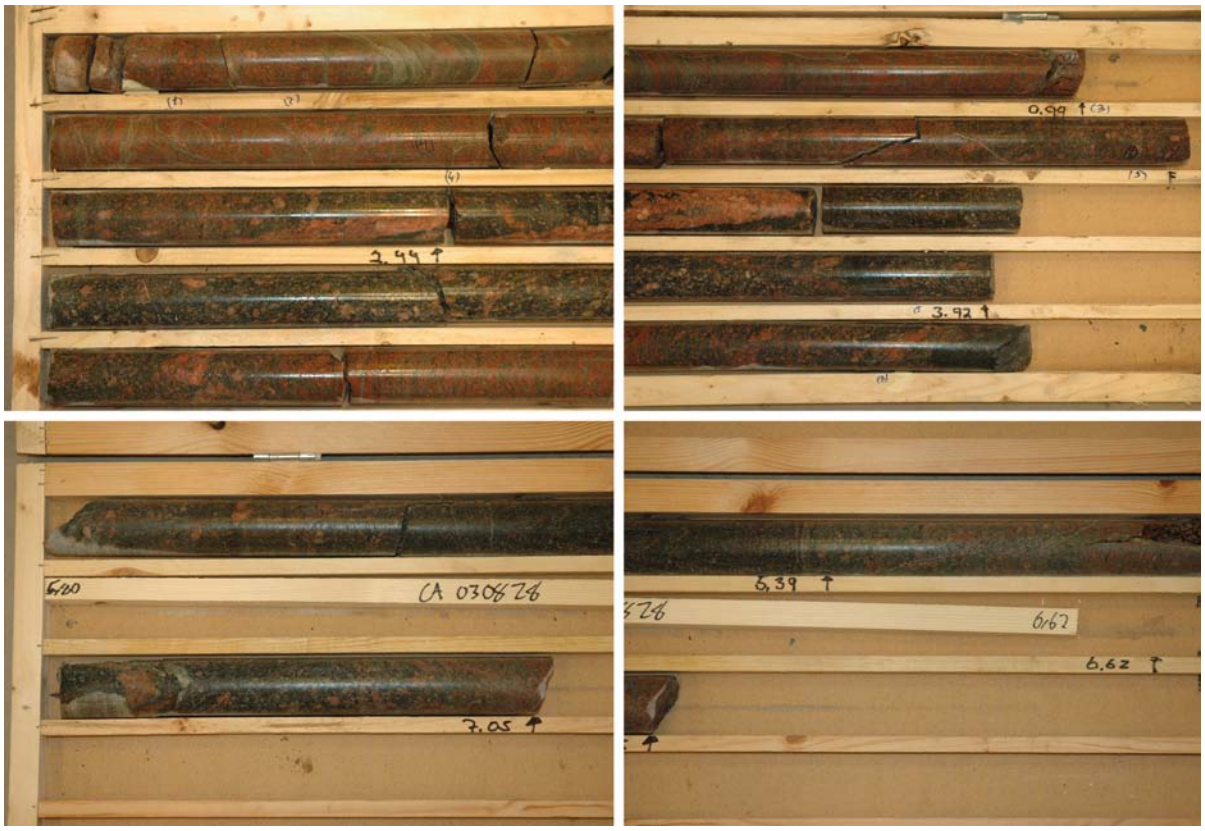

Figure 3-6. *Photograph of drill core from borehole KQ0048G01. The diameter of the core is 51 mm (and the borehole 76 mm). The rock type of the hole is a quartz monzodiorite, Äspö diorite.*

During Test 3 of the CAPS experiments the temperatures were monitored in two nearby 56 mm boreholes and the results are shown in Figure 3-7 (KQ0047G02) and Figure 3-8 (KQ0048G08). The SLITS test borehole (KQ0048G01) is closest to the borehole KQ0047G02, having a distance of about 0.3 m to this hole (Figure 3-3). The distance from the SLITS borehole to the wall of closest heated CAPS borehole is about 0.2 m less compared to the distance to boreholes KQ0047G02 and KQ0048G08 from this heated CAPS hole (cf. Figure 3-2 for borehole map). Therefore the temperature at the SLITS borehole is expected to have been at least in the order of temperatures shown in the diagrams of Figure 3-7 and Figure 3-8, and almost certainly somewhat higher, say about 80 degrees. This estimation of the highest experienced temperature, before the heating in SLITS pilot test starts, may also be made based on the isoplot of temperature of Test 3 constructed in Figure 3-9.

The breakouts that occurred in the 485 mm diameter heated borehole in CAPS Test 3 are shown in a photograph from the top downwards in the borehole in Figure 3-10. This figure also shows how the breakouts are located and oriented in the borehole (Figure 3-10 c). It is noteworthy that the occurrence is consistent and fairy continuous on both sides of the borehole and there is no breakouts in other directions of the borehole.

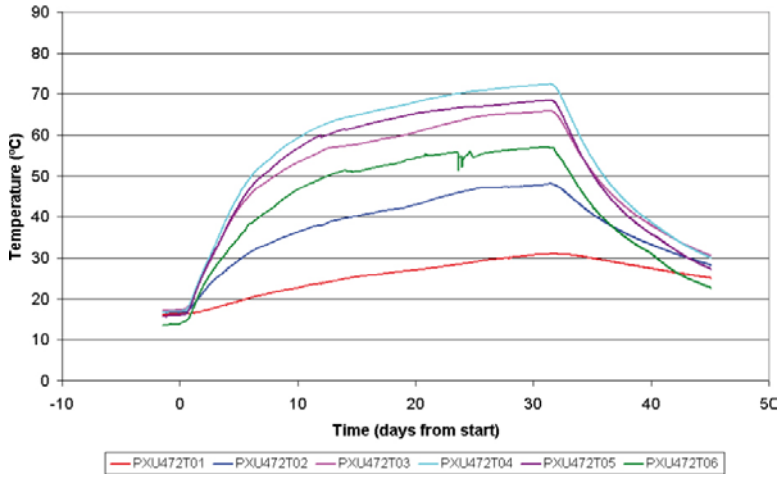

Figure 3-7. *Recorded temperature in borehole KQ0047G02 from Test 3 of the CAPS experiments (Glamheden et al. 2010).*

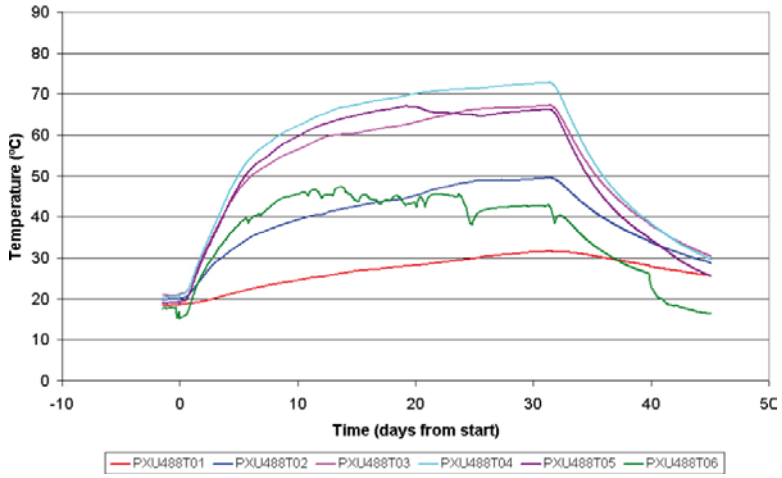

Figure 3-8. *Recorded temperature in borehole KQ0048G08 from Test 3 of the CAPS experiments (Glamheden et al. 2010).*

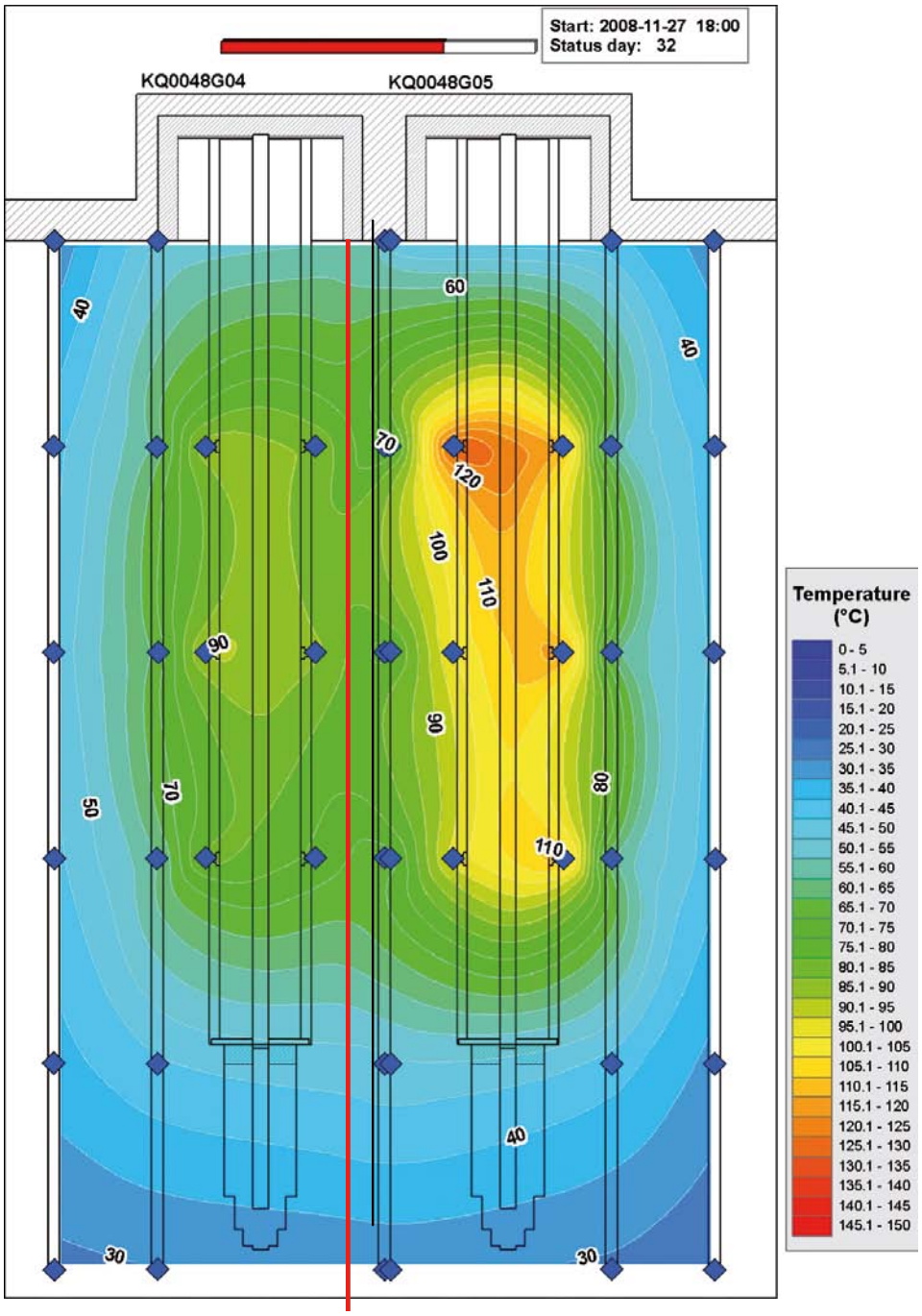

Figure 3-9. *Recorded temperatures, based on measurements in the blue square points in Test 3 of CAPS when the cooling phase was initiated. The CAPS Test 3 is located almost in the same section as the borehole tested in SLITS. It may be noted that the temperatures estimated with the isocurves reach about 80 degrees in the upper parts of borehole KQ0048G01. (See Figure 3-2 for location in plan view.) The upper part of the borehole heated in SLITS (KQ0048G01) is roughly indicated with a red line. Based on Glamheden et al. (2010).*

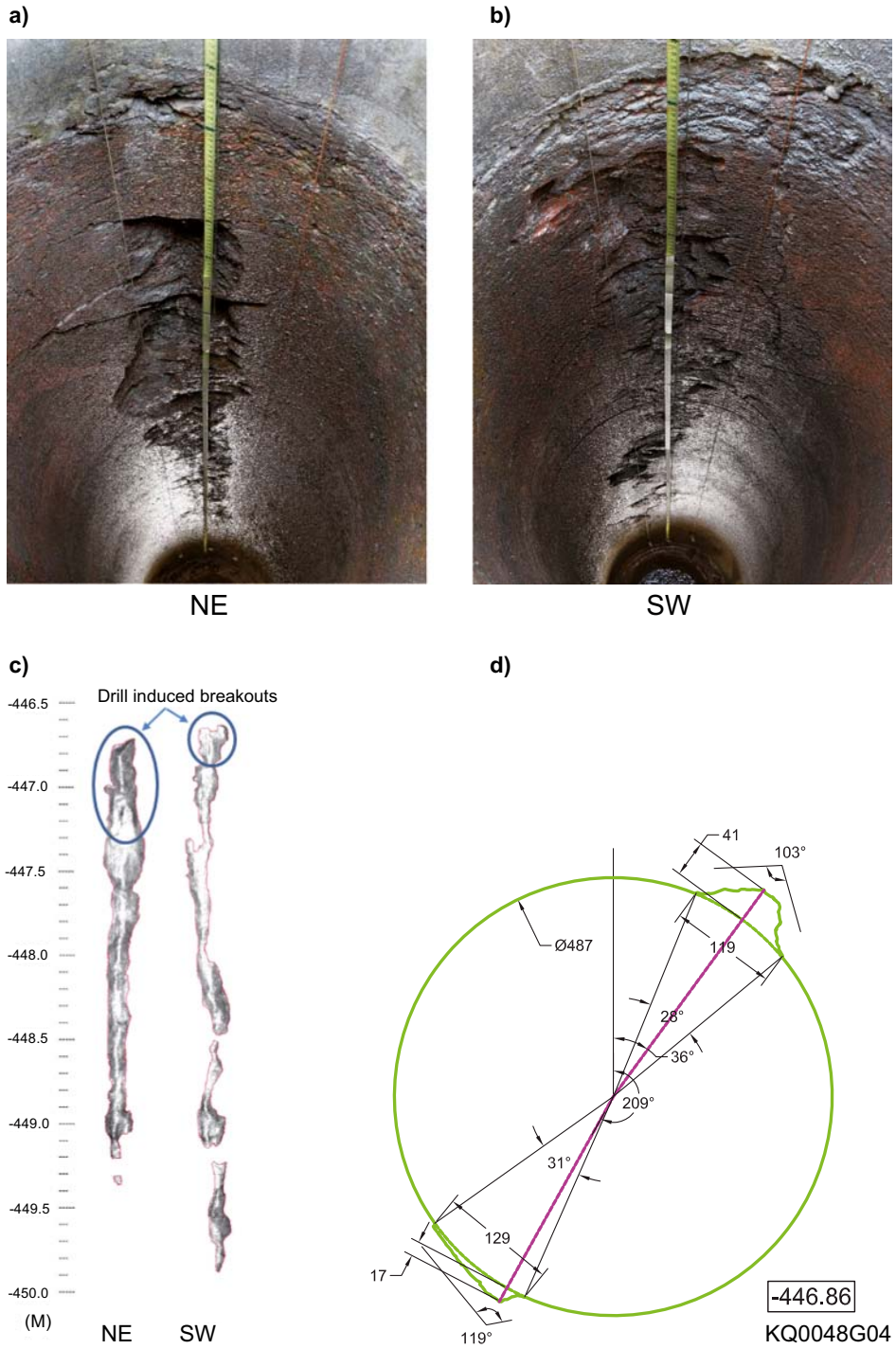

Figure 3-10. *a)–b) Spalls induced in the Test 3 (each side of KQ0048G04) of CAPS, after scaling the walls from loose fragments. c) The measured breakouts with depth on each side of the borehole KQ0048G04 based on laser scanning of the hole. The breakout marked occurred mainly before the heating. Note the fairly consistent occurrence and orientation of the breakouts along the hole d) Example of how the orientation of spalls orientation was determined in the CAPS thermal loading tests (red lines). The diameter of the heated boreholes in CAPS was 485 mm. From Glamheden et al. (2010).*

3.2 Equipment

3.2.1 Borehole heating equipment

The heating of the drill hole in the SLITS experiment was controlled by a Backer electrical heater element located in the centre of the 76 mm borehole (Figure 3-11). The length of the heater element was 4.2 m, but the active length of the element that generated heat was 4 m. The heating element itself has a diameter of about 25 mm.

The heating element was installed with the active part between level (this corresponds to about –446.4 and –450.4 m in the global coordinate system of the laboratory).

The output of the utilize heater element was reported to be limited to 2,300 W and the maximum allowable temperature of the element to 700°C. The heater power control was managed by Jumo thyristors, which were operated via the laboratory network. Additional technical specifications of the heater system are to be found in Glamheden et al. (2010).

3.2.2 Temperature measurements

The temperatures were measured in totally seven different points: at 3 depths in the heated borehole (KQ0048G01); on the heater itself; at the connection to the heater element where the rubber cable starts; in a borehole at 0.35 m distance (KQ0047G02) and in a borehole at about 0.75 m (KQ0048G08). The gauges used were Pentronic thermocouple Type K. In the heater borehole they were fixed to the heater itself (Figure 3-12) while in the nearby two boreholes (56 mm) they were simply lowered into the holes with the cable.

Since there was judged to be a risk of exceeding the allowed temperature at the connection to the cable above the heater a simple isolation was made above the heater element, and the temperature was monitored on the outer side of this isolation at the connection (see Figure 3-13).

The effect to the heater element and the temperatures measured was continuously monitored and a value collected every 10 minute. The values are digitally recorded directly to the laboratory network such that the test can be followed and controlled from the office.

Figure 3-11. *The heater equipment used for heating in the SLITS pilot test borehole. The length of the heater is 4 m. The heater is kept centred with three holders with the diameter of the borehole, 76 mm.*

Figure 3-12. *Close-up of the heater at the temperature gauge. This gauge is located at a distance of about 1 cm from the heater, i.e. in the gap between the heater and the borehole wall not leaning against the wall. This gauge was located at the bottom of the heated section (T01).*

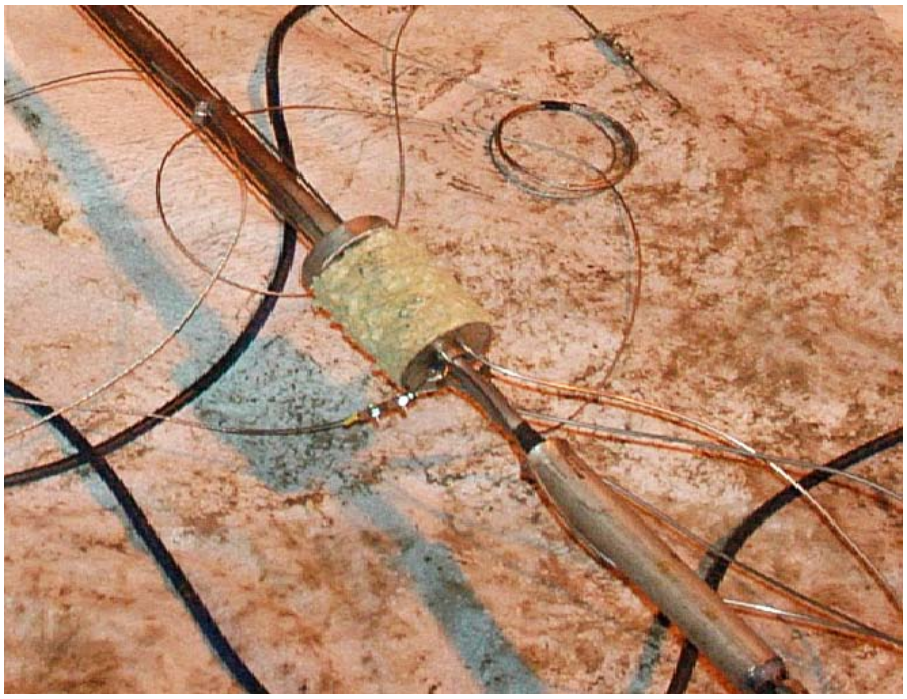

Figure 3-13. *The upper end of the heater element, the isolation and the connection to the electrical cable.*

It should be mentioned here that the location of the temperature gauges and the constancy of these gauge positions are important for the temperature readings since heat transfer is strongly distance dependent in any material. In these experiments, with several heating periods, the instrument must be taken out from the borehole and be reinstalled several times, and a repeated exact location of the gauges is important if direct comparison of the results is to be obtained.

3.2.3 Acoustic televiewer

The probe used for acquisition of data was a High Resolution Acoustical Televiewer, HiRAT, from Robertson Geologging Ltd. (www.geologging.com), Figure 3-14. The measurements were performed by Ramböll A/S. This equipment has been previously performed within the SKB site investigations and further explanation about the tool may for example be found in Ringgaard (2007).

The principle of this logger is to measure the amplitude and the time of an acoustic wave transmitted inside a borehole. The logger gave a value for each 0.7 mm large pixel size (1°), around the borehole periphery. The pixel size in the borehole depth direction is 1.25 mm. The amplitude value reflects the stiffness of the wall at the point and will also be sensitive to any geometrical changes and rock differences on the borehole wall.

Figure 3-14. *The HiRAT probe used for acoustic televiewer logging. The probe is centralized in the borehole with two bow spring centralizers (Ringgaard 2007).*

The wave velocity measurement gives the distance to the reflection of the borehole wall and, the accuracy of the radii measurement from these recording equals 0.075 mm (Ringgaard 2007). The acoustic wave velocity measurement is sensitive to the centralization of the probe. A small distance from the centre of the boreholes results in a little angle to the point on the borehole wall and difference in results. This effect is observed as dark shadows in the results plots along the boreholes on the two opposite sides. This is common in televiewer results and the results are often corrected for the decentralization.

The orientation of the data is based on measurement of the magnetic field. In this case this resulted in some accuracy problems at the top of the borehole because metal rings were placed close to the borehole on top of the CAPS boreholes. This made it impossible to calibrate the data in the uppermost meter, and a larger mismatch in terms of the orientation between measurements occasions is seen, but it does not influence the results from the spalling indications further down in the borehole.

The HiRAT probe requires a water filled borehole, and therefore the boreholes were filled with water between the heating periods. After the logging the borehole was again emptied from water before the next heating period.

The data from the logging is presented with the help of WellCad software. In WellCad the value in each pixel is presented according to a colour scale (amplitude) and a gray scale (radii), resulting in continuous pictures along the borehole. Apart from these images curves are presented giving the maximum/medium, minimum value for each depth. (Several examples will be presented in the result chapter.). The logging data are stored in the Sicada database, both in the form of raw data files and as WellCad files.

3.2.4 Optical logger

With an optical logger a continuous true colour image of the borehole wall is obtained. The optical logger used is the OBI52 probe (Electromind A.S.), Figure 3-15. The logger has a high resolution image of the whole (360°) borehole wall. The resolution of the optical logger is 360 pixels horizontally (for a 76 mm diameter borehole this means 0.7 mm) and 1 mm vertically. The logger may be used in 76–500 mm diameter holes.

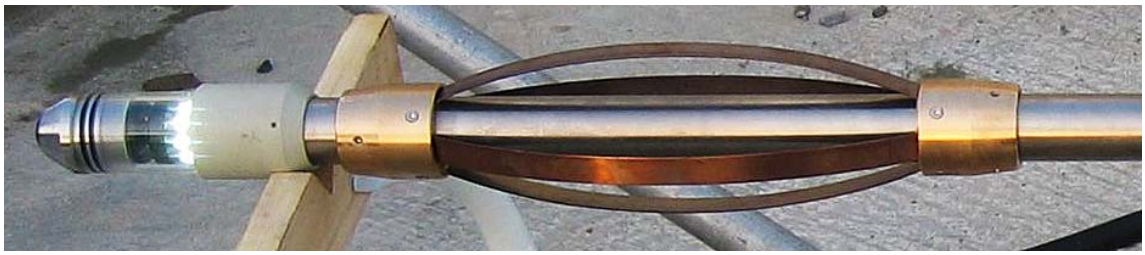

Figure 3-15. *The optical logger, OBI52 (Electromind A.S., www.electromind.eu), used in the SLITS pilot test.*

The optical logger may be used both in water filled and empty borehole. In this case the logging was made in water filled borehole, since the televiewer logging has to be made in water filled boreholes. Obviously, if the borehole is old the walls may have a thin film of bacteria or other oxidation materials, and the optical images of the borehole will become better if the walls are cleaned with high pressure water and/or a brush before the logging. After any steering of the borehole water there should be time to have the particles in the water to sink and to have fully clear water conditions. In the SLITS pilot test there was a first cleaning between the first and second optical logging and a slight improvement of the image colour could be noticed.

3.2.5 Ground water flow conditions

The heated borehole (KQ0048G01) is intersected by four open fractures (according to core logging results in Sicada). Out of these some, or at least one, is water bearing, probably at 6.7 m depth (Figure 3-6).

The water and humidity situation at the gauges are factors to consider in the experimental set-up. Since the borehole in the pilot test was only 7 m deep, the experience was that the water inflow was high enough to get the water level to rise up to the heated section during the time period of the test. When the temperature reaches the temperature gauge this will be clearly seen in the temperature measurement results. To avoid that the heated borehole was water filled in the heated section the two nearby boreholes (KQ0047G01 and KQ0048G08) were drained during the test period, and the inflow into the heated borehole was in this way minimized. Still the water level reached the lower temperature gauge in the last heating period (see further Section 3.3).

3.2.6 Borehole brushing and fragment collection

At three occasions during the heating sequence the borehole wall was scraped with a wire brush. (The objective was to remove any possible loose fragment on the borehole wall. After this the borehole bottom was emptied with a vacuum pump and the rock material in the filter collected.

Figure 3-16. *Brush used after heating periods to loosen any thermally spalled rock in the borehole wall.*

3.3 Temperature results

The temperatures were measured at three points in the borehole. The first (T01) at the bottom of heater at about 1 cm distance from borehole wall, and the second (T02) located at mid height of the heater, leaning against the borehole wall. The third temperature gauge (T03) was located at the top of the heater, also roughly at 1 cm distance. Further, the temperature on the surface of the heater was monitored and the temperature at the cable connection above the heating element. These measurements were made to make it possible to compare the different temperature results from tests with different heating sequences.

Four heating periods was applied in the boreholes. The first with gradually increase heater effect up to 800 W, the second with a constant effect of 800 W, the third with a constant 1,500 W and the forth with a constant heater effect of 2,100 W. The results from effect monitoring and temperature measurements for all heating periods are shown in Figure 3-17 and Figure 3-18.

Regarding the heater effect a general observation is that the levels are stable and that only for very low effect levels it may be difficult to keep a constant output effect. In the first heating a jump in temperature values is seen after about 7 hours, and this corresponds to a power break (the effect is zero) because an incorrect fuse was used by mistake. After the third heating there is also a gap in the temperature monitoring because the reading was first stopped and then restarted to enable a control also of the cooling stage. The unexpected abrupt changes in the temperature curves for the nearby boreholes KQ0047G01 and KQ0048G08 (Figure 3-18c) is judged to be caused by some movements of the gauges that were loosely placed in the boreholes.

If looking at the results from the three gauges T01, T02 and T03 a clear difference in temperature values may be noted. These differences are explained by the difference in distance to the heater and also the location along the heater in the hole, which means that the results should not be directly compared to each other. But curves from the same gauge after different heating periods may be compared. However, the location of gauge T02 has been changed before the third period and the gauge is in 3rd and 4th period leaning against the borehole wall. The other two gauges (T01 and T03) are at a distance from both the heater and the borehole wall, and the difference between them should be explained by the fact that T01 is at the bottom of the heater where there is more cooling from surrounding rock.

The highest temperature that was measured in T02, at the borehole wall at middle height of the heater, was 130°C in the 4th period (and this is absolute temperature not the temperature increase). This temperature was reached after about 1 day of heating and did not increase significantly during the three more days of heating with 2,100 W constant heater effect. The temperature at the wall should not be taken as exactly equal to the temperature inside the rock of the borehole wall surface, but it is certain that the temperature inside the wall rock should not be higher than the temperature measured in the air at the wall contact of the gauge.

After about 1 day in 4th heating and after 3 days in the 3rd heating the water level in the borehole seem to have reached the lowest gauge T01 (dark blue curve) and the temperature registered drops (see also Section 3.2.5). After about 4 days of heating in the 4th period the top gauge (T03) starts to be unstable. The reason for this is not known but a hypothesis is that it is an effect of high humidity, partly boiling, condense and dripping from the gauge itself. The gauge T03 is oriented downwards while T02 is oriented upwards, which could possibly explain that the same phenomenon is not seen in T02.

The generally stable temperature recordings show that the gauges work well and that it is possible to perform the test also in an environment with some other ongoing activities. The distance from the measurement section to the tunnel itself, and simple arrangement for the cables from the borehole, enabled the pilot test to be carried out with a minimum disturbance from, or to, the other activities in the laboratory. When the heater is mounted in the borehole the test need no staff and almost no space apart from the borehole itself, which must be protected from water inflow or debris falling into the borehole.

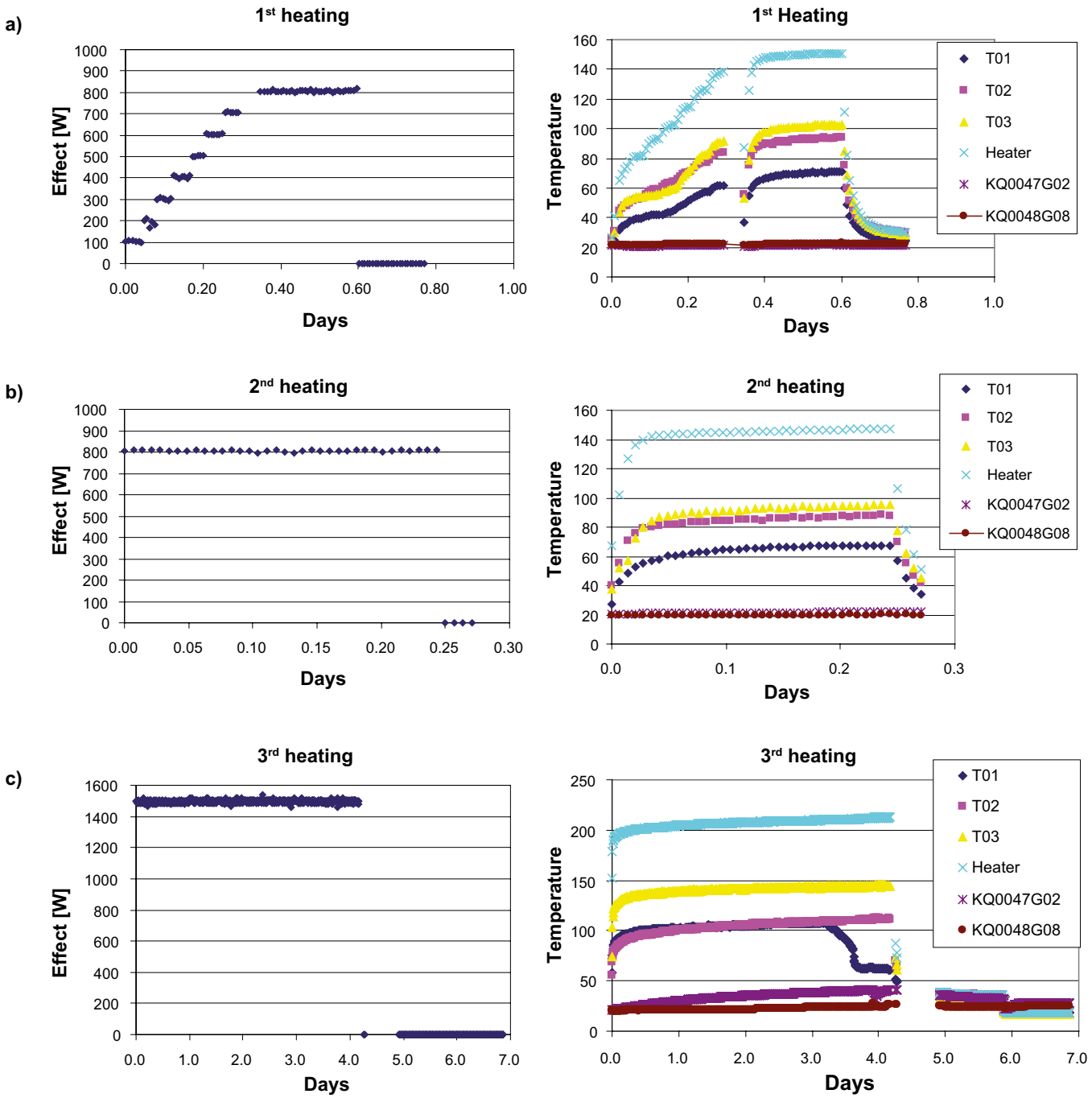

Figure 3-17. *The effect in the heater (left) and temperatures (right) during a) the first heating period, b) the second heating period and c) the third heating period. The gauge T01 is at the bottom, T02 at mid height and T03 at the top of heater. The gauge T02 is in 1st and 2nd period located at a distance from the borehole wall (moved before 3rd heating). Note that these values are not the temperature inside the borehole wall rock, but the temperature of the air of the borehole gap where the gauges are located. See Figure 3-2 for borehole locations.*

From the acoustic logging results, which will be presented in next section, it became clear that no additional spalling was induced by the two first heatings. The temperatures that was reached in the borehole after these periods was also not higher, but in this same order of what this borehole had experienced already during the CAPS test (Section 3.1). Therefore it was decided that higher heater effects should be applied in the following heatings.

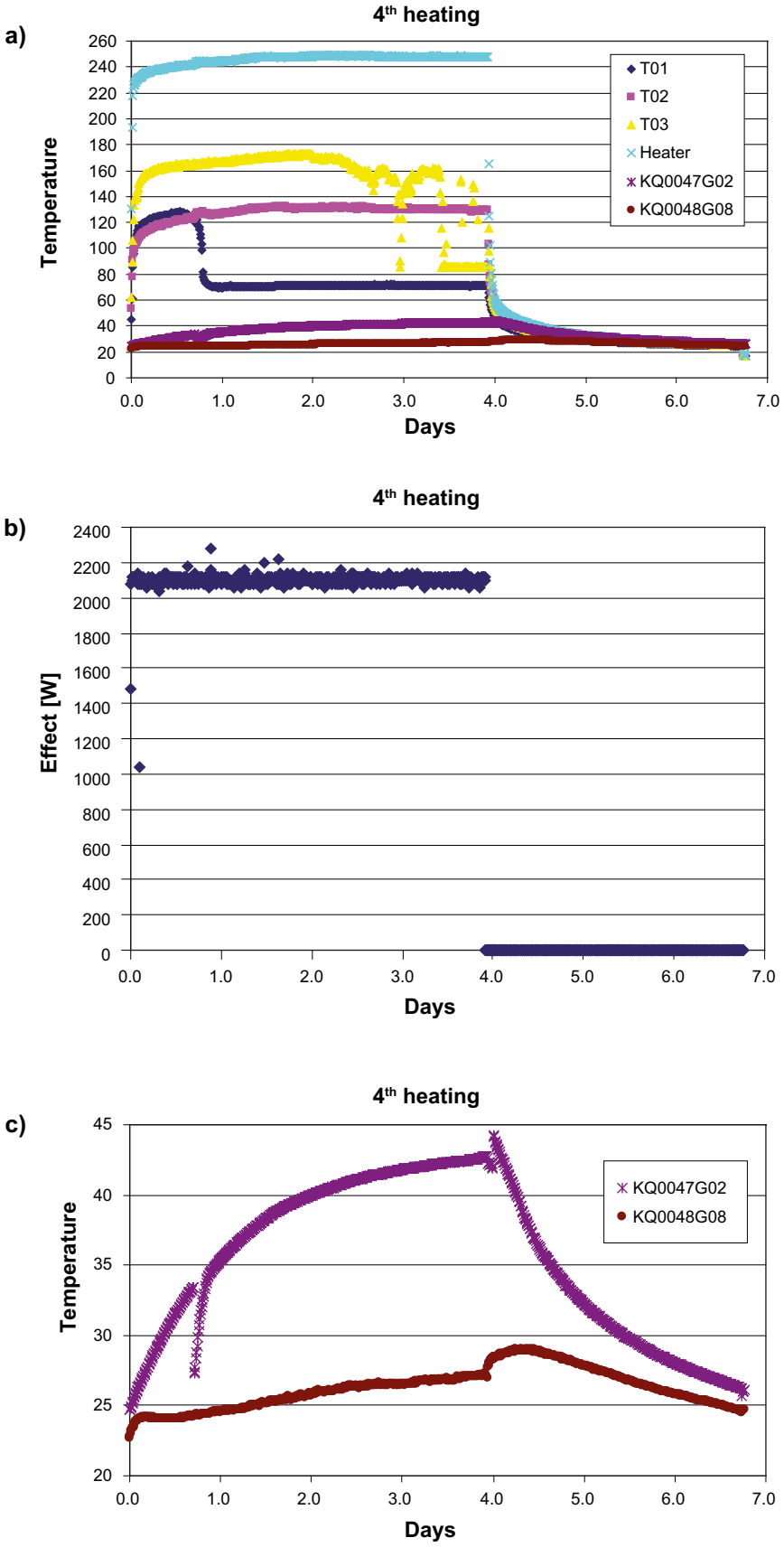

Figure 3-18. *a) The temperature recorded during the third heating. b) The effect in the heater during forth heating period. c) Detail of the diagram in a) with different y-axis scale, showing the results from temperature measurements in the two boreholes nearby. See Figure 3-2 for borehole locations.*

3.4 Acoustic and optical logger results

Acoustic and optical loggings were performed at five occasions: before, between and after the four heatings. Two examples of the results is given in Figure 3-19 and Figure 3-20, where all three types of logging data are presented in parallel along the borehole. The corresponding complete result from the logging is presented in Appendix A–D, and the underlying data is available from SKB Sicada database.

The yellow-brown colour scale of the middle image indicate the difference in amplitude of the acoustic wave, which in turn is a measure of variability in surface smoothness or differences in surface stiffness of the borehole wall rock. The y-axis in the plot is the borehole depth and the x-axis is along the unfolded periphery of the borehole wall mantle surface (360°). The analysis may be made using different y-axis scales for different purposes. In this case the x and y scales are fairly similar and thus giving a fairly undistorted image compared to the real shape of the rock features in the wall.

From the image in Figure 3-19 and Figure 3-20 it may be noted that there is a clear correspondence between anomalies for the radii curves, in the amplitude images and the optical images. Also it may be concluded that it is not so easy to detect the very small wall displacements or spalling, which is here the concern, in the optical images. Also there are natural features that show up in the amplitude images such as fractures and mineral changes.

The results shows that already at the first logging, before the SLITS heating started, break-outs existed in the borehole, for example those seen as dark features at 3.9 m and 4.2 m depth in Figure 3-19. It is not known for certain if these initial breakouts were caused already at the drilling of the borehole, or if they developed during CAPS experiments when the temperatures became elevated in the area. Although this condition was not foreseen (because the close proximity to the CAPS borehole was not realized in the planning) this was not considered as a major problem to carry through the pilot test, since the major part of the borehole was still without spalling indications and the main objective for the pilot test was to evaluate the tools required and the interpretation procedures.

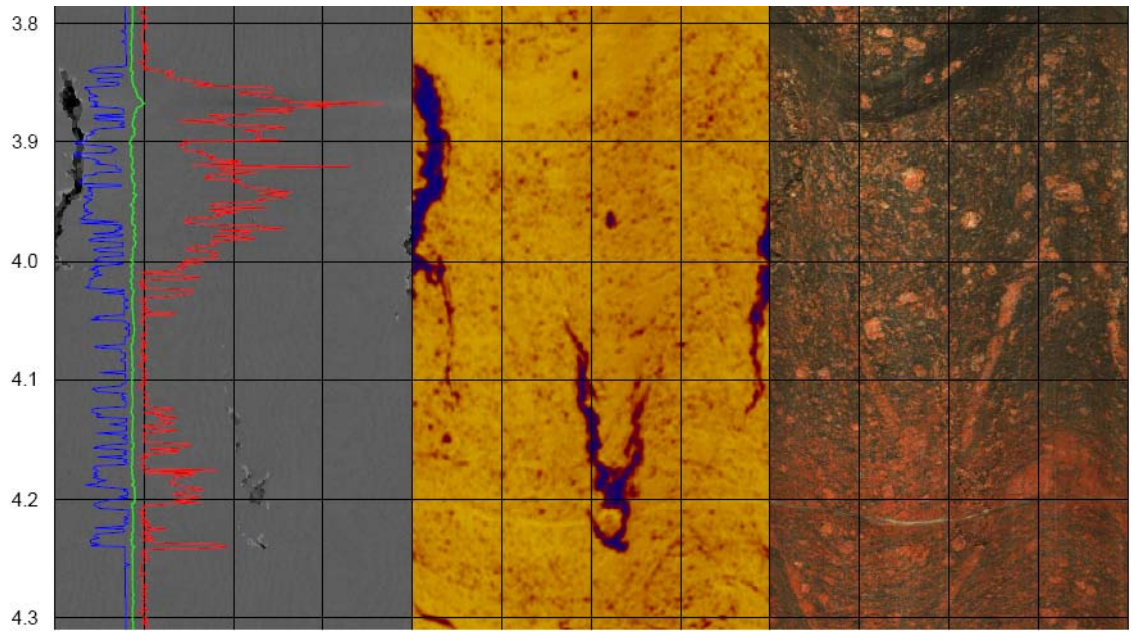

Figure 3-19. *Example of logging results. Left image: Gray-scale indicating the radii. Red line is the maximum value, green the medium value and blue the minimum radius in the same depth level row, Middle image: Acoustic amplitudes; Right image: the optical image. Each image starts from magnetic north to the left and show the 360°, with 90° between the lines. The real distance along the periphery of the borehole wall is ca 239 mm, i.e. 60 mm between the vertical lines in the images. The distance between the horizontal lines is 100 mm and thus the images are in this case not significantly distorted.*

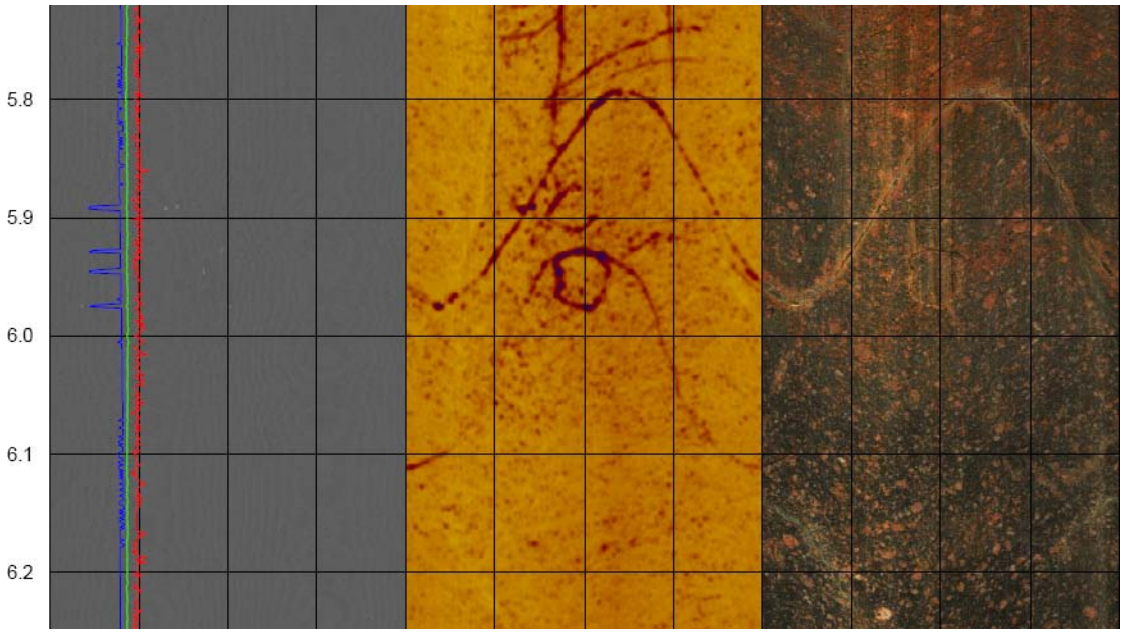

Figure 3-20. *(cont.) Example of logging results. The natural fracture is possible to observe both in the optical image and the acoustic amplitude image. The small edges or cavities are easier to observe in the amplitude image than in the optical. The mineralogy and texture of the rock type appears only in the result from the optical log.*

The development of a spall in a borehole wall passes different stages, as was documented with photographs taken in the CAPS experiments where video cameras were installed inside the large diameter heated boreholes (See Figure 3-21). The first sign would be a small bulge into the borehole and thereafter one small edge sticking in to the borehole. The fracture propagates along the borehole wall and into the rock. In particular note in Figure 3-21 that the entire loose rock fragment is still connected to the wall after the 15 days of heating. The experience from the CAPS experiments was also that there was a major part of the spalled rock that was loosened from the wall only during the mechanical scaling performed after the heatings. This means that an indication off a spalling mechanism in the acoustic logging results could potentially both be found as a decrease in borehole radius and, after a fragment is fallen off, as an increase.

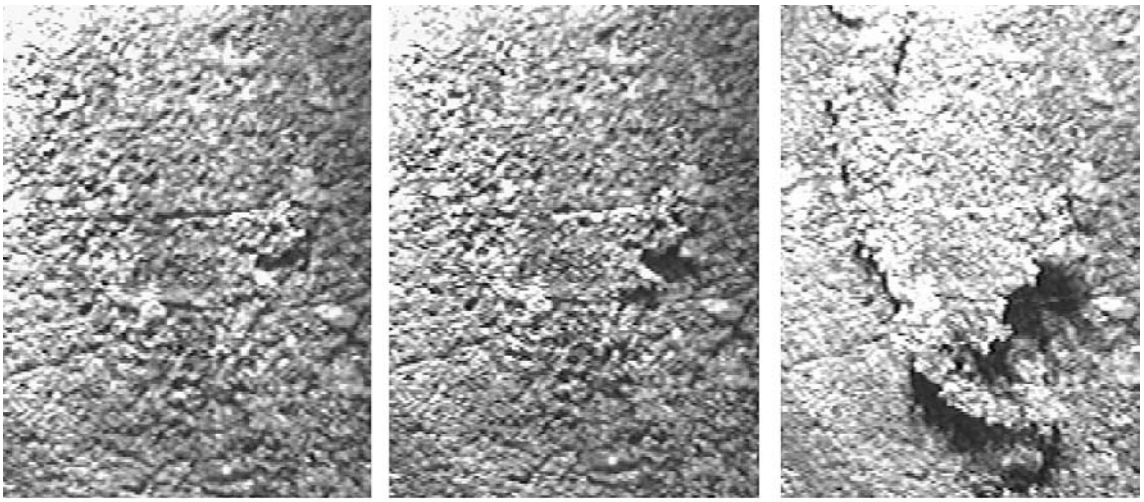

Figure 3-21. *The pictures show the development of a thermal spall in the wall during 15 days of heating in CAPS Field Test 1. The images are from monitoring cameras of the borehole wall. Image height is ca 30 cm. From Glamheden et al. (2010).*

How, in detail, the half developed spalls would influence the acoustic wave amplitudes, in different part of the fragment and at different times, is not known, and therefore we consider that any kind of changes between stages should be used in the analysis for stress determination. Change indication requires that there is one logging before a heating and one logging after. To only analyse one single logging looking for spalls or breakouts is also possible, and this is what has been done in the POM and PLU projects. However, in such cases only the more pronounced breakout can be reliably identified, and this may require high stress levels. In SLITS project the aim is to try and use the heating to induce stress levels high enough also in areas where the in situ stress is not high enough to produce borehole spalling or breakouts (we here use the two terms spalling and borehole breakouts almost interchangeable, while the former refers more to the mechanism behind and the latter rather to the result (the cavity) when the fallout is significantly large).

In SLITS the borehole diameter is small compared to previous thermal spalling studies at the laboratory, and therefore the size of the studied object is much smaller and the resolution of the measurement important. The specific observation of geometrical change, due to the heating, will naturally only be possible to observe if there is logging result from both before and after the heating.

The different results from different measurements are presented as examples from a section in Figure 3-22. It can be noted that the repeatability of the tools are very good and that there are only small differences between the loggings. At a first glance the images look quite identical. Differences in orientation (location in horizontal direction on the plot) of a particular “object” are visible between the stages, in particular in the upper part of the borehole. This should not, however, be interpreted as the best possible orientation uncertainty since, as explained above (Section 3.2.3), the conditions for orientation were not optimal in the upper part of the SLITS pilot test hole due to the metal rings in the nearby CAPS boreholes.

To find all small differences between the patterns from different measurements, a detail comparison between each of the loggings have been be performed. Note that it is mainly the image patterns (relative differences in image) that are compared, not the absolute amplitude or radius values, Some very small difference should be expected between different measurements, also if nothing has changed in the borehole, because the location of each measurement point (pixel) in the borehole wall will not be repeated fully and this means that the location of each measurement area (pixel) is not perfectly the same. Nevertheless, the repeatability for the logging must be regarded as very good. Examples of the repeated logging results for a 1 m long section in terms of the amplitude images and the optical images, respectively, are given in Figure 3-22.

The most convenient procedure to find the changes in geometry between repeated logging is to start and study an overview plot of the radii results, see Figure 3-23. From the maximum and minimum radii curves it is fast to identify the sections where some significant irregularities exist in the borehole wall. It may be concluded that the maximum and minimum values often occur at the same places, and this is not surprising since free edges at the side of a tiny cavity may tend to move inwards, and there is a combination of loosened and stuck pieces as discussed previously. Actually the analysis was first performed with a presentation of the maximum radius curve only but in the further study it was realized that the minimum value is more sensitive and therefore probably a better indicator of a beginning spalling phenomenon.

The thermal spalls in the slim boreholes, in contrast to what has been observed in the larger scale field experiments, are very small and in the scale of the rock type mineral grains. In some cases there is also a correspondence interpreted between an observed anomaly and a certain mineral grain. For example this is seen in Figure 3-19 at 3.97 m depth (200°). The dark dot in the amplitude image coincides exactly with a large feldspar grain in the optical image. (To study details in the logging data the WellCad file should be utilized, where there is a possibility to zoom in, and the image resolution is better than what can be conveyed here in this printed report.)

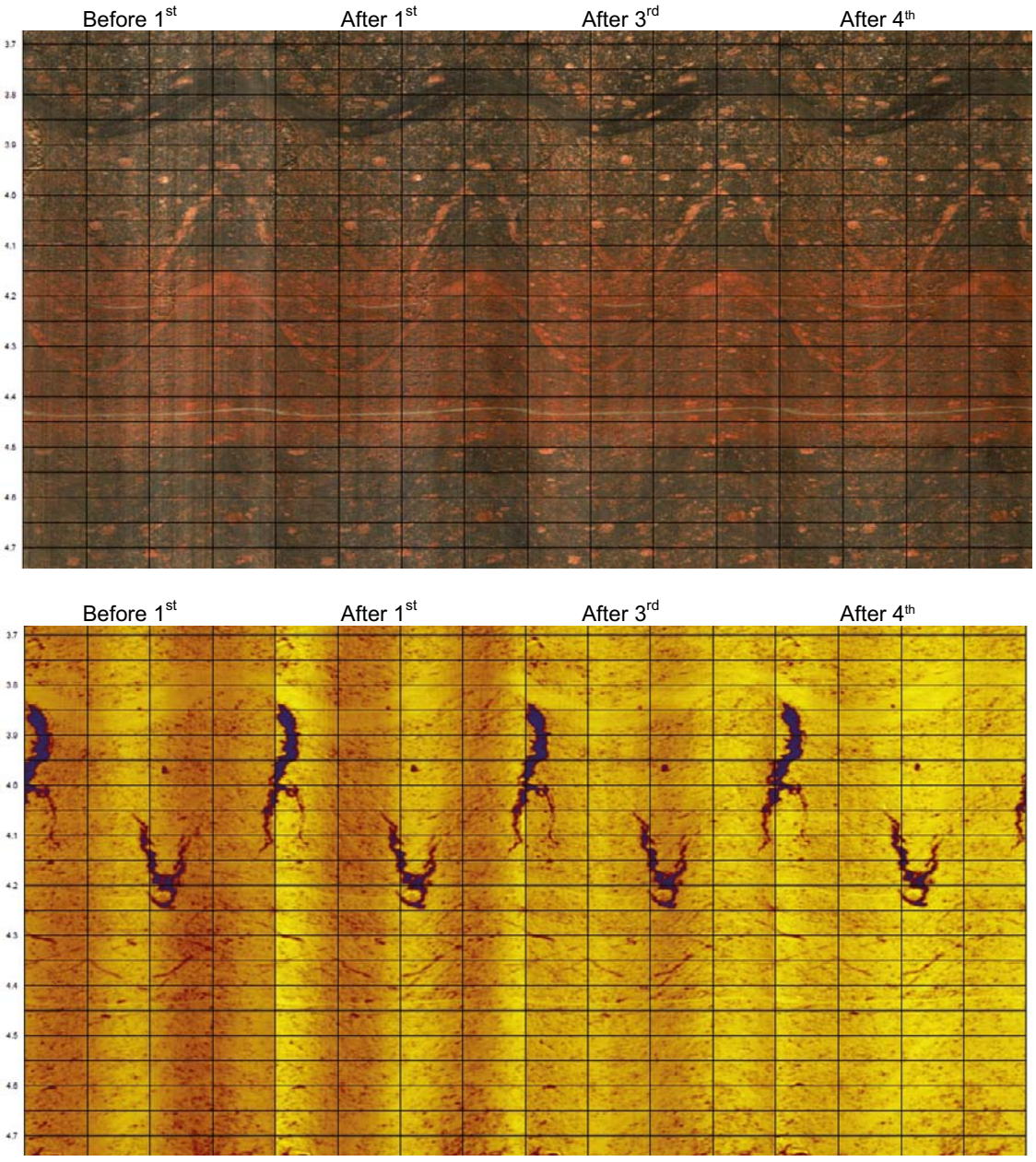

Figure 3-22. *Example of results presented for about 1 m long section of the borehole. Four different measurements, performed at different occasions, are compared. The upper image is the optical logging results and the lower image is the acoustic wave amplitude results. The results (the patterns) are almost identical. The breakage of the wall rock that has taken place at 3.8–4.2 m depth is easy to detect in the amplitude image while requiring much more effort in the optical images,*

Looking closer at the anomalies at 3.95 m depth (Figure 3-24) it is noticeable that there is a change with time even if it is very small. The cavity widens slightly and the length extension increases a little in both direction. Generally, when the white parts decreases (lower radii values and blue line), i.e. when some small grains at the edges fall of, the dark areas at the same point increase (higher radii values and the red line).

One point along the borehole where a change was observed, and where the location was not affected already before the first heating, was at 4.9 m depth (see Figure 3-23). At this depth an indication of lower radius turn up after the 3rd heating and remains in the log after the 4th, but does not show in logs before this. Close up images at this point is given in Figure 3-25. One may note that no anomaly occurs for the red curve and this is thus an example where the minimum curve is helpful. The next step is to see if any lighter point is found on the radii image. This location gives the point along the periphery.

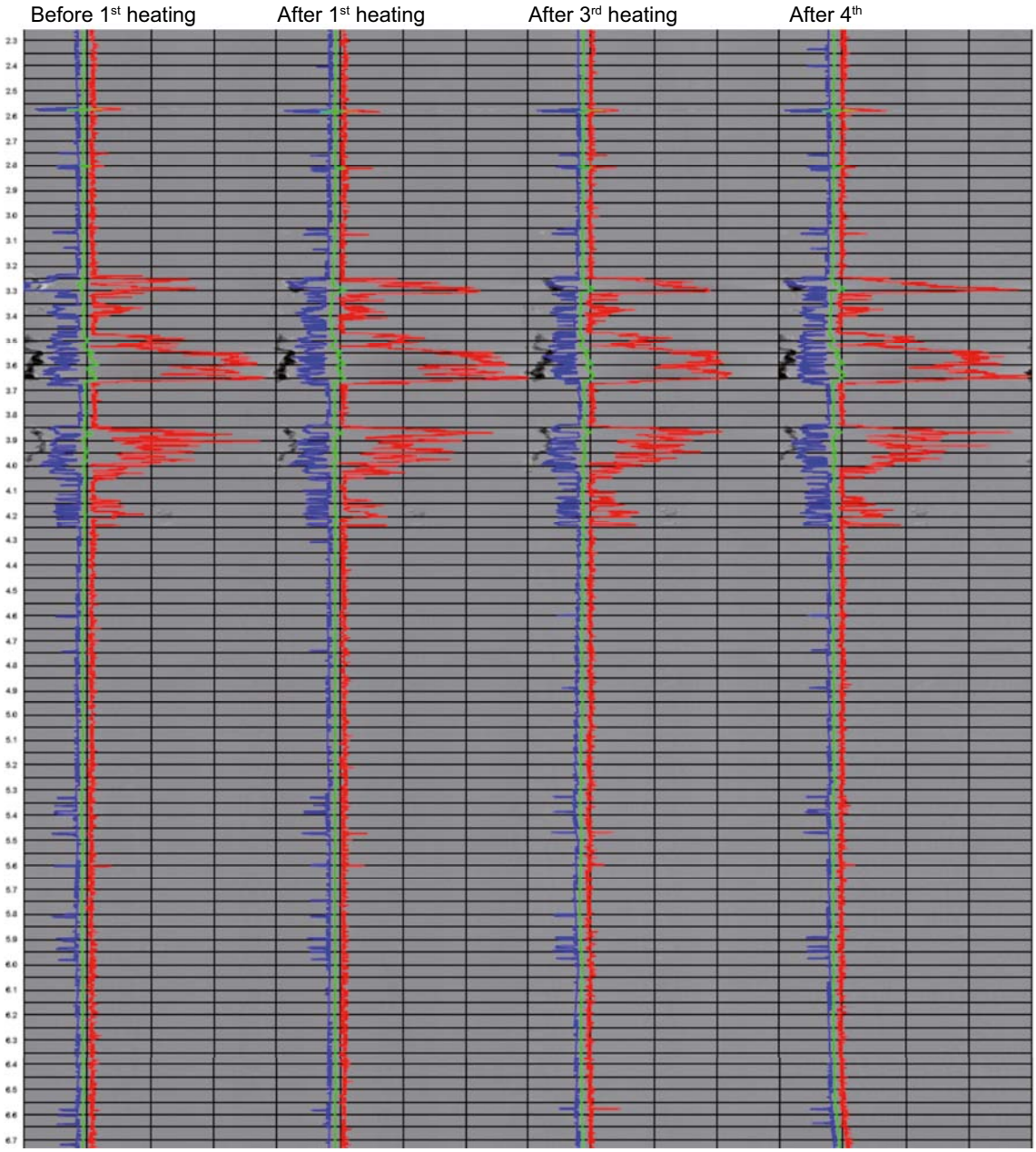

Figure 3-23. *Radii result from 4 measurement occasions. Thy y-scale is compressed such that the whole borehole (2.3 – 6.7 m) can be seen and provide an overview. For explanation of lines refer to text and Figure 3-19.*

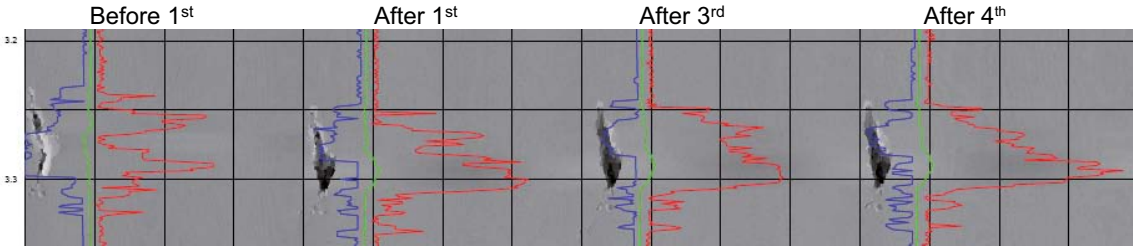

Figure 3-24. *Ten cm long detail of the borehole showing the radii measurement result. An increase in maximum radius values (red) may be noticed, and also the corresponding slight enlargement in the spalled area during the heating periods.*

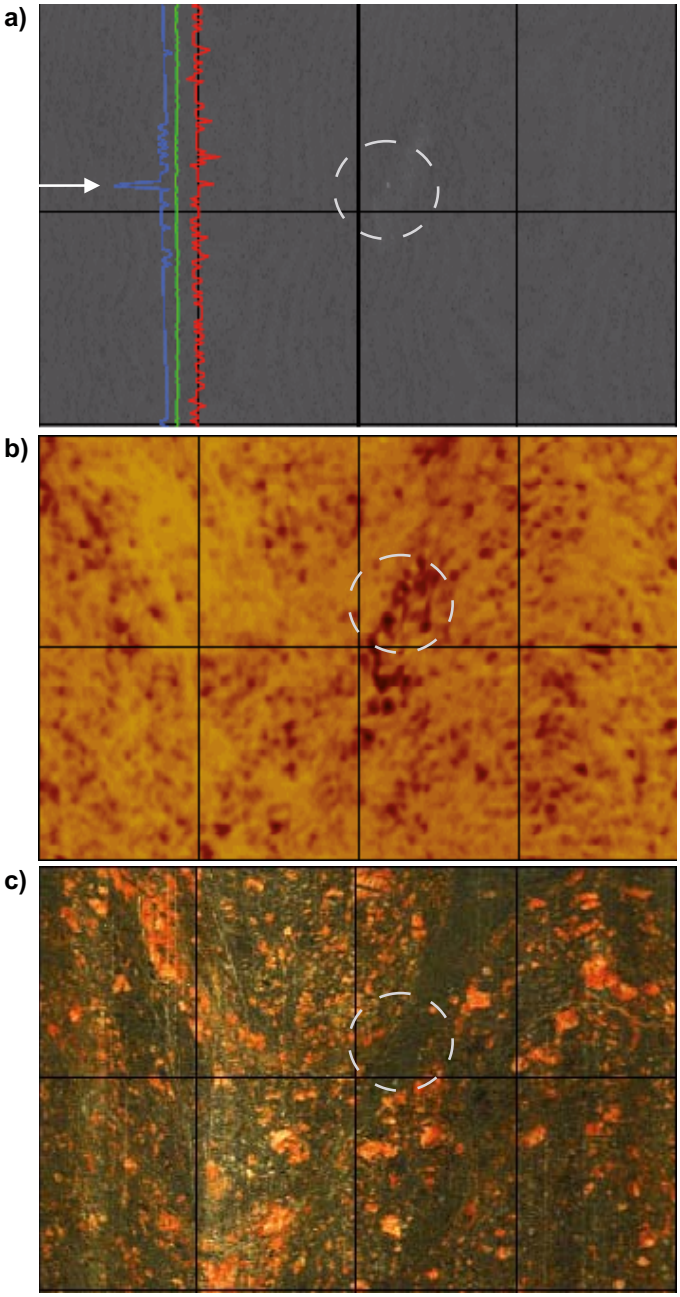

Figure 3-25. *Logger results from the stage after 4th heating. a) A 20 cm long section of the results from radii measurements. (For explanation of lines refer to text and Figure 3-19.) The grey-scale area gives the radii values at each wall surface point. b) Corresponding acoustic televiewer amplitude results. The darker spots correspond either to a less stiff mineral or to some roughness in surface. c) The result from the optical logger shows the corresponding borehole section, and a thin loosened fragment of rock was found in the marked area.*

Having this indication from the radii results, it is the next suggested step to check this location in the amplitude images and see if there is a corresponding change seen also in this log parameter. This comparison is made in Figure 3-26. The increase in dark areas is not large in extent but clear when the location is known. The change is gradual from the first to the last logging.

To further check what the character is of this anomaly the final stage is to check in the optical image (Figure 3-25c and Figure 3-27). The actual point displays a change in geometry that looks like a small thin piece has fallen off. The area increases slightly from after the 3rd to after the 4th heating. But practically it would be hard to identify these small differences in images if the location to search was not known. The high resolution optical logging is required for this step.

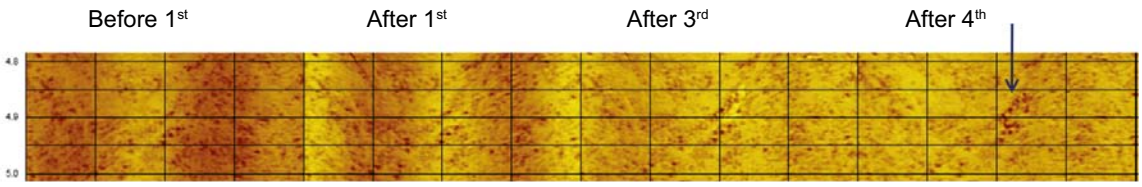

Figure 3-26. *Acoustic amplitude results at borehole depth 4.8–5.0 m. Comparison between different measurements. The signs of the small spall develop gradually.*

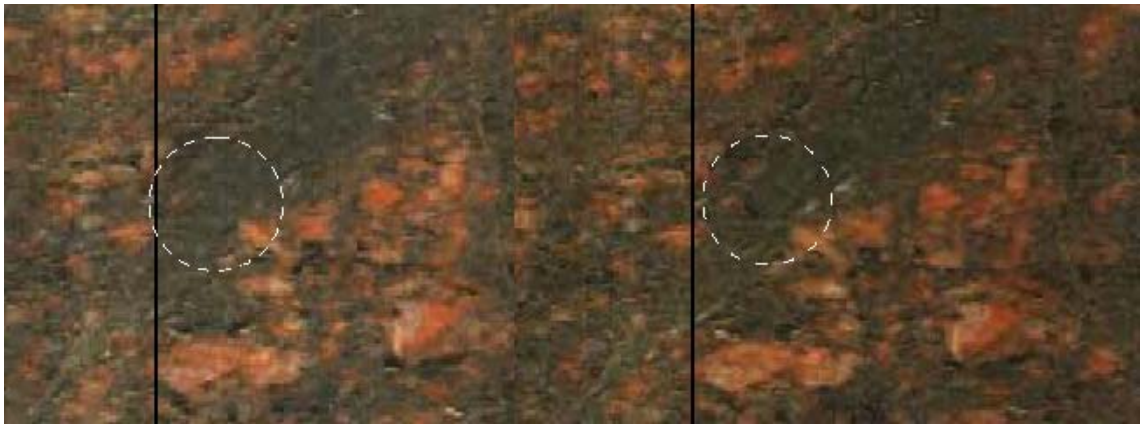

Figure 3-27. *The same location as shown in Figure 3-25 and Figure 3-26. The left image is the optical logger result from 30/8 after the second heating and the right image is from 9/9, after the third heating.*

3.5 Collected fragments and alsphaltite

A collection of fragments war performed after 1st, 2nd and 4th heating period. The first gave about 360 g of rock fragments, the second about 60 g and the last about 10 g. The first collection is hard to draw any conclusions from since it is unclear how emptied and protected the borehole has been before the experiments at the site. Focus here in the study has been on the two later collections.

Four of the fragments collected after the 3rd heating were clearly larger than others. Photographs of these fragments are shown in Figure 3-28. The upper image is taken from the side and the lower image from above. The flat and elongated shape of the fragments can be noticed. For one of the fragment the probable original location in the borehole wall was found, based on the resemblance in shape seen when comparing fragments and the image of the borehole wall at 4.9 m depth (Figure 3-29).

As a comparison, the fragments collected in the CAPS experiments (Figure 3-30), where the borehole diameters was 485 mm compared to 76 mm, show the same general thin wedges shaped fragments. The size of the borehole was six times larger in CAPS compared to SLITS, and the smaller fragments in Figure 3-30 are also about six times larger than the fragments from the slim SLITS borehole.

Clearly, most of the fragments are small, in the size order of the grains, 0.1–0.5 mm. Each fragment most often consists of one single mineral, but all the different minerals in the rock type is occurring, see examples in Figure 3-31 and Figure 3-32.

The metallic looking spheres among the rock fragments is drops of the fracture filling material alsphaltite (Swedish “bergbeck”). This is a carbonaceous material which is liquid at high temperature (melting point about 100°). It is only among the fragments collected after the last 4th heating, where the temperature at the borehole wall reached to 130° that alsphaltite was found. The colour and character of the alsphaltite grains vary and examples are shown in close-up images in Figure 3-33 and Figure 3-34. It was not investigated further from which fracture in KQ0048G01 that the asphaltite has originated. It is not believed that the asphaltite occurrence has any importance for the spalling

behaviour and the potential for the SLITS method. However, if any kind of automatic collection of fragments below the heated section is arranged in future attempts it may be beneficial to be aware of this possibility for inflow of asphaltite.

In the future, if there is a possibility to choose the heated section, it should be preferable to avoid sections with fractures and water flow. If sections without fractures are avoided there would be less material that loosend along edges just due to scraping with wire brush.

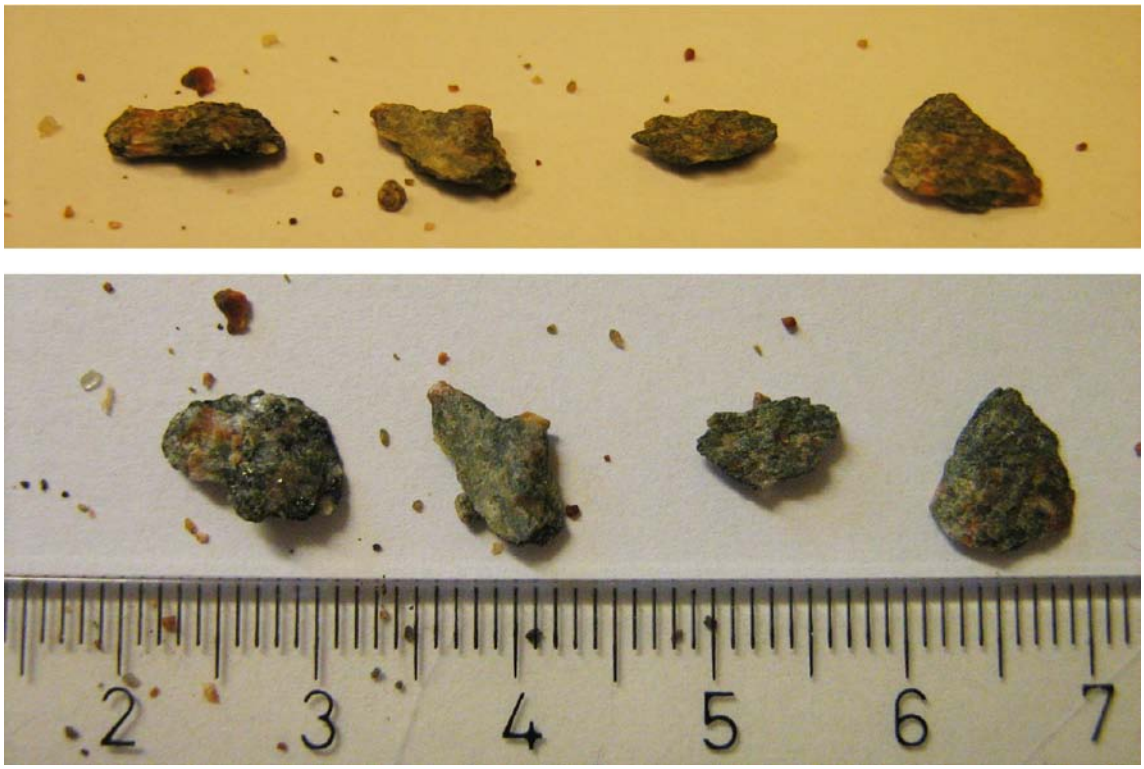

Figure 3-28. *Four of the fragments collected were clearly larger than others. The upper image is taken from the side and the lower image from above. The flat and elongated shape of the fragments can be noticed.*

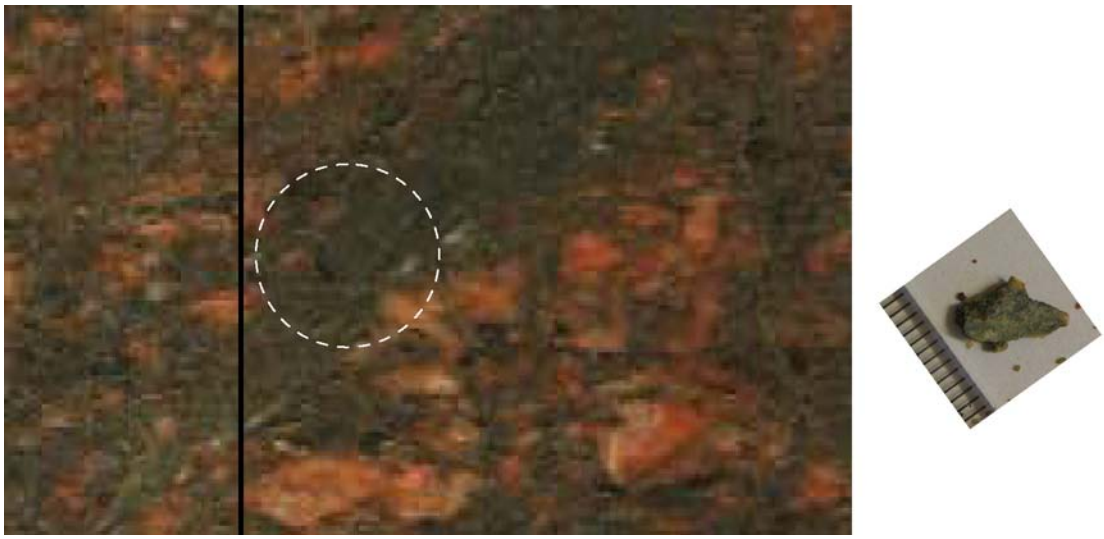

Figure 3-29. *For one of the fragments collected it seems that the shape and size fits with the place where we found a missing piece in the logging results. The left image is the optical logger result from after the third heating and the right image is the mirror image of the fragment, for comparison.*

Figure 3-30. *The larger fragments collected from a heated borehole (450 mm) CAPS Test 1, shown here for comparison of the shape to the fragments collected in the slim borehole (75 mm) of SLITS (Figure 3-28). The scale in the centre of the image is 10 cm long (Glamheden et al. 2010).*

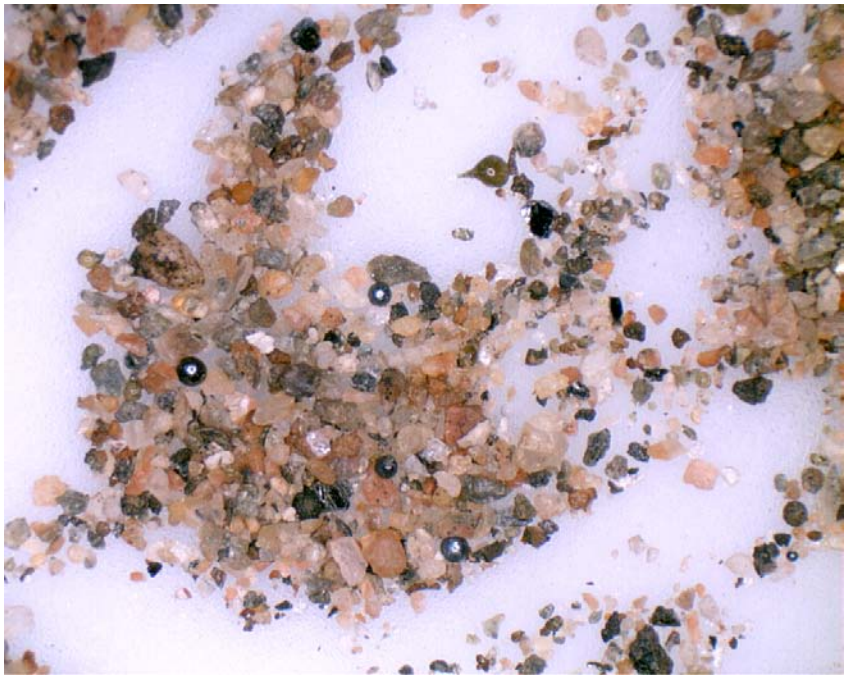

Figure 3-31. *Example of typical look of the most common small fragments collected after the last heating. The size of the image is about 12 mm.*

Figure 3-32. *Close-up image of typical small fragments collected. Three spheres of asphaltite. The image is about 1.5 mm wide.*

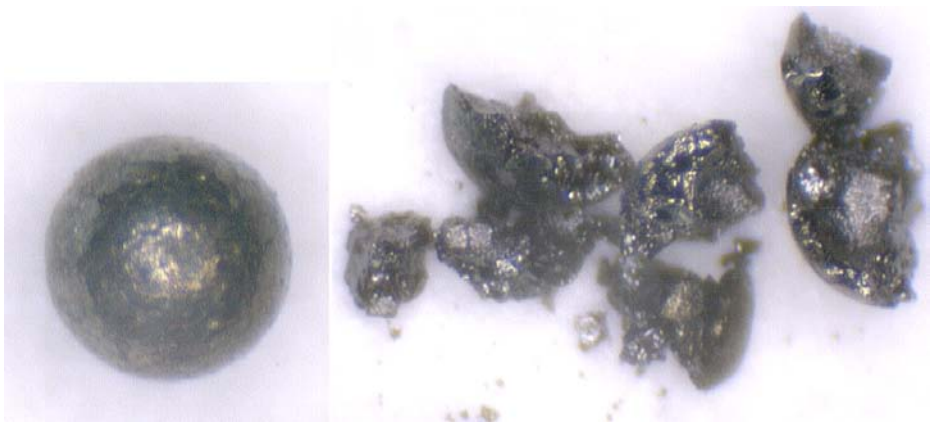

Figure 3-33. *Example of a typical small asphaltite sphere collected in the heated borehole after the last heating. The diameter of the hollow sphere is about 0.4 mm and it is easy to break. The material seems to be a mixture with very small mineral grains inside the asphaltite liquid.*

Figure 3-34. *Example of asphaltite collected among the fragments after the last heating. The particle is transparent and having drop shape. The image is ca 1.5 mm wide.*

3.6 Determination of in situ stress orientation

3.6.1 Stress orientation at the SLITS borehole

For the locations in the borehole, where it is interpreted that there has occurred a spalling phenomenon in the borehole wall, a determination of the orientation of the central point was made. The determination was made manually based on the acoustic amplitude images, as described in an example given in Figure 3-35. The orientation is in this example about 202° (from magnetic north). Consideration should be made that the half spalled rock often has a ”double-crack” appearance, with one crack showing up on each side of the not-yet-loose fragment. At the very start the spall is thin and with small width and it widens as the break propagates (cf. photos from CAPS in Figure 3-20 and APSE in Figure 1-3).

Most certain is the orientation of the breakout, or beginning thermal spalls, when there is an observation on each side of the borehole with 180° separation, as in this example case (Figure 3-35). However, this may not always be the case due to the variation, or anisotropy, in rock material properties. In the example of Figure 3-36 the opposite side of the clear spalling has instead a band of minor darker dots (marked in figure). This might be interpreted as a beginning of a spalling behaviour, but the interpretation is uncertain. The grey-scale (acoustic wave velocity) image of the radii may be used to further strengthen the identification and localization of the deepest anomalies.

It will be difficult to define objectively what should be considered “one” observation along a borehole, and also slightly subjective what observations to include in the interpretation and which to disregard. Keeping this in mind the section selected as a support for the estimation of stress orientation is presented in Table 3-1. In the table a mean value is also calculated, giving the weight according to length along hole and counting both sides separately. The mean orientation becomes 17° from magnetic north for the spalling indicating a direction of the maximum stress of 107°. This orientation is the estimation of the actual minor horizontal stress orientation at the borehole. However, since the stress situation at the hole (i.e. the secondary stress field) in this case is governed also by the nearby excavations, an adjustment to this value must be made to arrive at the estimation of the virgin in situ stress (primary stress field) orientation. This correction is made in the next section.

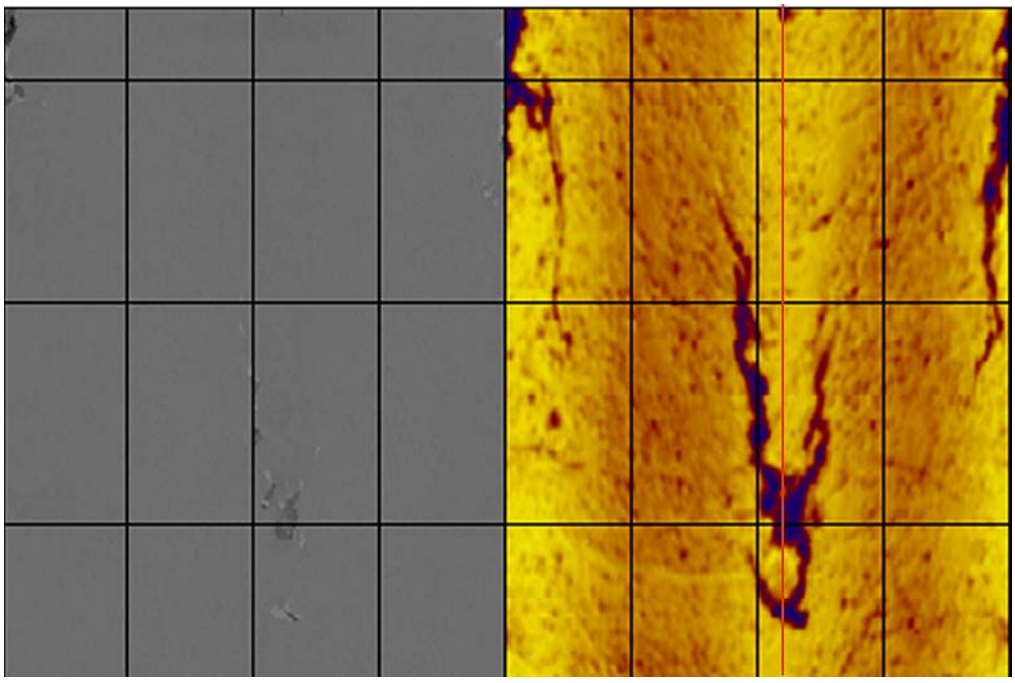

Figure 3-35. *Example of spalling/breakout in the pilot SLITS borehole (KQ0048G01). To the left: Image of radii determined using acoustic wave velocity. To the right: The acoustic wave amplitude results. The centre line of the breakout it determined manually by interpretation on the log result image. The red line positioned where the centre of this break is interpreted, at 200° from magnetic north. Slightly higher up in the borehole there is a spall on the opposite side, with the centre at about 18°.*

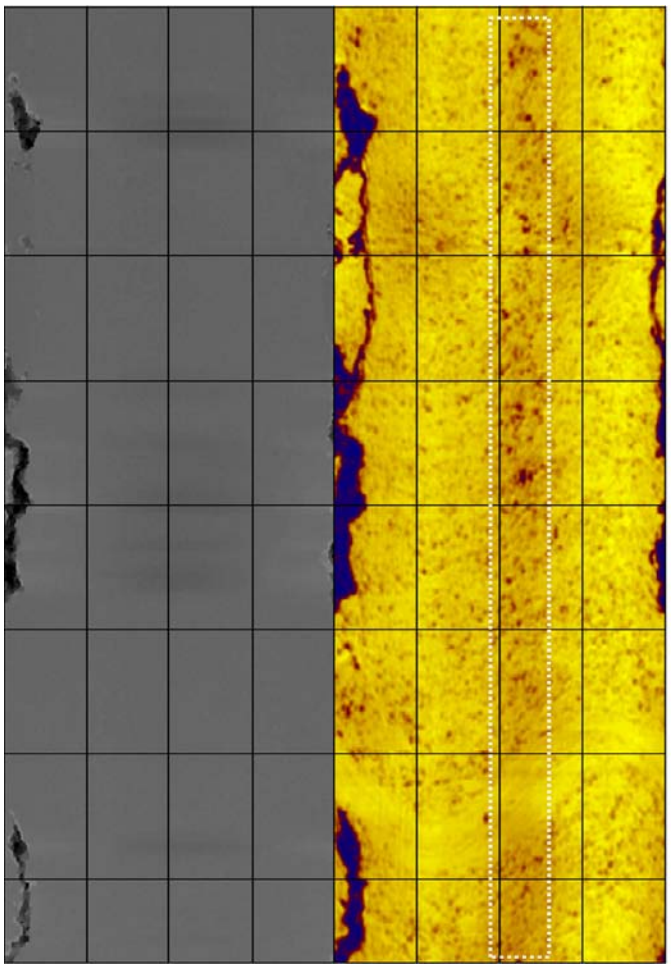

Figure 3-36. *Acoustic televiewer logger results from ca 3.2–4.0 m depth section of the borehole. Note that apart from the clear breakout occurring about 0°–30° N there is also a tendency for darker small dots on the opposite side at about 180°–210° N and these may be interpreted as a beginning spalling also on this side of the borehole.*

Table 3-1. The logged borehole sections utilized for interpretation of the stress orientation.

No.	Section depth in borehole [m]	Length [cm]	Orientation of spall centre in borehole wall	Reduction by 180° for all obs. >90°	Comment
	0.65 – 0.70	5			*Not relible orientation, uncertain character.*
	1.50 – 1.58	8			*Influence from drilling possible. Uncertain orientation.*
1	1.64 – 1.70	6	5°	5°	Could be influenced by natural feature?
2	3.05 – 3.08	3	18°	18°	
3	3.24 – 3.33	9	21°	21°	
4	3.33 – 3.52	19	15°	15°	
5	3.52 – 3.67	15	15°	15°	
6	3.84 – 4.03	19	18°	18°	
7	3.96 – 3.97	1	202.5°	22.5°	
8	4.07 – 4.24	17	202.5°	22.5°	
9	4.60 – 4.61	1	39°	39°	Uncertain.
10	4.73 – 4.76	3	39°	39°	Uncertain.
11	4.87 – 4.90	13	207°	27°	
12	5.87 – 5.92	5	170°	–10°	
13	5.93 – 5.98	5	0°	0°	Could be influenced by natural fracture.
	Weighted mean value			17°	

3.6.2 Calculation of influence on stress field from CAPS boreholes

The borehole KQ0048G01 is located too close to the CAPS boreholes to be unaffected in terms of the stress redistribution around these holes. Using a numerical calculation the amount of the influence was estimated. A two-dimensional FLAC model was built where the CAPS Field test 3 boreholes are included. With this analysis the three-dimensional effect from the tunnel itself is assumed negligible compared to the influence from the CAPS boreholes and the analysis is simplified to a two-dimensional question. The boundary stresses are assumed lying in parallel with the axis between the two 485 mm diameter boreholes. The magnitudes and the elastic properties are assumed in accordance with Andersson (2007). The Figure 3-37 shows isocurves of the maximum principal stress and Figure 3-38 shows a close-up at the location of KQ0048G01 (the excavation of the little borehole itself is not simulated) with the stresses in each calculation element shown as stress trajectories.

The FLAC analysis was made under the assumption that the major principal stress direction was applied in the direction perfectly perpendicular to the tunnel axis. This direction is –56° from magnetic north. The influence in orientation of the principal stresses at the location of the borehole KQ0048G01 (red circle in the plot) is 15° anticlockwise from the applied direction at the boundary. Therefore, if we here assume that the breakouts (or spalling) seen are caused by the stress situation prevailing after the CAPS boreholes were drilled (and not even earlier) the maximum in situ stress direction according to the SLITS observation is 17° + 90° + 15° = 122°. This should be compared then to the direction perpendicular to the tunnel which is about 180°–56° = 124°.

If, instead, the real in situ direction is actually slightly inclined from the perpendicular direction to the tunnel (6°) as suggested by Andersson (2007), see Figure 3-39, the influence on the stress orientation at the SLITS borehole would be less than the 15° in the FLAC calculation, say about 9°. The results from the SLITS measurements should then be indicating an in situ maximum stress direction of 17° + 90° + 9° = 116° and this is also comparable to the assumed direction of (124°–6°) = 118° N.

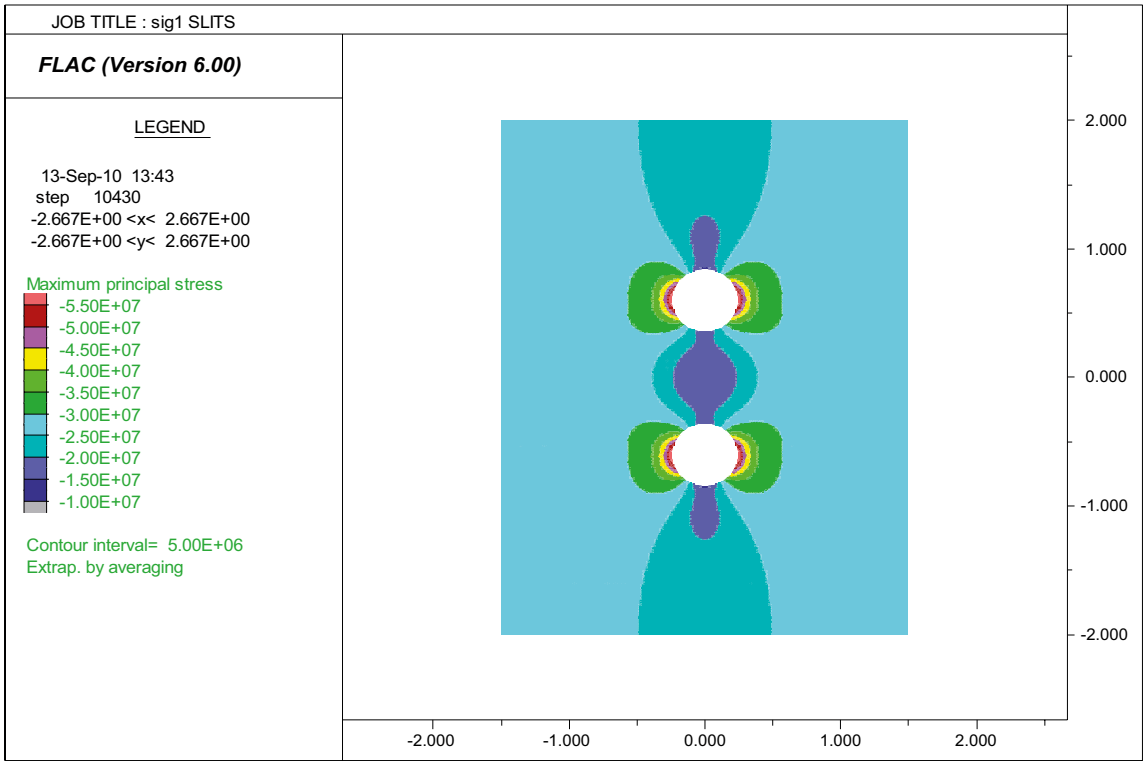

Figure 3-37. Isocurves of maximum principal stress around two excavated boreholes, simulating the situation around the CAPS Test 3 boreholes where the SLITS pilot test borehole is located.

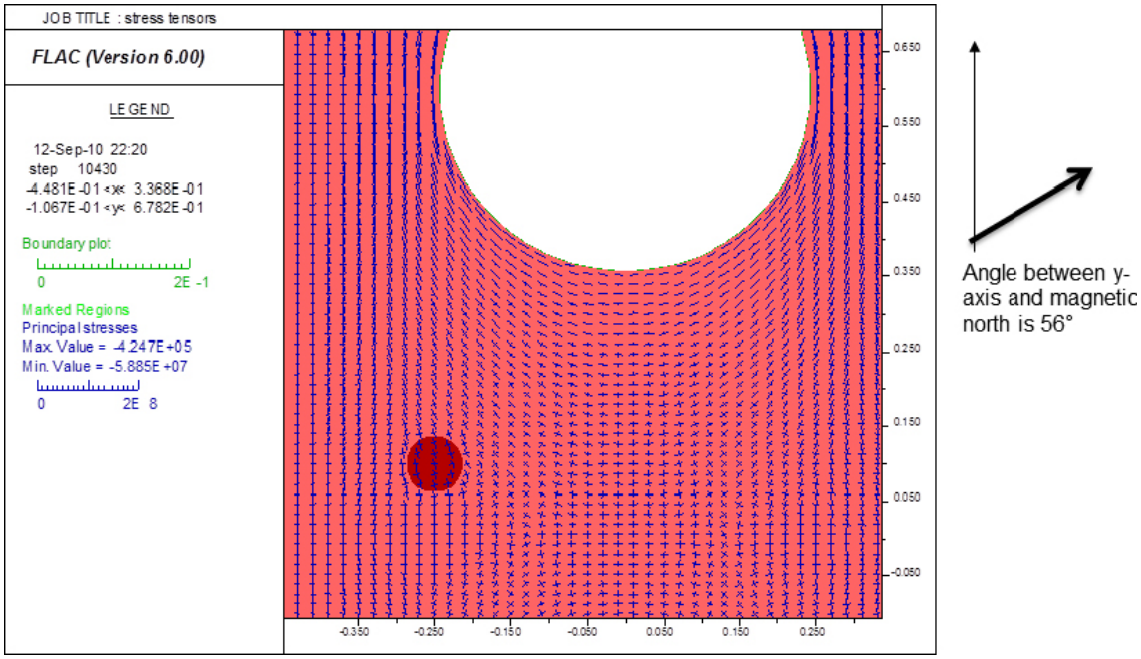

Figure 3-38. *Trajectories of the principal stress around the CAPS heater hole closest to the SLITS borehole (marked in red). The stress magnitudes and orientation in each mesh elements calculated and the influence of the excavated CAPS hole at the location of the SLITS borehole was estimated from these results. At the SLITS borehole the inclination is about 15°.*

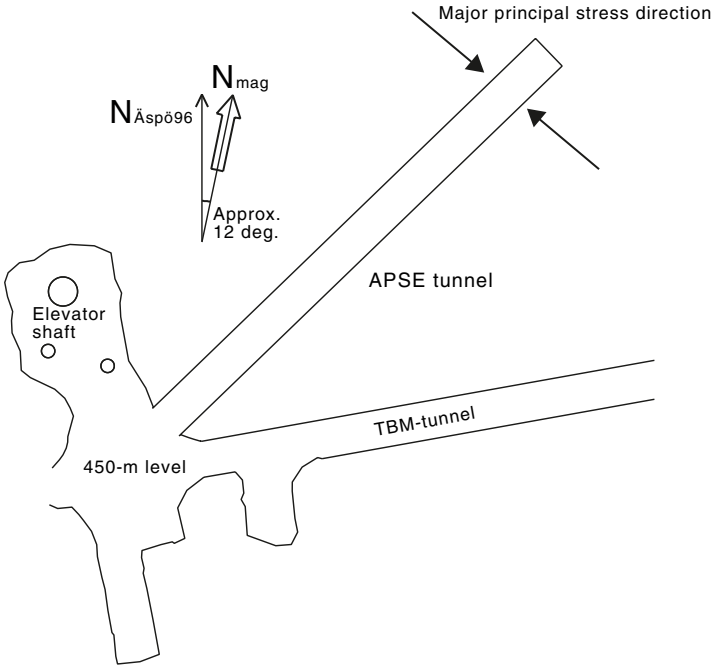

Figure 3-39. *The orientation of the experiment tunnel in relation to the direction of the major principal stress and the relationship between the Äspö-96 coordinate system and magnetic north. From Andersson (2007).*

3.6.3 Comparisons with previous observations at site and in the region

The results from the plot SLITS determination compare well with the observations of stress orientation made through other methods, as seen from the compilation in Table 3-2.

Another comparison which may be made with previous experiences concerns the continuity of the spalling. In the SLITS borehole it may be concluded that only some part of the borehole exhibit spalling behaviour. The explanation to this may be two: the stress values may vary along the hole

and the spalling strength may vary. Concerning the first explanation it is expected that the stress is highes at the top of the borehole, due to the stress increase from the tunnel itself, and that the stressese are lower in the bottom of the hole. This trend is observed to some extent but the upper part of the borehole does not have any spalling. This could in turn possibly be explained by the fact that no heating has been perfomed in the very upper part of the boreholes.

However, a significant part of the variation is also probably explained by the variation in the rock properties. This is accordance with the results seen in the CAPS experiments (Glamheden et al. 2010) and also in laboratory tests on samples from the Q-tunnel (Figure 3-40). The spalling strength is expected to be proportional to the uniaxial compressive strenght (UCS) and the spalling strength should therfore also be varying with the rock mineral variation. According to Martin (2007) the ratio between UCS and the spalling strength is in the order of 0.57, i.e. a rock type with the UCS of about 200 MPa should experience spalling at about 114 MPa tangential stress in the borehole wall. However, this empirical spalling critera is based mainly on observation on larger scale boreholes and tunnels.

Table 3-2. Compilation of selected data on the rock stress orientation in the Äspö Hard Rock Laboratory, in the Q-tunnel where the pilot SLITS test was performed and adjacent locations, for comparison.

Source of data	Orientation of major horizontal in situ stress (mean value if several) In degrees from magnetic north (i.e. not in Äspö coord system)	Reference
APSE, Convergence measurements analysis	118°	Andersson 2007
CAPS, Test 1, Location of spalling	122.5°	Glamheden et al. 2010
CAPS, Test 2, Location of spalling	128.5°	Glamheden et al. 2010
CAPS, Test 3, Location of spalling	127°	Glamheden et al. 2010, see also Section 3.1 in this report
CAPS, Test 4, Location of spalling	127.5°	Glamheden et al. 2010
Mean of 17 breakouts locations in 5 slim boreholes of site invvestigation SDM-Site Laxemar (located in the region of Äspö laboratory)	133.4°	Hakami et al. 2008
Overcoring, Borre probe, KF0093A01	118°	Janson and Stigsson 2002
Overcoring, Borre Probe, KA3579G	113°	Janson and Stigsson 2002
Hydraulic fracturing, KA2599G01	119°	Klee and Rummel 2002
Pilot SLITS, KQ0048G01 (After correction due to secondary stress field)	116°–122°	Section 3.6.1 and 3.6.2 in this report

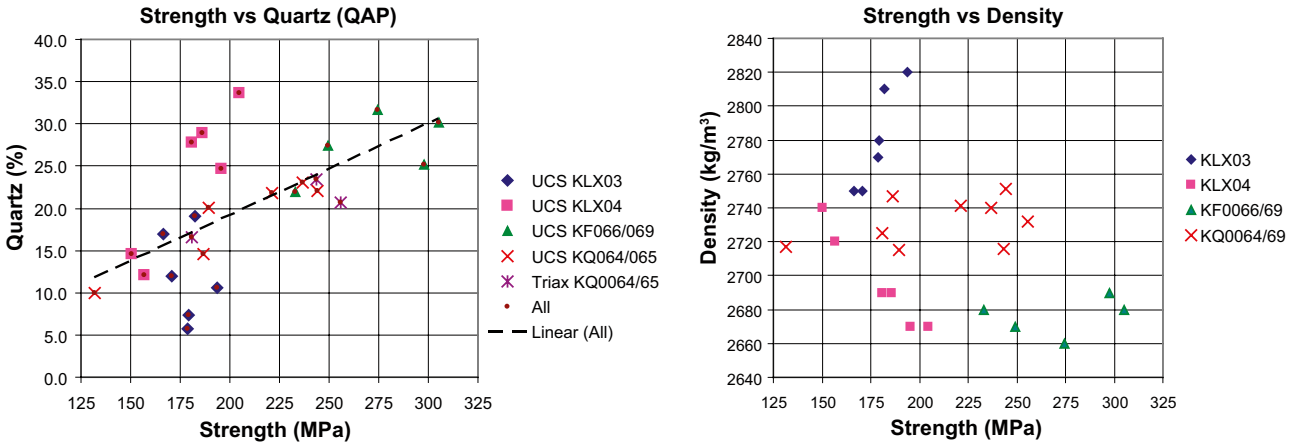

Figure 3-40. *Strength test results on quartz monzodiorite samples from the same tunnel as the pilot SLITS test (KQ Samples), together with other results from the region, showing the variation in strength and the correlation with mineral composition. From Janson et al. (2007).*

4 Field test at ONKALO

4.1 Geological conditions at the site

The pilot test in the Posiva research facility ONKALO was performed in the borehole ONK-PP259, located in the experimental niche POSE (Posiva Spalling Experiment), see Figure 4-1. This borehole was drilled vertically from the tunnel floor at a depth level of –344 m, and the total length is 7.5 m (Figure 4-2). Photos of the drill core from the borehole are provided in Figure 4-3.

The main rock type intersected by the drill holes in the POSE tunnel is pegmatitic granite (PGR) and veined gneiss (VGN). For the borehole ONK-PP259 the division into the different rock types are described in Table 4-1. Further description of the geological conditions at ONKALO is found in Toropainen (2010).

Table 4-1 Geological description of drill core from ONK-PP259 (Toropainen 2010). See also corresponding photographs in Figure 4-3.

M_From	M_To	Rock_Type	Leucosome %	Description
0.00	0.34	Concrete		
0.34	1.13	VGN	20	Moderately banded VGN with sillimanite and cordierite. Lots of cordierite in contact to PGR. Unweathered/ unaltered.
1.13	4.81	PGR		Pale coloured coarse grained PGR with garnet and cordierite. Weak shear bands and microfracturing. Very weak epidotization locally. At 3.80–4.00 m mica bands.
4.81	5.16	VGN	15	Short section of moderately banded VGN. Very weak spotty kaolinitization.
5.16	7.48			Pale coloured coarse grained PGR with garnet and cordierite, locally apatite. Weak shear bands and micro fracturing. Very weak epidotization locally.

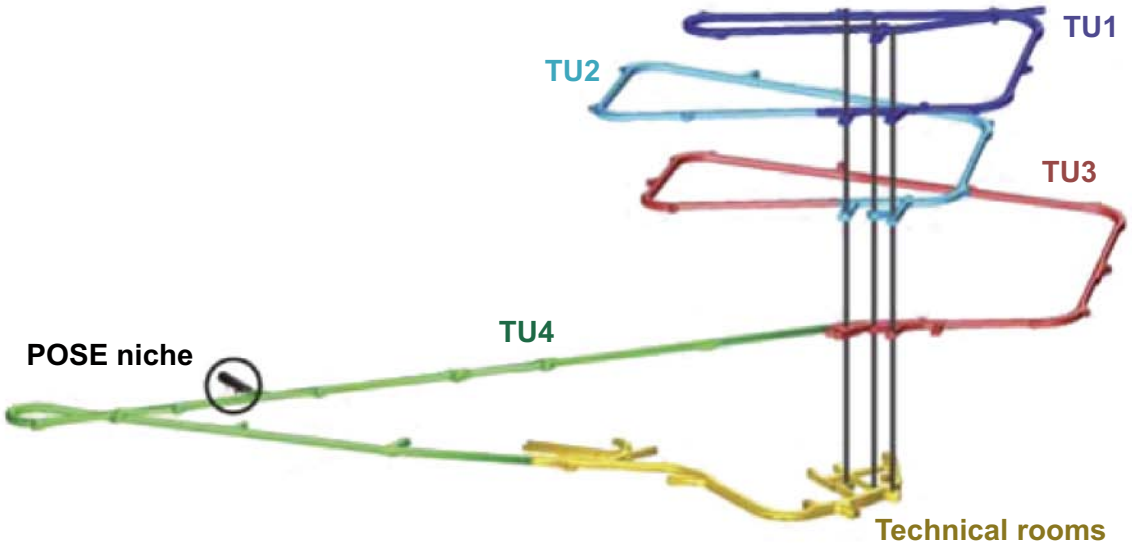

Figure 4-1. *Location of the rock mechanics investigation tunnel (ONK-TKU-3620) at access tunnel chainage 3620 (Siren 2011).*

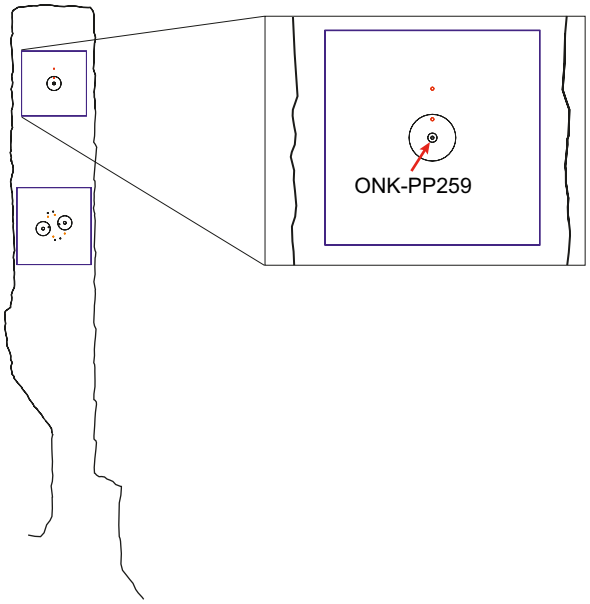

Figure 4-2. *Location of the borehole utilized for the SLITS pilot test at ONKALO, POSE experimental site. The borehole ONK-PP259 is drilled in the centre of the planned larger diameter borehole in the inner part of the tunnel niche.*

Figure 4-3. *Drill core from the borehole (ONK-PP259) used for the pilot SLITS test at ONKALO. The diameter of the core is 83.7 mm (while the diameter of the borehole is 101.3 mm. The upper box includes cores down to 2.31 m depth, the middle box to 4.87 m and the lower box down to the end of hole at 7.48 m depth. The first 0.34 m is concrete in the tunnel floor. (Toropainen 2010).*

4.2 Equipment

4.2.1 Borehole heating equipment

The heating in borehole ONK-PP259 was made using the same heating equipment as was used in the Äspö Hard Rock Laboratory, but the difference was that the fixtures to centralize the heater was adjusted to the larger diameter borehole of 101 mm. The heat effect was increased gradually in four steps, 500 W, 1,000 W, 1,500 W and 2,000 W. During the period with 1,500 W the temperature increased to nearly approximately 130 degrees, in the air of the heated borehole, and after 7 days the effect was increased to 2,000 W. This increased the temperature to 160 degrees in two days. The temperature was more than about 150 degrees in the borehole at least for six days before ending the heating period.

4.2.2 Temperature measurements

The temperatures were measured in two boreholes at a distance from the heated borehole. The distance was 0.5 and 1.5 m, respectively (ONK-PP260 and ONK-PP261, Figure 4-2). No temperature measurement gauge was located inside the heated borehole itself during heating. Using a numerical model for the heat spread in the area a fit of the model against the measured temperatures, the temperature at the borehole was estimated and the thermal stresses induces calculated.

4.2.3 Acoustic televiewer

The acoustic televiewer logging was performed by Suomen Malmi Oy. The probe used is an ABI40 Televiewer (Advanced Logic Technologies). Results are presented in similar way as in the Äspö test. The difference is that that there is no radii result presented and the resolution of the logging is less, 1.4 mm/pixel. In this case there was also no optical logging performed.

4.3 Temperature results

The results of the temperature measurements are given as the dots in the diagram of Figure 4-4. The y-axis in the diagram indicated the temperature increase (not the absolute temperature). Having a starting temperature of 14°, the result indicates that the maximum temperature at the heater borehole wall reached about 70°C.

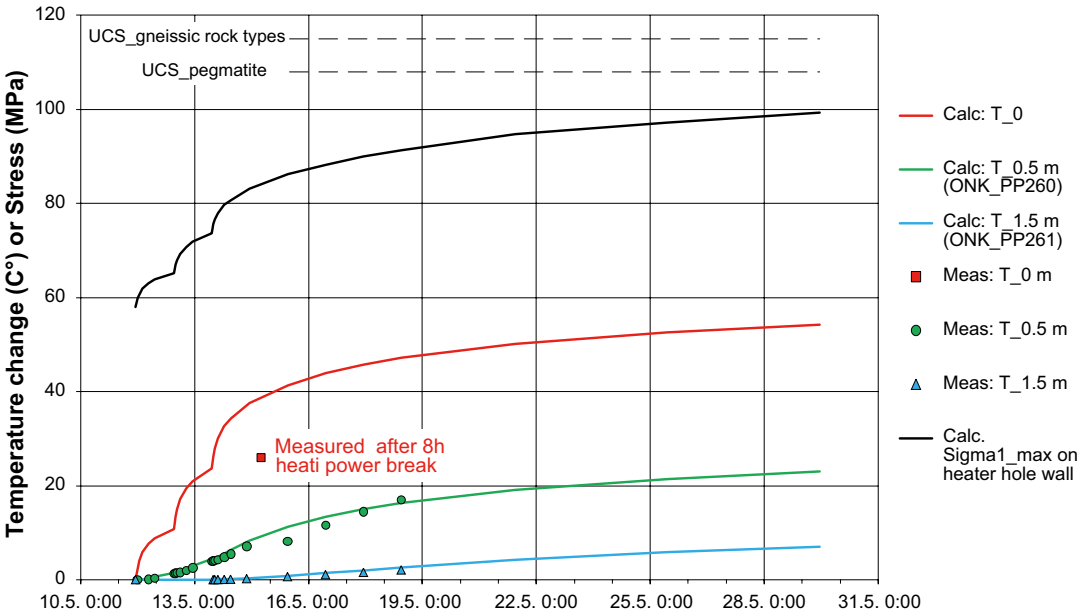

Figure 4-4. *Measured temperatures in boreholes at two different distances from the heating borehole, and calculated temperatures according to the numerical model. No temperature measurements were taken inside the heater holes during the heating. The solid black line indicates the estimated rock stress in the borehole wall (different unit on the y-axis) (Kemppainen, personal communication).*

A numerical model was also used to estimate the tangential stress expected due a thermal expansion of this order. These results are given as the black line in Figure 4-4. The maximum tangential stress after the last heating period is estimated to 100 MPa.

At ONKALO the rock types has a UCS in the order of 110 – 120 MPa (Remes et al. 2009), and since the spalling strength is proposed to be clearly lower (40%–60%) than the UCS (Martin 2007) the thermal load applied was believed to be sufficient to cause some spalling in the borehole wall.

4.4 Logging results

The logging results were presented using WellCad in a similar way as for the acoustic amplitude loggings performed at Äspö. One example section of the results, where the logging before and after the heating periods may be compared is provided in Figure 4-5. It may be concluded that the images are fairly identical, and that there is no clear breakage in the borehole wall, even after the heating. Note that it is the relative colour pattern that should be compared, not the absolute yellow-brown scale value because this value is more sensitive to small changes in measurement conditions, such as how much the instruments deviates from the borehole centre. The complete borehole logging result is given in Appendix E. Studying the images in detail a few difference was found in the pattern before and after heating that was used to estimate stress orientation.

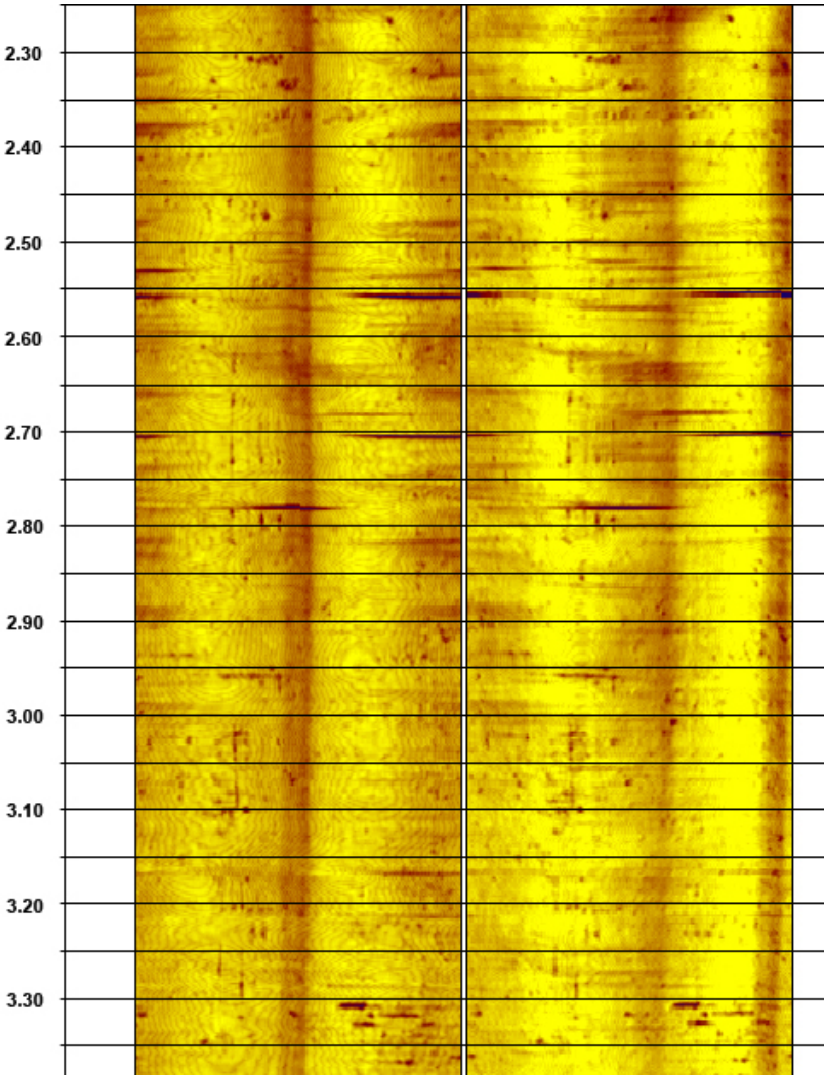

Figure 4-5. *Acoustic televiewer logger result from a ca 1.1 m long section of the borehole ONK-PP259. The left image is the logging before heating and the right image is from logging after. The colour scale indicates the amplitude of the acoustic wave amplitude.*

4.5 Stress orientation results

The determination of interpreted stress orientation was performed in the same manner as described in Section 3.6.1. Three small difference were found in the loggings from before the heating and afterwards, and these locations in the logging results are shown in Figure 4-6. The mean value for the spall location of these three points is 78°. This means that the best estimate of the maximum stress direction from the SLITS pilot test is 168° N, i.e. the major horizontal stress is expected in a direction between N-S and NNW-SSE. There is a minor shift in the orientation of presented logging results between the two logging occasions. In the evaluation it was assumed that the last logging has the best orientation.

4.6 Comparisons with previous measurements at site.

The results from the SLITS pilot test at ONKALO, although the amount of spalling was limited, seem to compare well with the results from other measurements at this site. Based on LVDT measurements during overcoring in the tunnel wall in the investigation niche in the POSE area, the understanding about the stress direction of the time (2010) was that the maximum stress should have an NNW-SSE orientation, about 170°–350°N, see Figure 4-7. The SLITS pilot results are also shown in the diagram for comparison. The average values for the methods compare well.

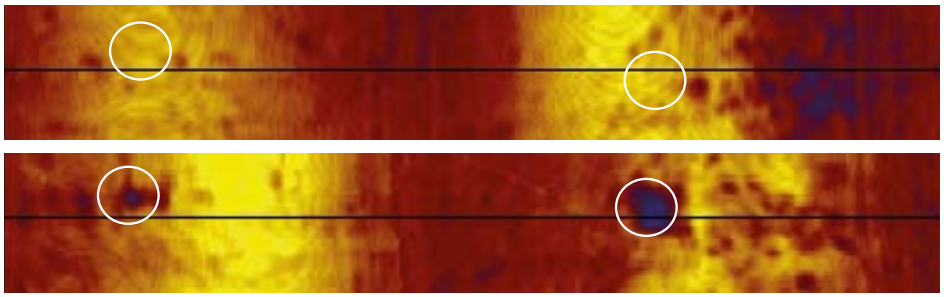

a) 0.7 m depth, ca 247°

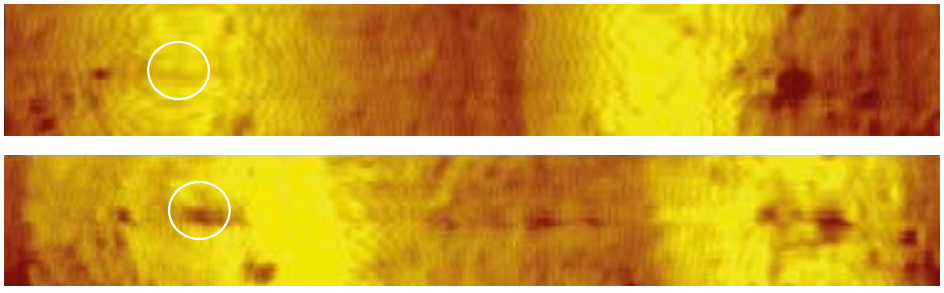

b) 1.1 m depth, ca 78°

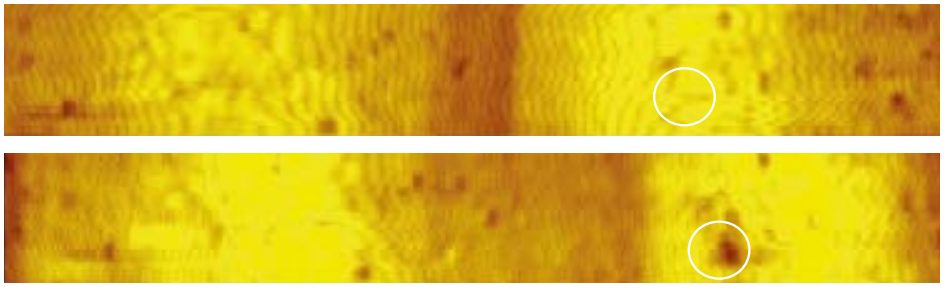

c) 2.0 m depth, ca 270°

Figure 4-6. *Three small differences were observed between the televiewer logger results before (upper image) and after (lower image) the heating periods in the borehole ONK-PP259. (Images show 0°–360° with N to the left.)*

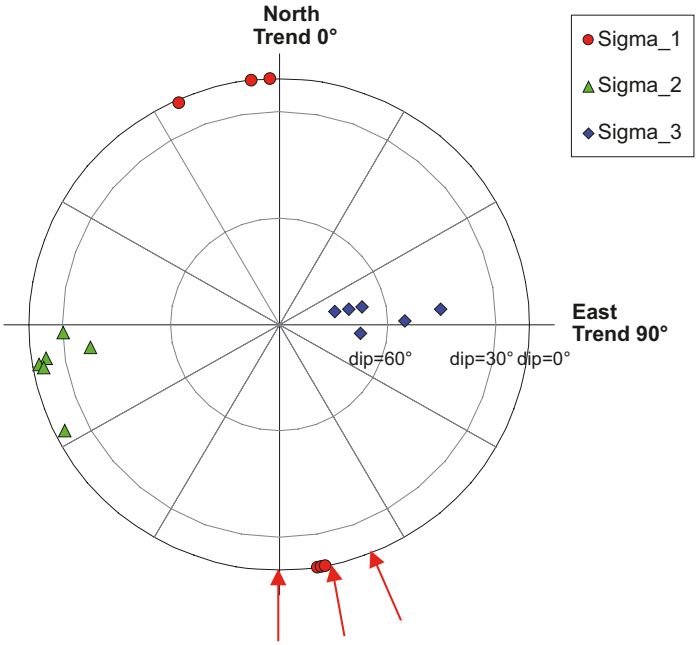

Figure 4-7. *Stress determination results based on LVDT measurement during large diameter short overcorings in the tunnel wall in the POSE site (Kemppainen K 2010, personal communication). The red arrows indicate the stress orientation from the three SLITS indication shown in Figure 4-6.*

5 Conclusions and recommendations

The pilot test with heating in slim boreholes at two different sites as a method to determine stress orientation worked out satisfactory, in view of the fact that the stress orientation interpreted from of the spalls was shown to be the same as the expected orientation based on other measurement methods at both pilot test sites. The spalling observed from the SLITS method indicated an orientation that was consistent and identical to the expected orientation based on other methods. The difference between the average trend from SLITS compared to other methods was less than ten degrees, both at Äspö and ONKALO.

The amount of induced spalls was small and less than what was expected based on empirical spalling strength criterion for tunnels. This may be an indication of different spalling strength for different borehole sizes due to the fact that the induced spalling is in the scale of the mineral grains. There also seems to be a difference in spalling sensitivity between the two sites, where spalling was less in the ONKALO case, probably mainly due to differences in rock type properties.

The time needed for one single measurement using SLITS was in this pilot study about a week, including one logging before and one logging after the heating and the analysis. It is recommended that in future efforts the induced spalling be tested with higher heater effect to increase the thermal load and amount of spalling, and also decrease the time needed for the test. The use of immediate high heating effect, not a stepwise increase, is recommended to further speed up the thermal load around the borehole.

One of the limitations for higher effects is the limit on temperature for the cable connecting the temperature gauges to the heater. The temperature at the cable did reach to fairly high levels in the pilot experiment since the distance to the heater was short. If the rubber cable is connected at a longer distance from the heater the risk for too high temperatures also for measurements at longer distance into boreholes will be eliminated.

The fragments that may fall of during the heating, if fully loosened spalls are developed, could be collected by a devise connected below the heater. In this way, having a continuous collection of fragments from the specific heated borehole section, the point of time when spalling occur may be readily detected. This time span may be useful to assess spalling properties of the rock.

A standardized (i.e. fully repeatable) measurement procedure would be beneficial in that it would enable direct comparisons and assessment of differences in spall potential between different points. Such comparisons could be used to indicate potential variation in the prediction for thermal spalling in the deposition holes, and also increase the possibilities to use SLITS measurements for estimation of stress magnitudes, not only stress orientations.

The interpretation in the pilot experiment was naturally fairly time consuming, as the method as such was also developed during the course of the project. However, if this method is to be used in several or longer sections, procedures for fast identification and interpretation of the spall locations from the logger results can be developed.

Since the experience from site investigations is that there may be small spalls or breakouts in the small diameter (76 mm) investigation boreholes also without the heating, possibly partly induced by the local heat developing during the drilling of the borehole, the potential for purposely using the drilling equipment to obtain high temperatures and inducing breakouts while drilling, may also be investigated.

In the pilot tests two different rock types were involved, a medium grained monzodiorite and a weaker fine grained anisotropic gneiss, and there was indication of differences in results that might be explained by the difference in the rock properties. Further tests in other rock types are recommended if the robustness of the SLITS method as a general method is to be evaluated.

6 References

SKB's (Svensk Kärnbränslehantering AB) publications can be found at www.skb.se/publications.

Andersson C J, 2007. Äspö Hard Rock Laboratory. Äspö Pillar Stability Experiment, Final report. Rock mass response to coupled mechanical thermal loading. SKB TR-07-01, Svensk Kärnbränslehantering AB.

Ask D, Ask M V S, 2007. Forsmark site investigation. Detection of potential borehole breakouts in boreholes KFM01A and KFM01B. SKB P-07-235, Svensk Kärnbränslehantering AB.

Glamheden R, Lanaro F, Karlsson J, Lindberg U, Wrafter J, Hakami H, Johansson M, 2008. Rock mechanics Forsmark. Modelling stage 2.3. Complementary analysis and verification of the rock mechanics model. SKB R-08-66, Svensk Kärnbränslehantering AB.

Glamheden R, Fälth B, Jacobsson L, Harrström J, Berglund J, Bergkvist L, 2010. Counterforce applied to prevent spalling. SKB TR-10-37, Svensk Kärnbränslehantering AB.

Hakami E, Fredriksson A, Lanaro F, Wrafter J, 2008. Rock mechanics Laxemar. Site descriptive modelling, SDM-Site Laxemar. SKB R-08-57, Svensk Kärnbränslehantering AB.

Janson T, Stigsson M, 2002. Test with different stress measurement methods in two orthogonal bore holes in Äspö HRL. SKB R-02-26, Svensk Kärnbränslehantering AB.

Janson T, Ljunggren B, Bergman T, 2007. Oskarshamn site investigation. Modal analyses on rock mechanical specimens. Specimens from borehole KLX03, KLX04, KQ0064G, KQ0065G, KF0066A and KF0069A. SKB P-07-03, Svensk Kärnbränslehantering AB.

Klee G, Rummel F, 2002. Äspö Hard Rock Laboratory. Rock stress measurements in the Äspö HRL. Hydraulic fracturing in boreholes KA2599G01 and KF0093A01. SKB IPR-02-02, Svensk Kärnbränslehantering AB

Martin C D, 2007. Quantifying in situ stress magnitudes and orientations for Forsmark. Forsmark stage 2.2. SKB R-07-26, Svensk Kärnbränslehantering AB.

Remes H, Kuula H, Somervuori P, Hakala M, 2009. ONKALO Rock Mechanics Model (RMM), version 1.0. Posiva Working Report 2009-55, Posiva Oy, Finland.

Ringgaard J, 2007. Mapping of borehole breakouts. Processing of acoustical televiewer data from KFM01A, KFM01B, KFM02A, KFM03A, KFM04A, KFM05A, KFM06A and KFM07C. SKB P-07-07, Svensk Kärnbränslehantering AB.

Siren T, 2011. Fracture mechanics prediction for Posiva's Olkiluoto Spalling Experiment (POSE). Posiva working report 2011-23, Posiva Oy, Finland.

SKB, 2009. Underground design Forsmark. Layout D2. SKB R-08-116, Svensk Kärnbränslehantering AB.

Staub I, Andersson J C, Magnor B, 2004. Äspö Pillar Stability Experiment. Geology and mechanical properties of the rock in TASQ. SKB R-04-01, Svensk Kärnbränslehantering AB.

Toropainen V, 2010. ONKALO Pose experiment – core drilling of drillholes ONK-PP223...226, ONK-PP253...261 and ONK-PP268...272 in ONKALO at Olkiluoto 2009–2010. Posiva Working Report 2010-86, Posiva Oy, Finland.

Optical loggings in KQ0048G01

Appendix A

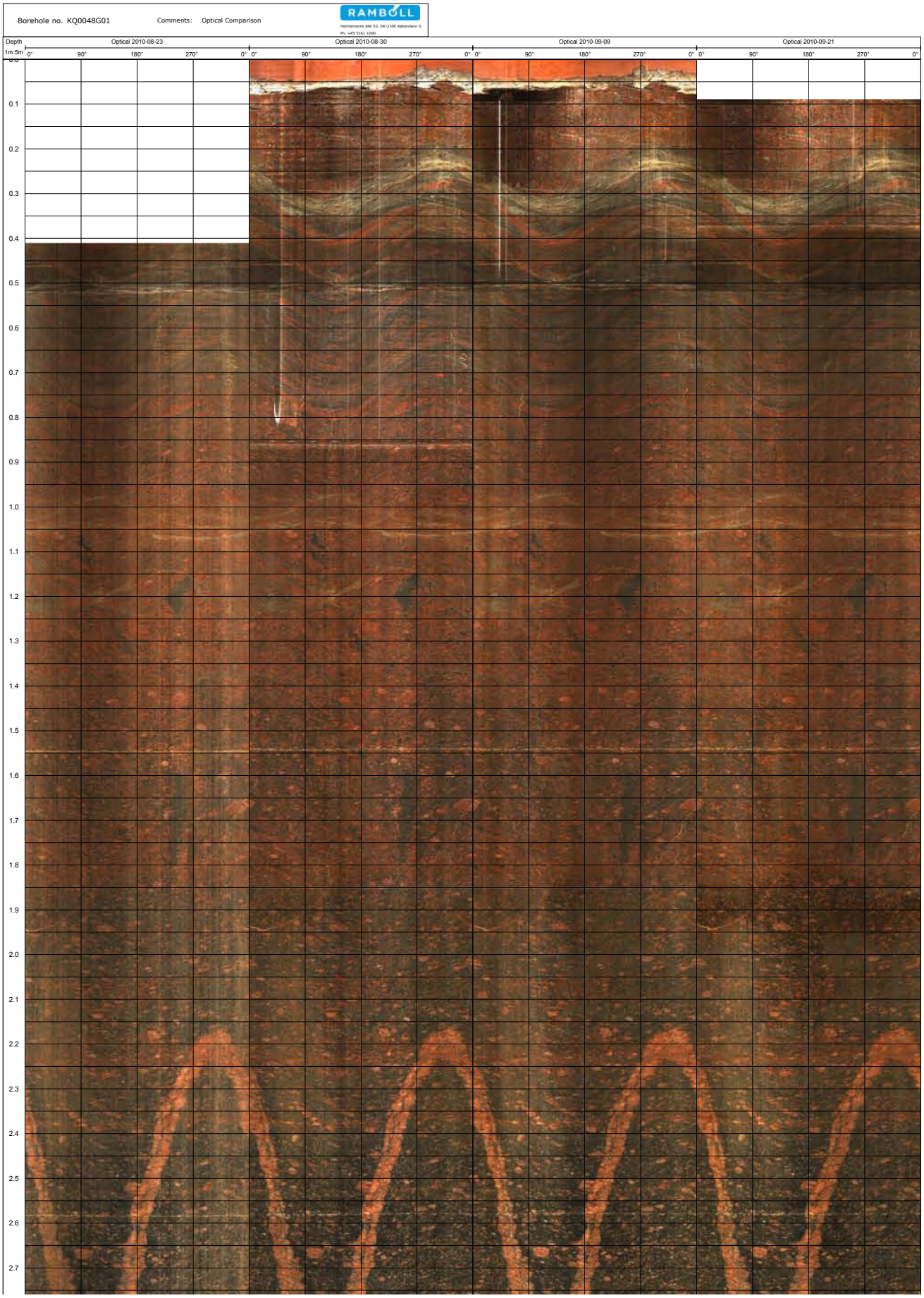

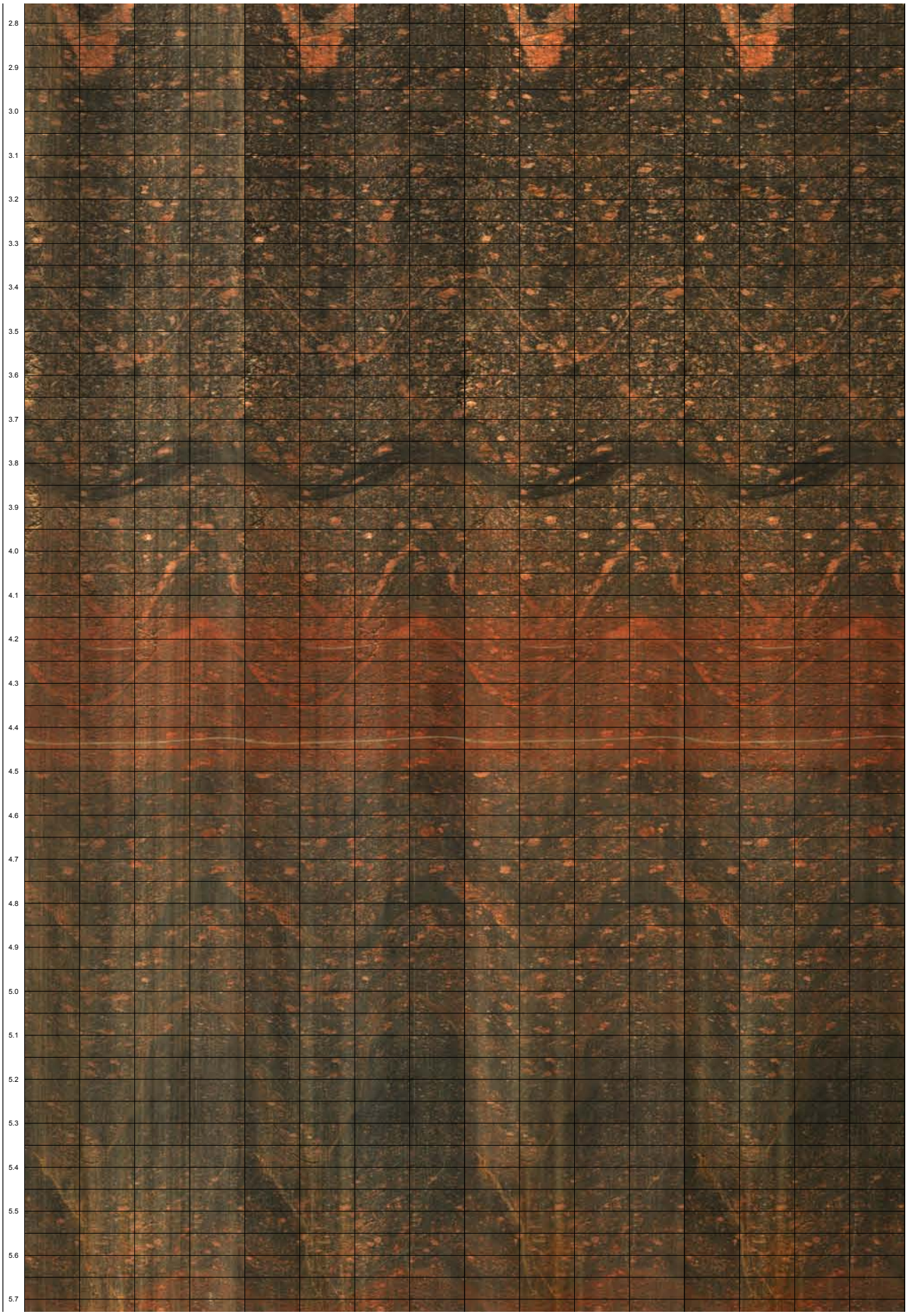
2.8
2.9
3.0
3.1
3.2
3.3
3.4
3.5
3.6
3.7
3.8
3.9
4.0
4.1
4.2
4.3
4.4
4.5
4.6
4.7
4.8
4.9
5.0
5.1
5.2
5.3
5.4
5.5
5.6
5.7

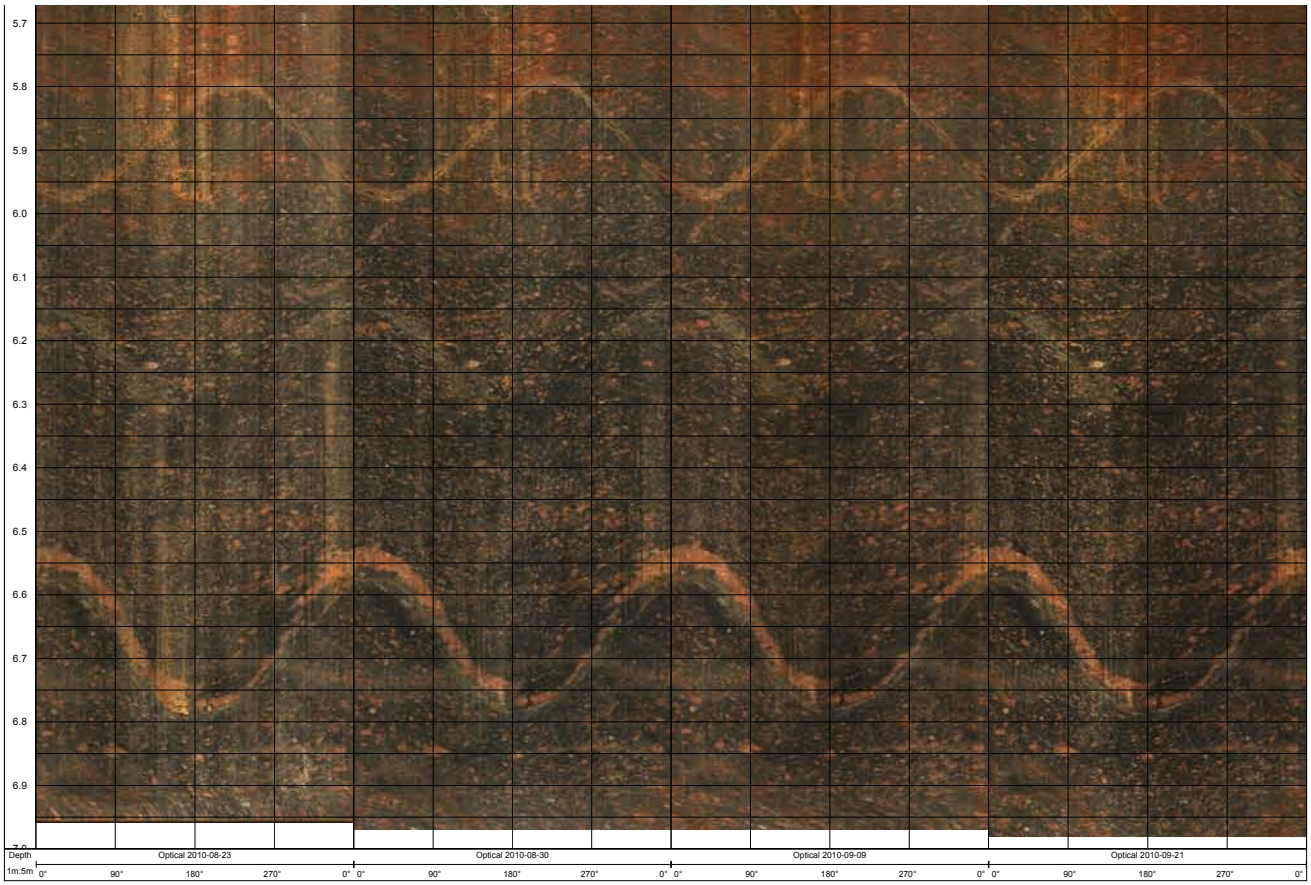
5.7
5.8
5.9
6.0
6.1
6.2
6.3
6.4
6.5
6.6
6.7
6.8
6.9
Depth
1m:5m
Optical 2010-08-23
Optical 2010-08-30
Optical 2010-09-09
Optical 2010-09-21
0° 90° 180° 270° 0° 0° 90° 180° 270° 0° 0° 90° 180° 270° 0° 0° 90° 180° 270° 0°

Amplitude measurements

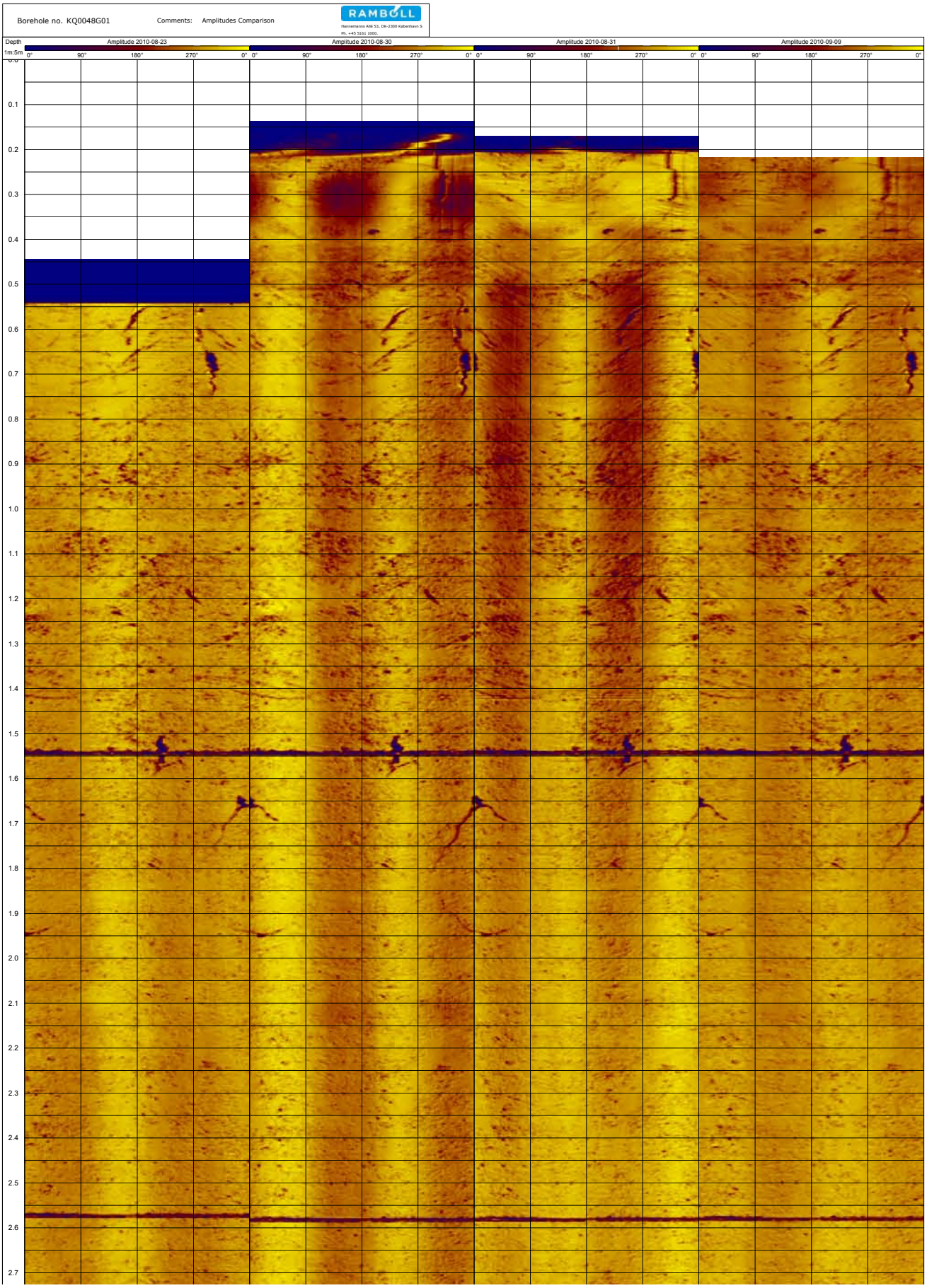

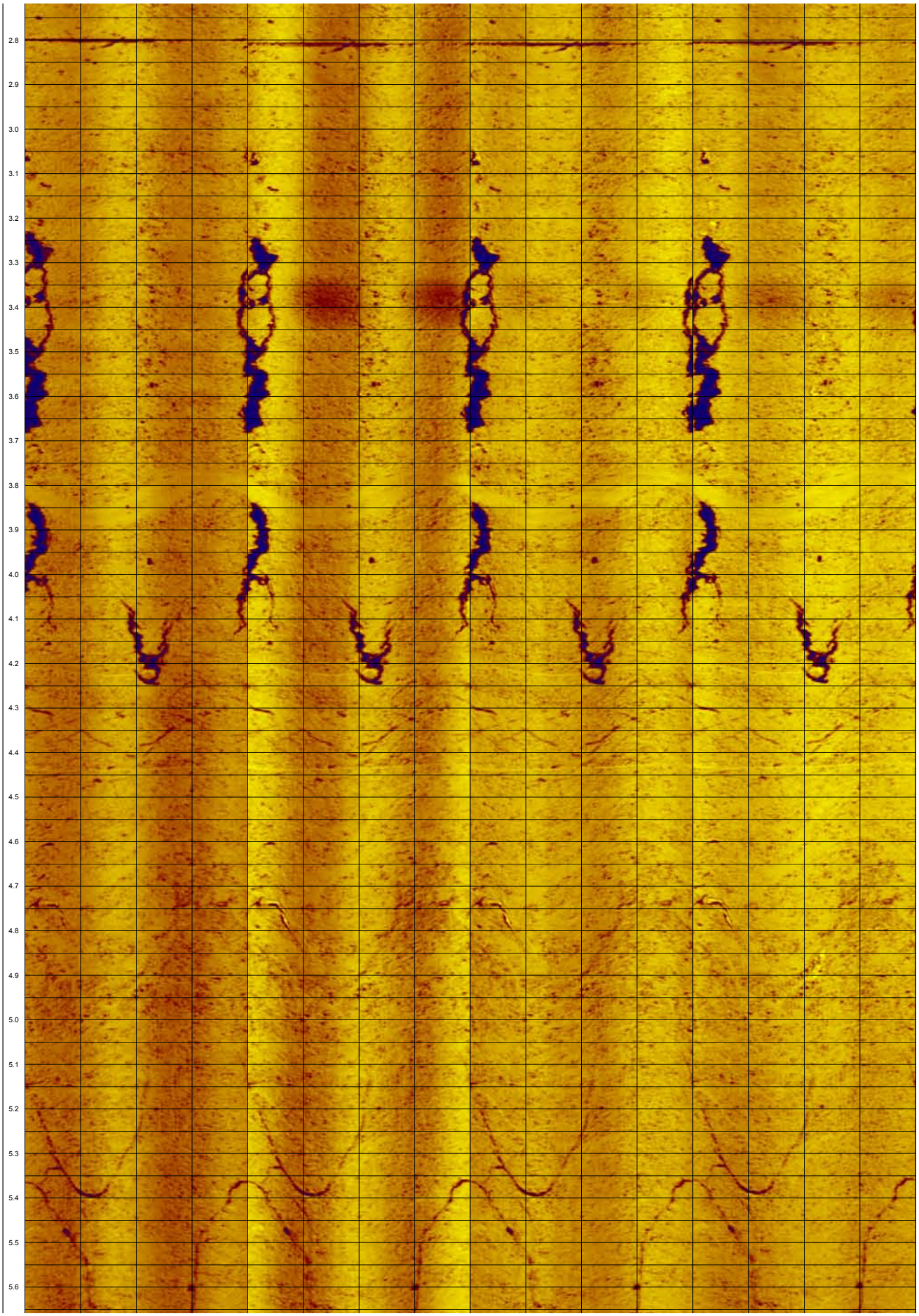
2.8
2.9
3.0
3.1
3.2
3.3
3.4
3.5
3.6
3.7
3.8
3.9
4.0
4.1
4.2
4.3
4.4
4.5
4.6
4.7
4.8
4.9
5.0
5.1
5.2
5.3
5.4
5.5
5.6

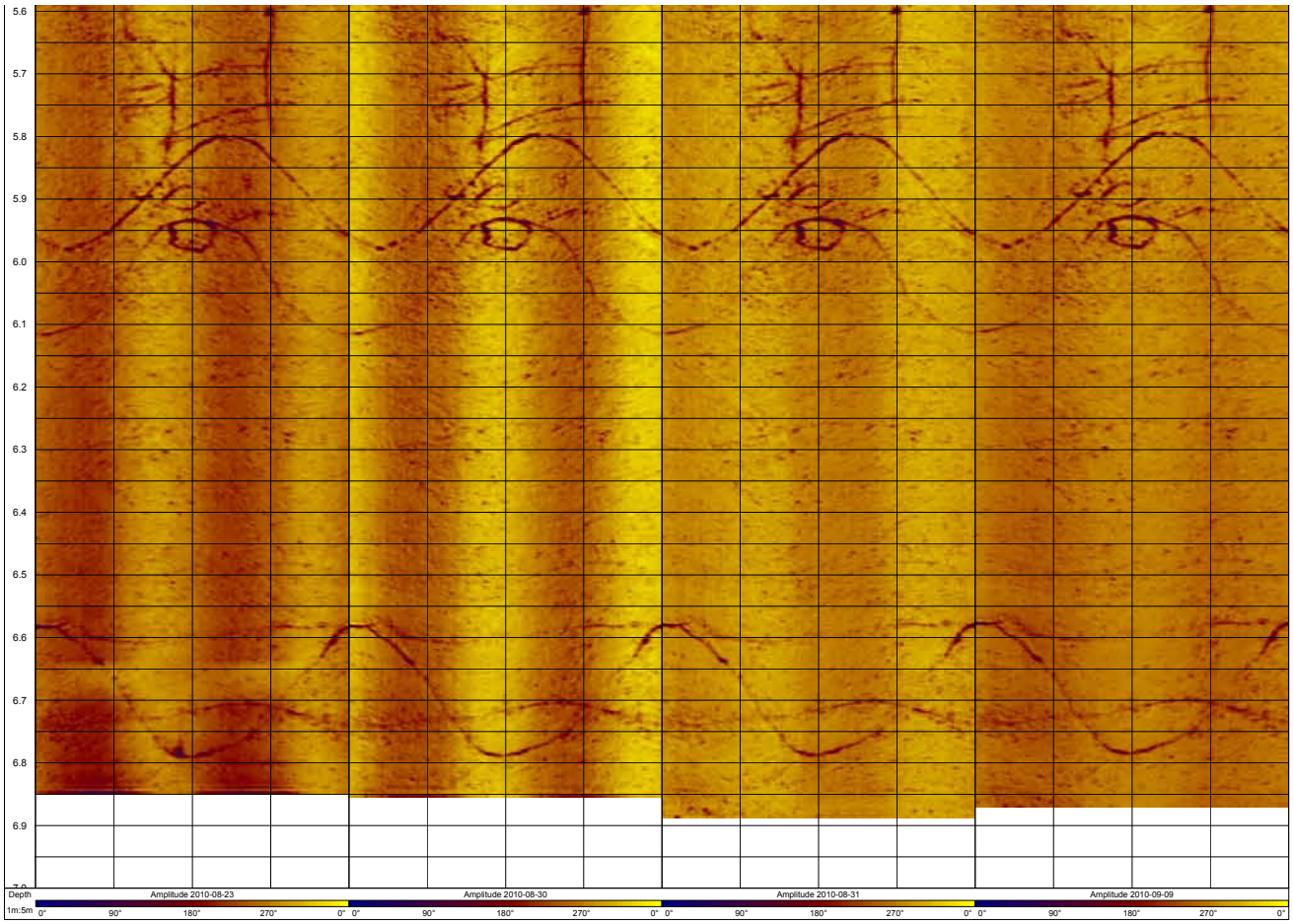
5.6
5.7
5.8
5.9
6.0
6.1
6.2
6.3
6.4
6.5
6.6
6.7
6.8
6.9
Depth
1m:5m
Amplitude 2010-08-23
Amplitude 2010-08-30
Amplitude 2010-08-31
Amplitude 2010-09-09
0°
90°
180°
270°
0°

Radii measurement comparison between stages

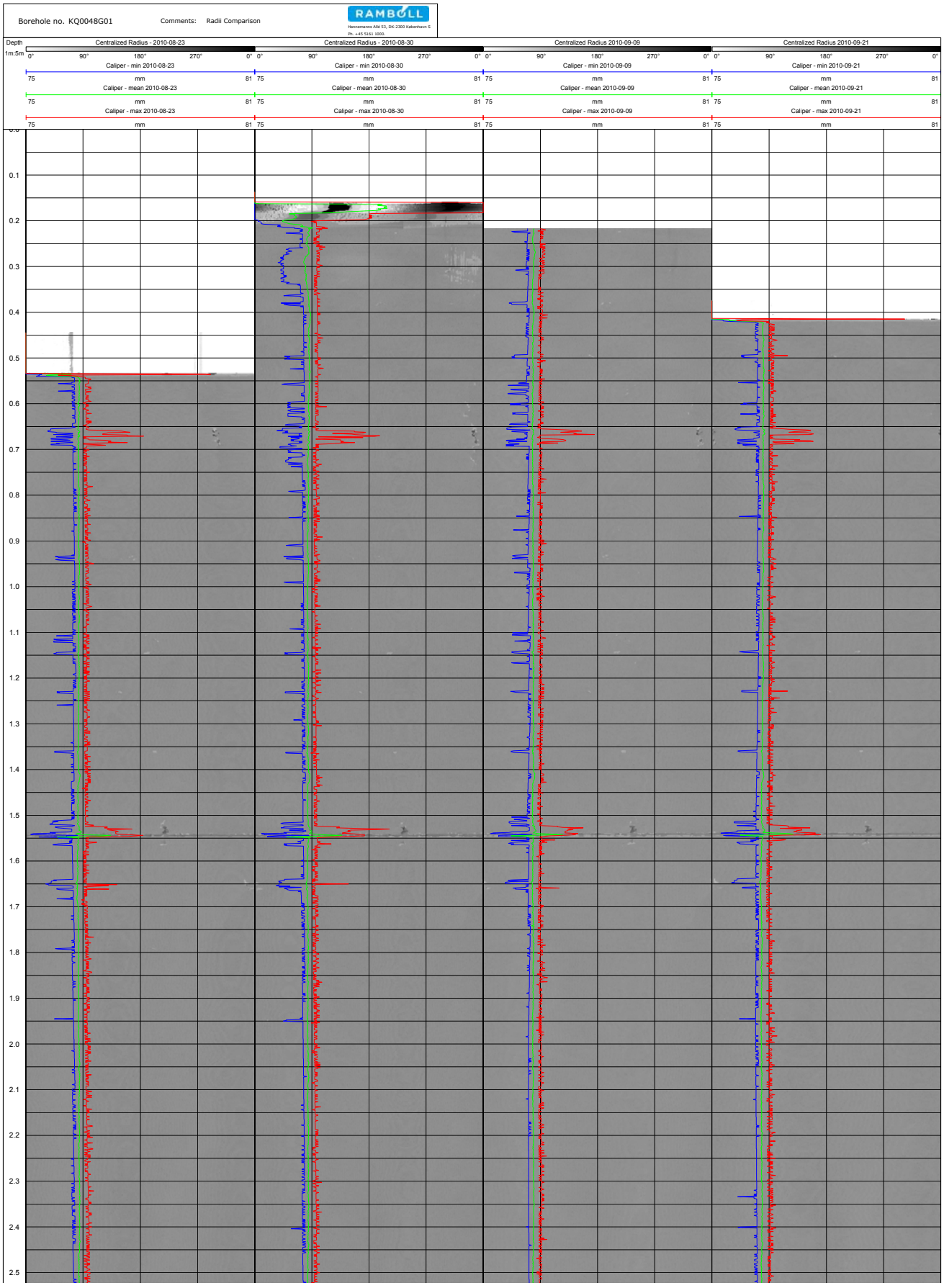

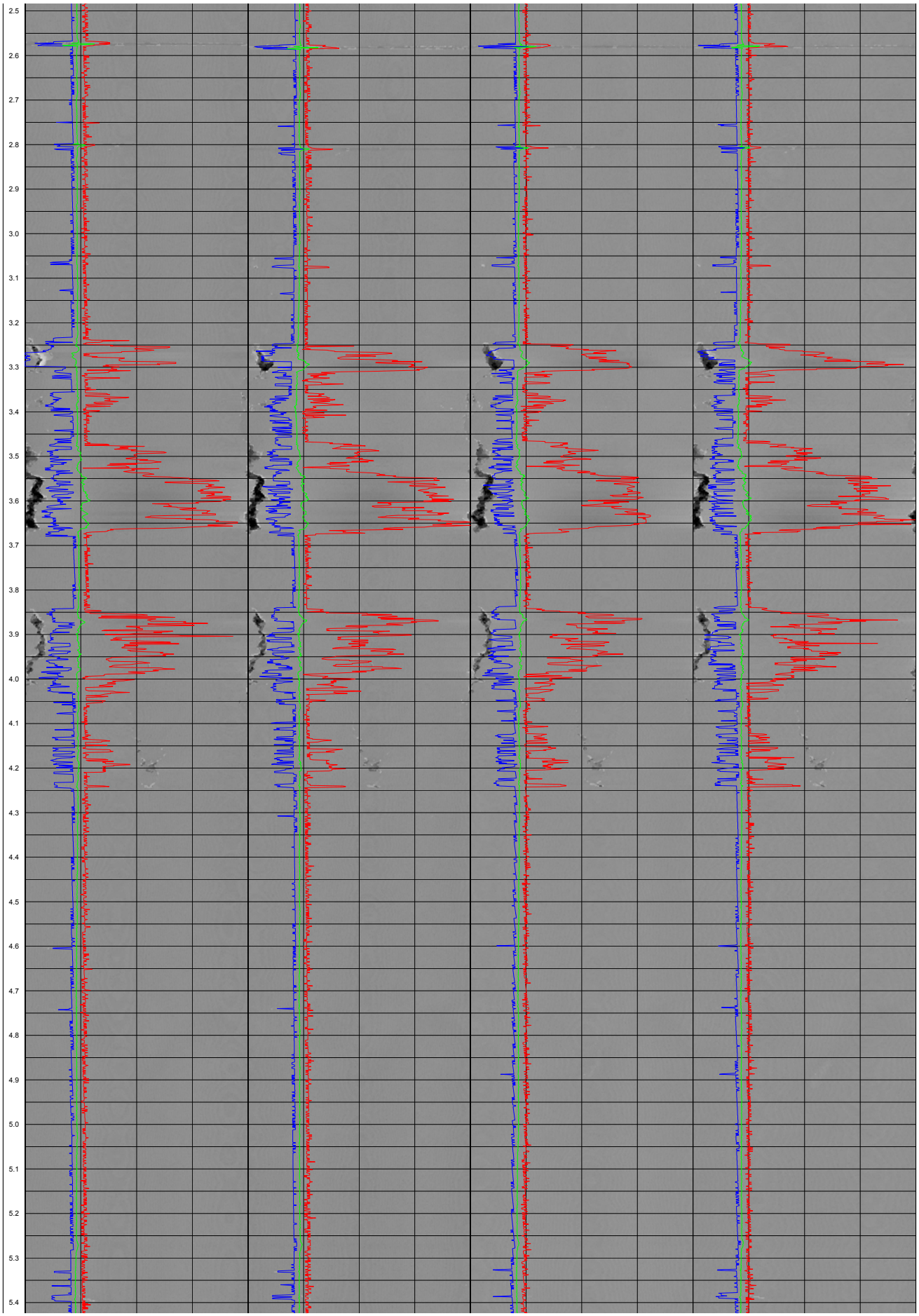
2.5
2.6
2.7
2.8
2.9
3.0
3.1
3.2
3.3
3.4
3.5
3.6
3.7
3.8
3.9
4.0
4.1
4.2
4.3
4.4
4.5
4.6
4.7
4.8
4.9
5.0
5.1
5.2
5.3
5.4

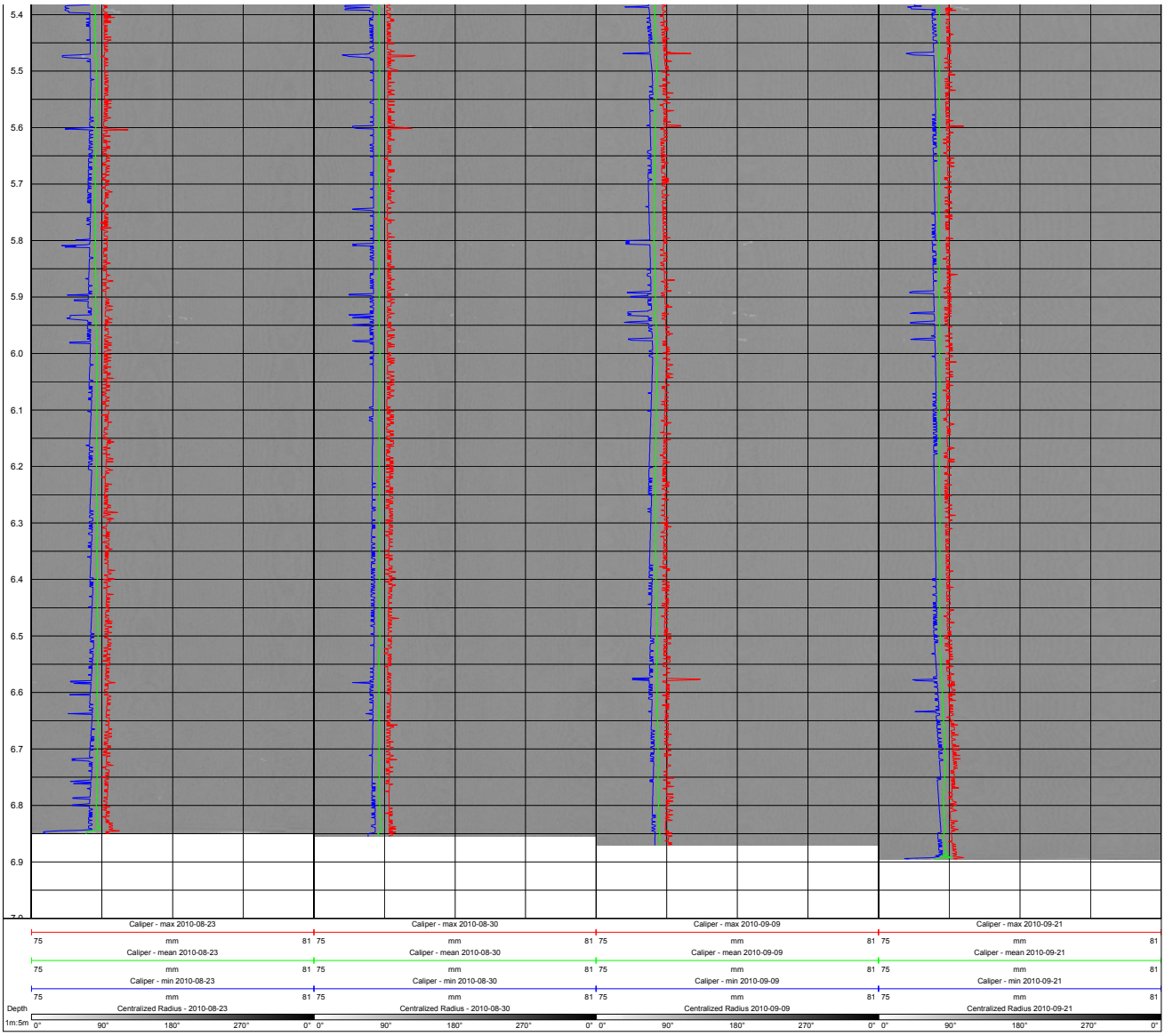
5.4
5.5
5.6
5.7
5.8
5.9
6.0
6.1
6.2
6.3
6.4
6.5
6.6
6.7
6.8
6.9
Caliper - max 2010-08-23
Caliper - max 2010-08-30
Caliper - max 2010-09-09
Caliper - max 2010-09-21
75 mm 81
Caliper - mean 2010-08-23
Caliper - mean 2010-08-30
Caliper - mean 2010-09-09
Caliper - mean 2010-09-21
Caliper - min 2010-08-23
Caliper - min 2010-08-30
Caliper - min 2010-09-09
Caliper - min 2010-09-21
Centralized Radius - 2010-08-23
Centralized Radius - 2010-08-30
Centralized Radius 2010-09-09
Centralized Radius 2010-09-21
Depth
1m:5m
0° 90° 180° 270° 0°

Logging results from all three methods after last heating in KQ0048G01

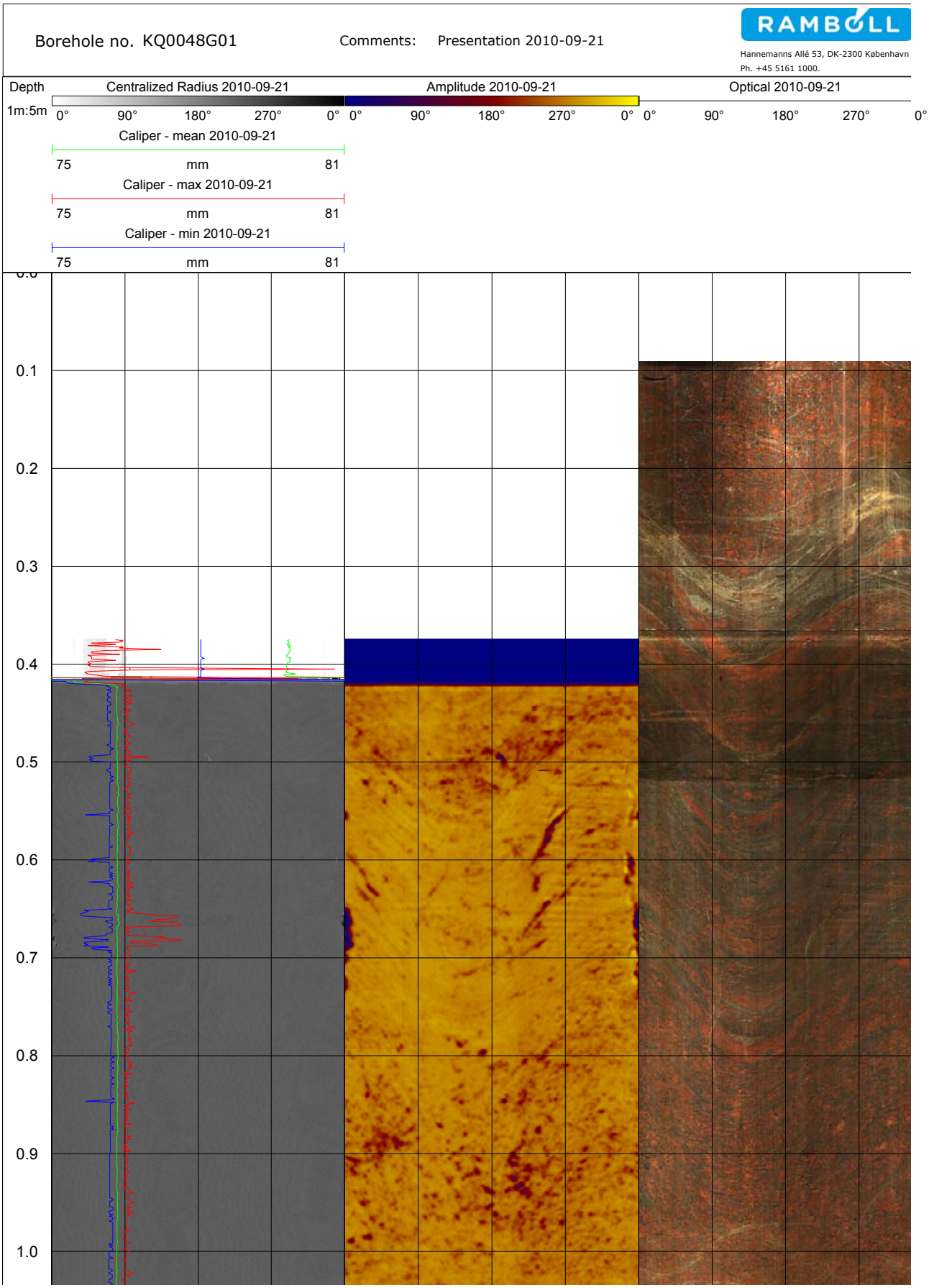

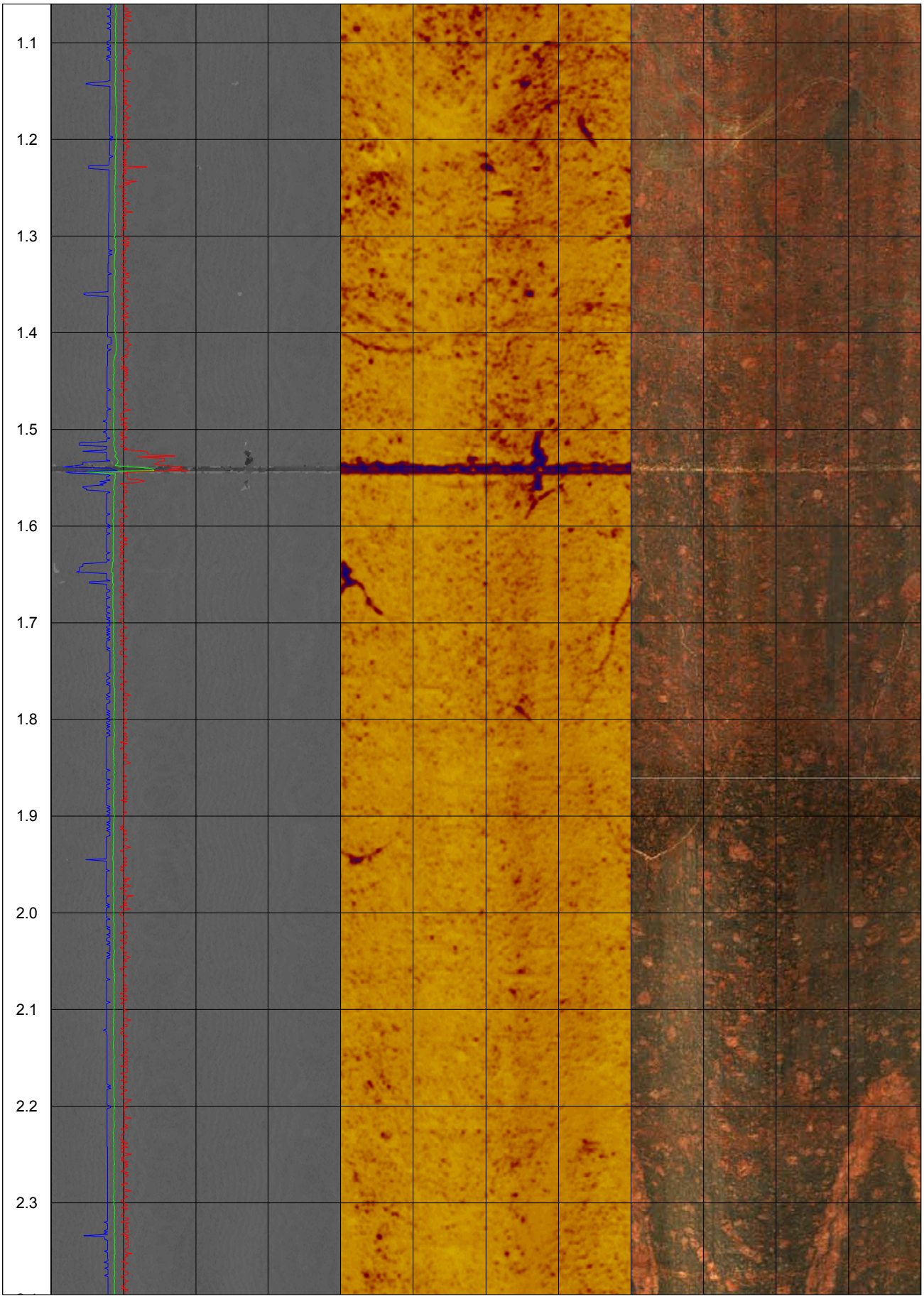
1.1
1.2
1.3
1.4
1.5
1.6
1.7
1.8
1.9
2.0
2.1
2.2
2.3

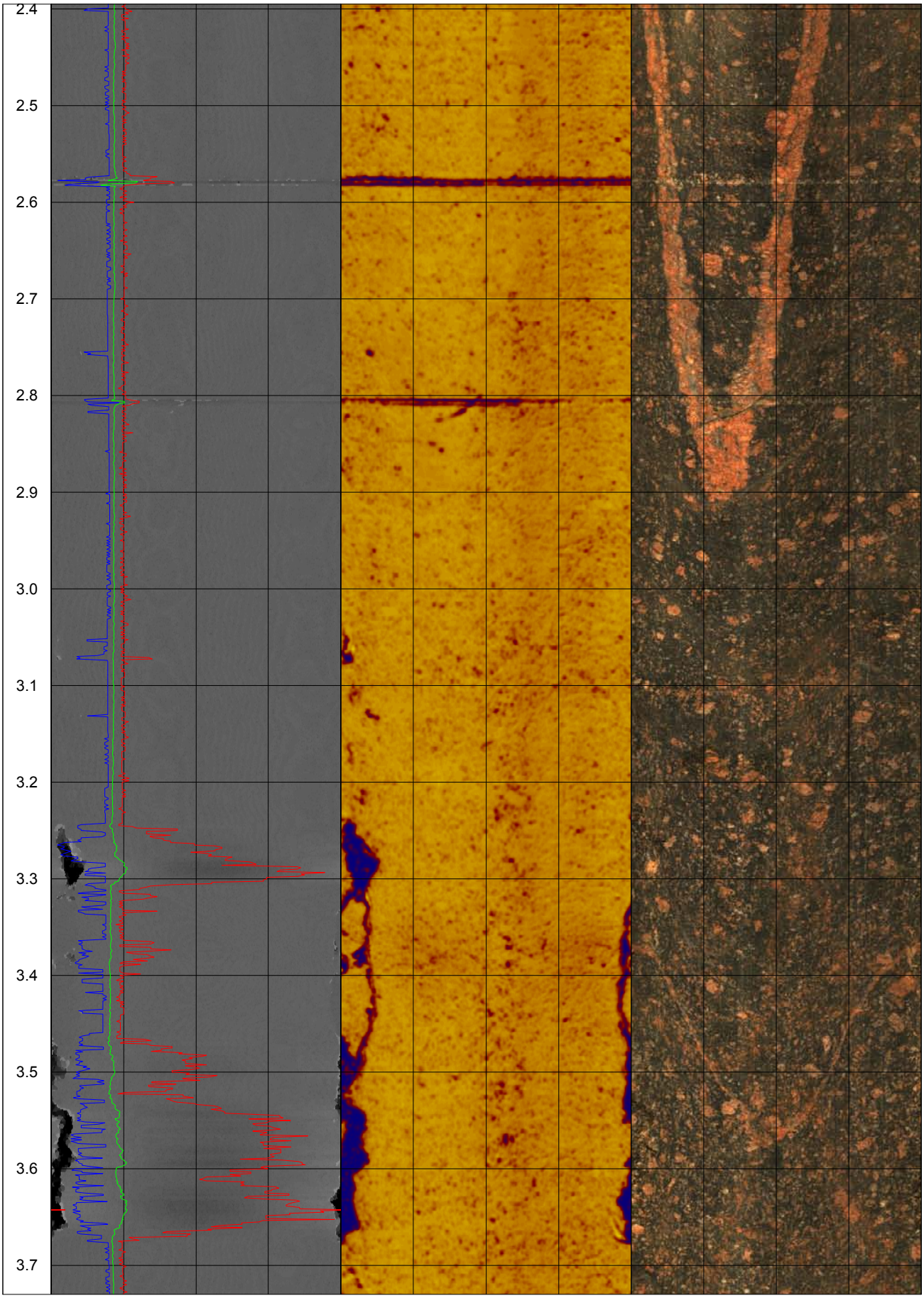
2.4
2.5
2.6
2.7
2.8
2.9
3.0
3.1
3.2
3.3
3.4
3.5
3.6
3.7

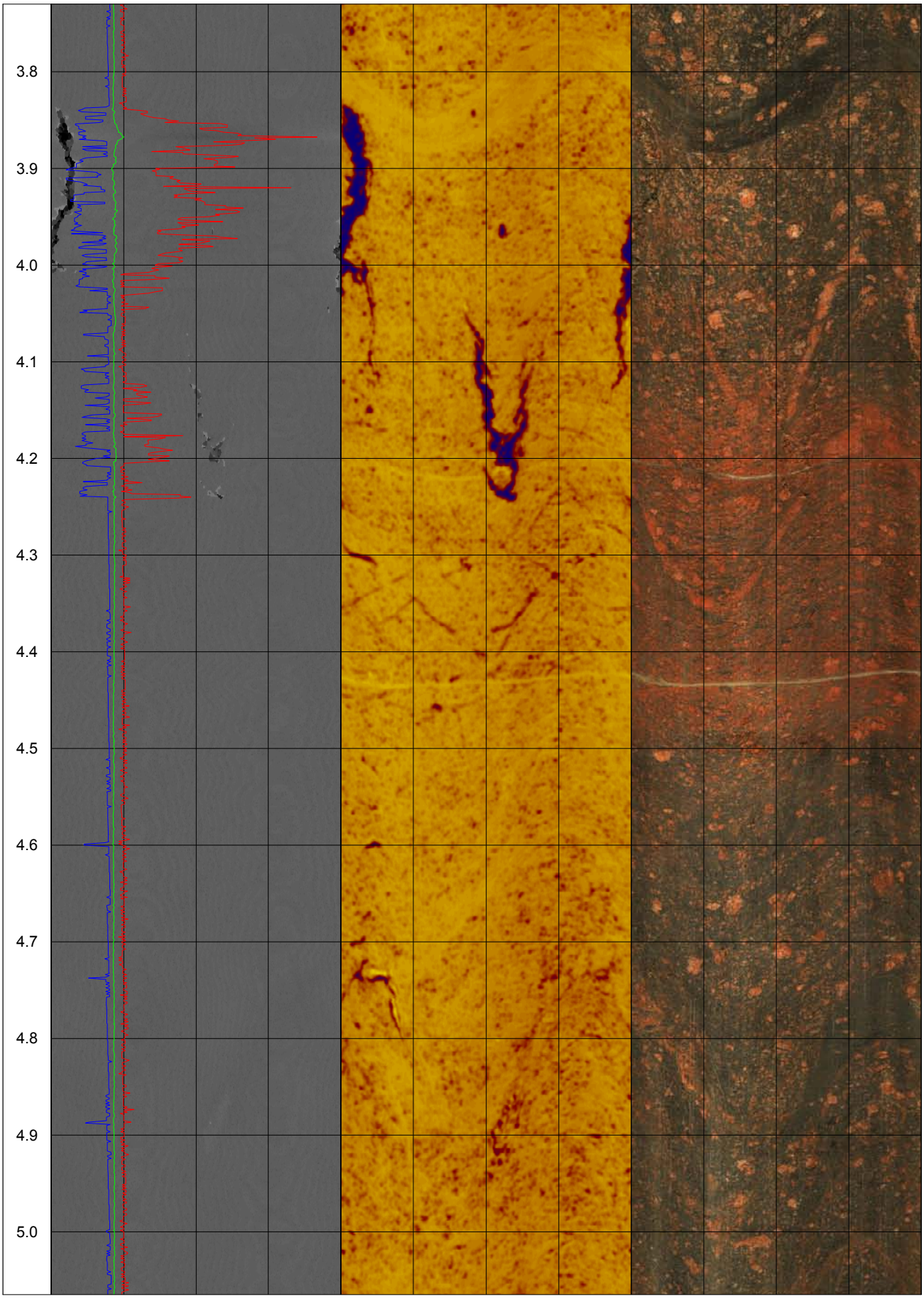
3.8
3.9
4.0
4.1
4.2
4.3
4.4
4.5
4.6
4.7
4.8
4.9
5.0

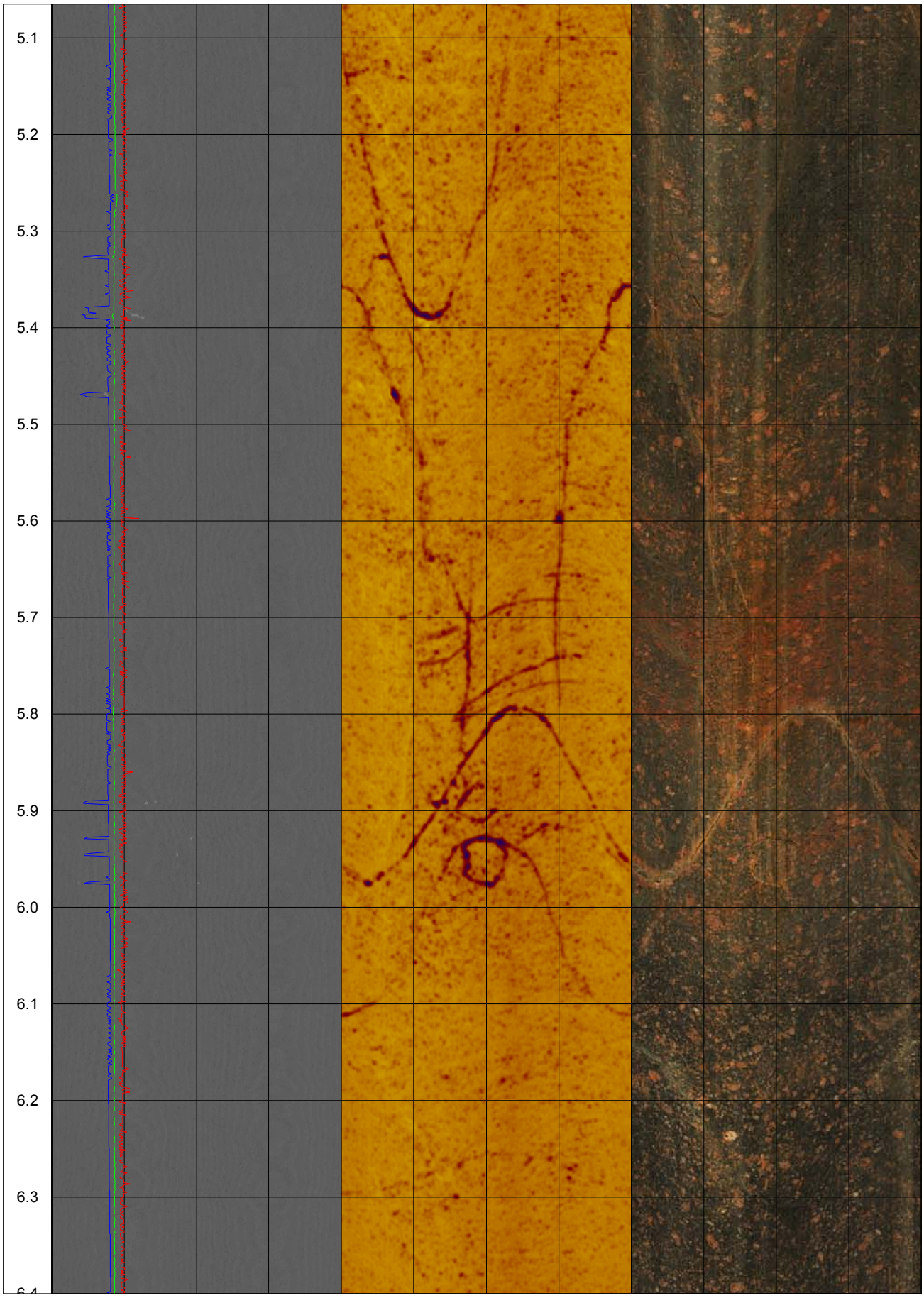
5.1
5.2
5.3
5.4
5.5
5.6
5.7
5.8
5.9
6.0
6.1
6.2
6.3

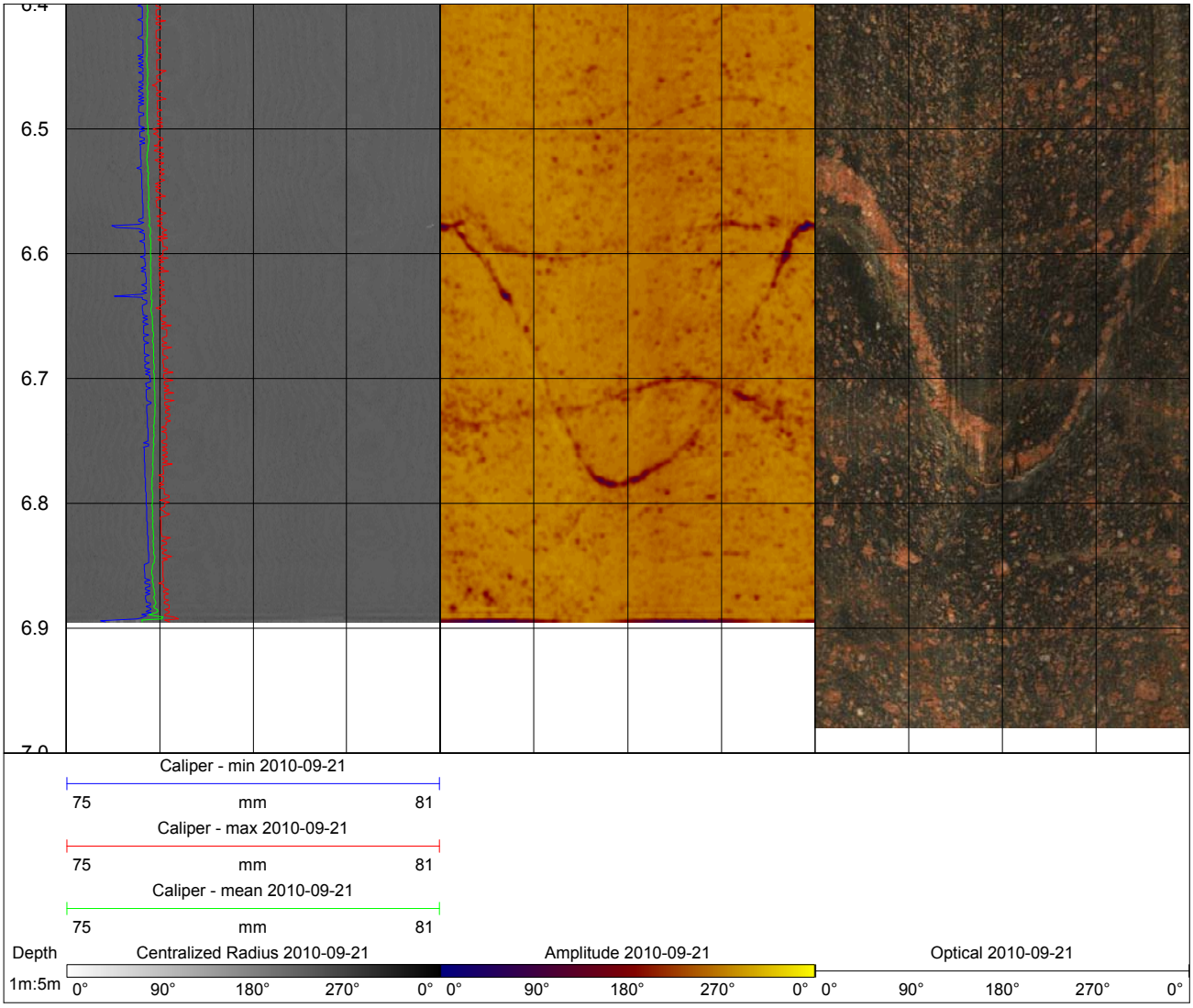
6.5
6.6
6.7
6.8
6.9
Caliper - min 2010-09-21
75
mm
81
Caliper - max 2010-09-21
75
mm
81
Caliper - mean 2010-09-21
75
mm
81
Depth
1m:5m
Centralized Radius 2010-09-21
0°
90°
180°
270°
0°
Amplitude 2010-09-21
0°
90°
180°
270°
0°
Optical 2010-09-21
0°
90°
180°
270°
0°

Client: Posiva	**Hole no:** ONK-PP259	**Ø:** 101 mm	**Surveyed by:** HL
Site: Olkiluoto	**X:** 6792336.67	**Length:** 7.48	**Survey date:** 4.5.2010
Project no: 9252-10	**Y:** 1525463.51	**Azimuth:** 0.0	**Reported by:** AT
	Z: -351.930	**Dip:** 90.0	**Report date:**

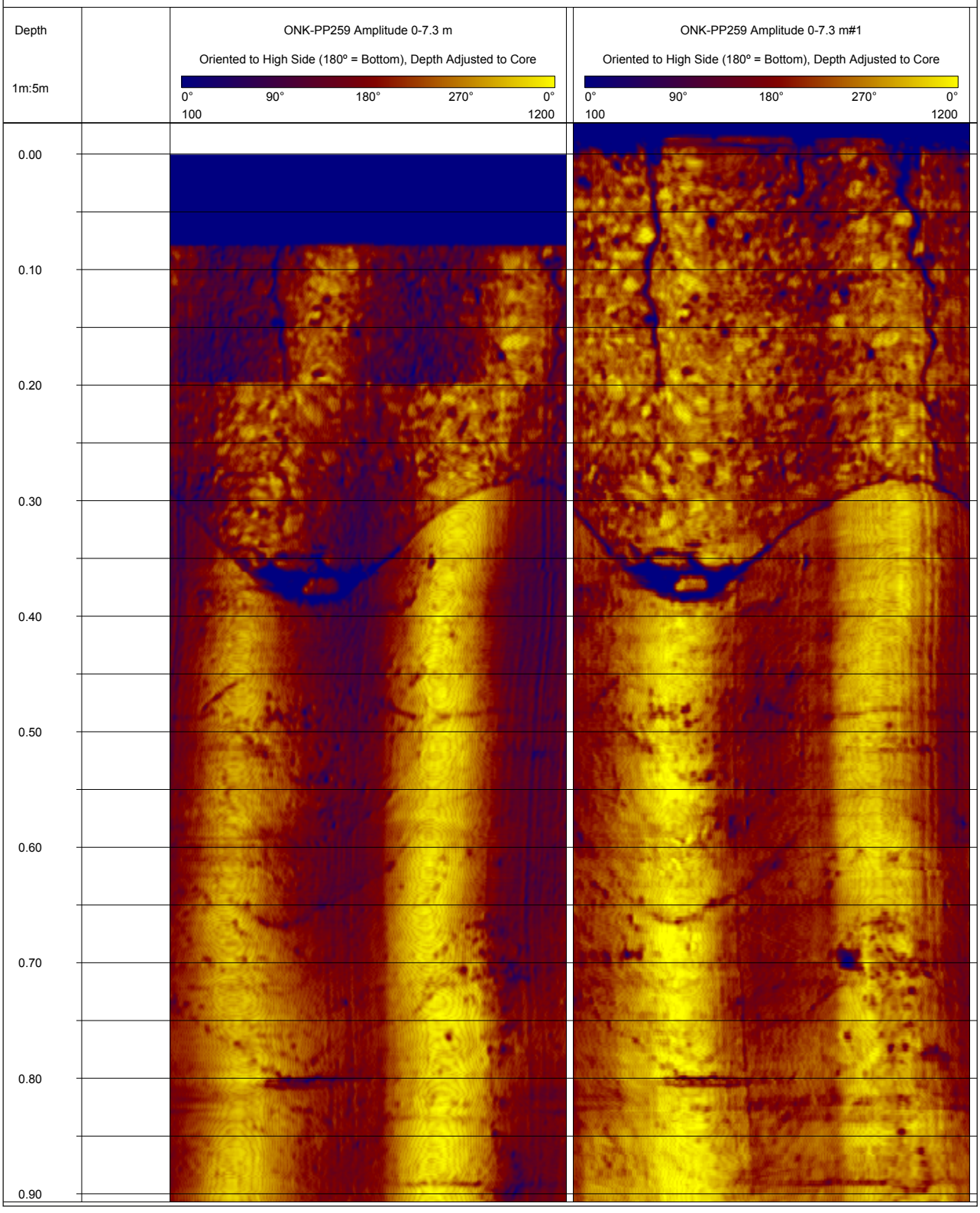

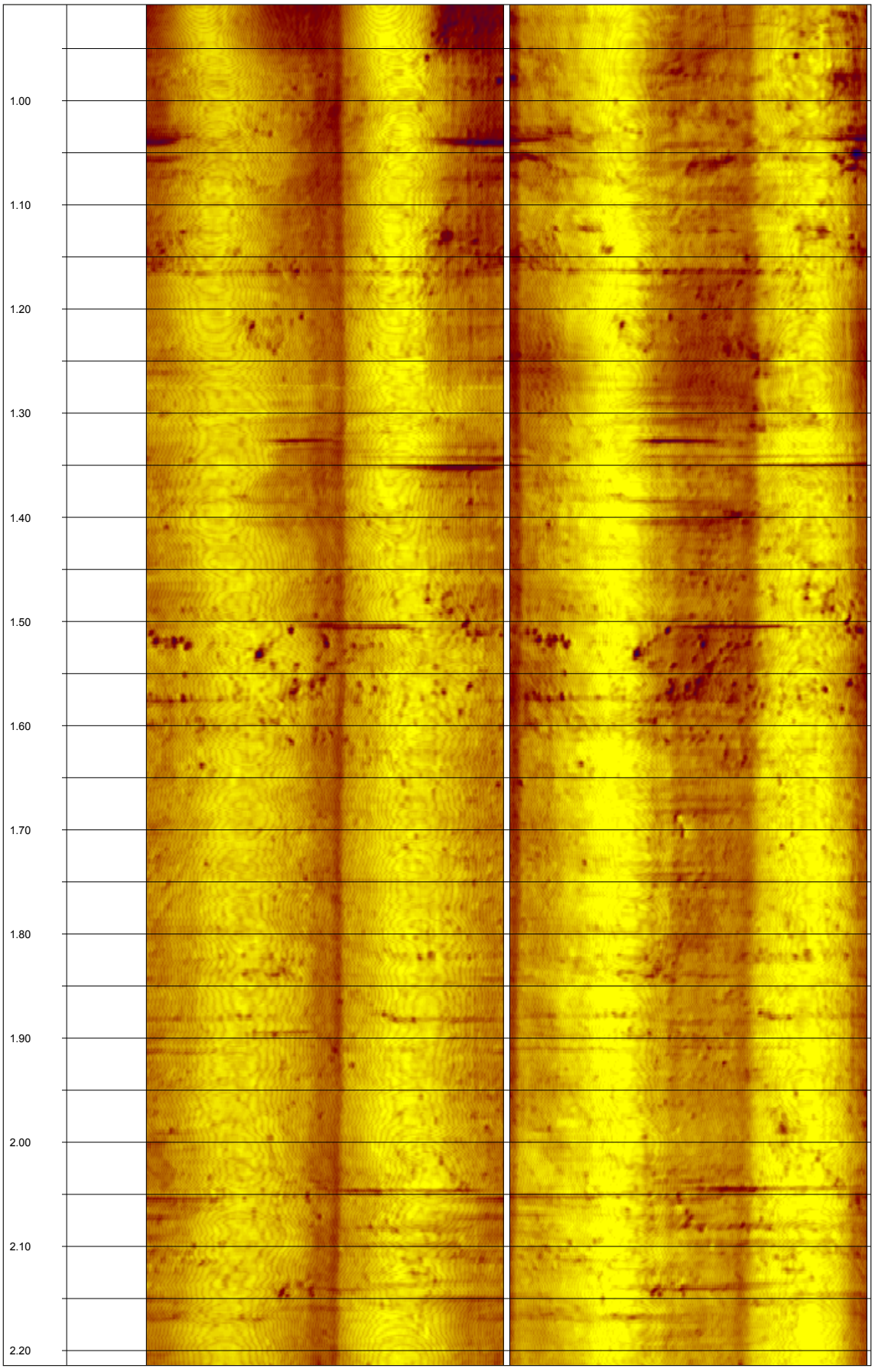
1.00
1.10
1.20
1.30
1.40
1.50
1.60
1.70
1.80
1.90
2.00
2.10
2.20

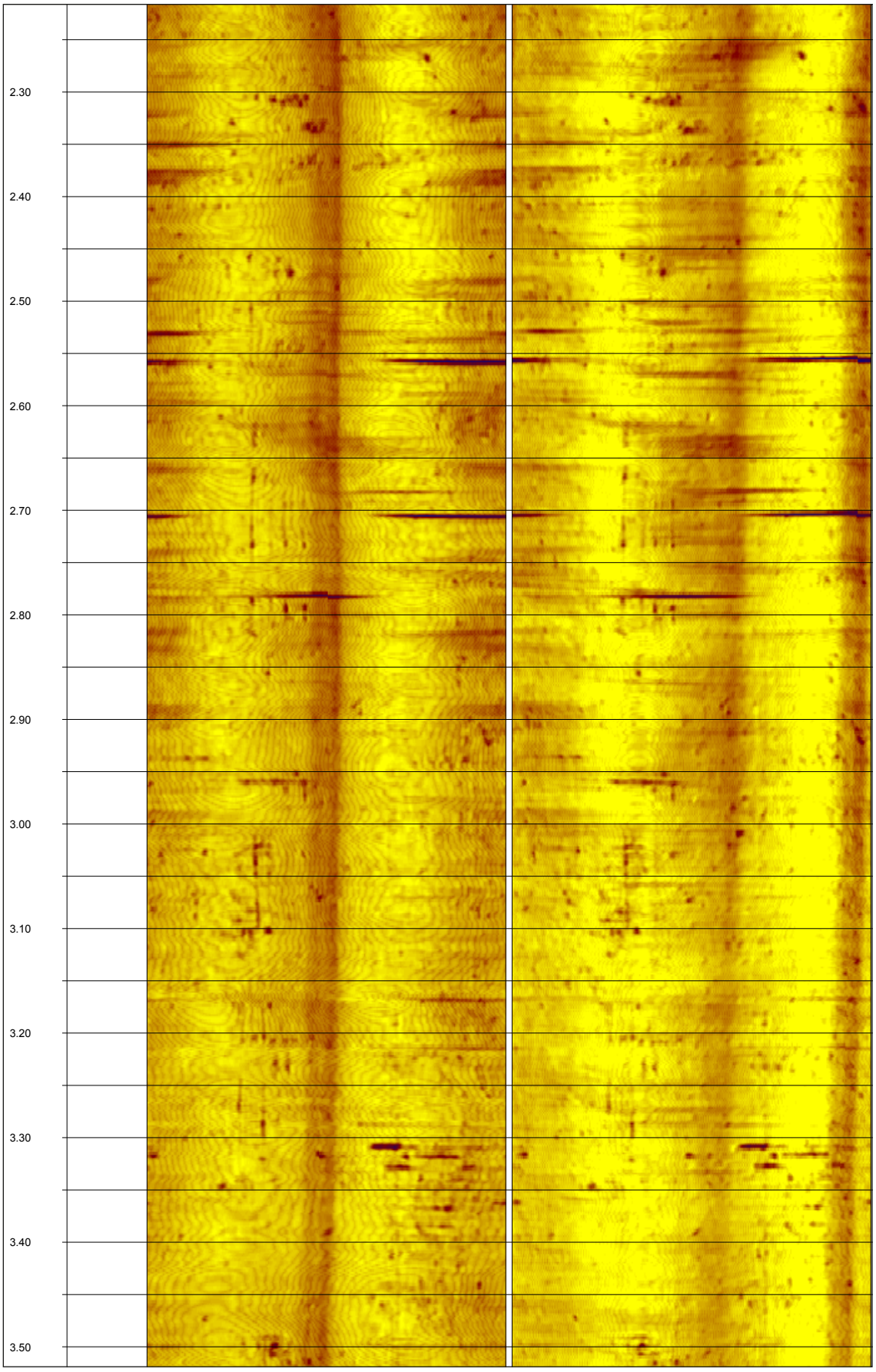
2.30
2.40
2.50
2.60
2.70
2.80
2.90
3.00
3.10
3.20
3.30
3.40
3.50

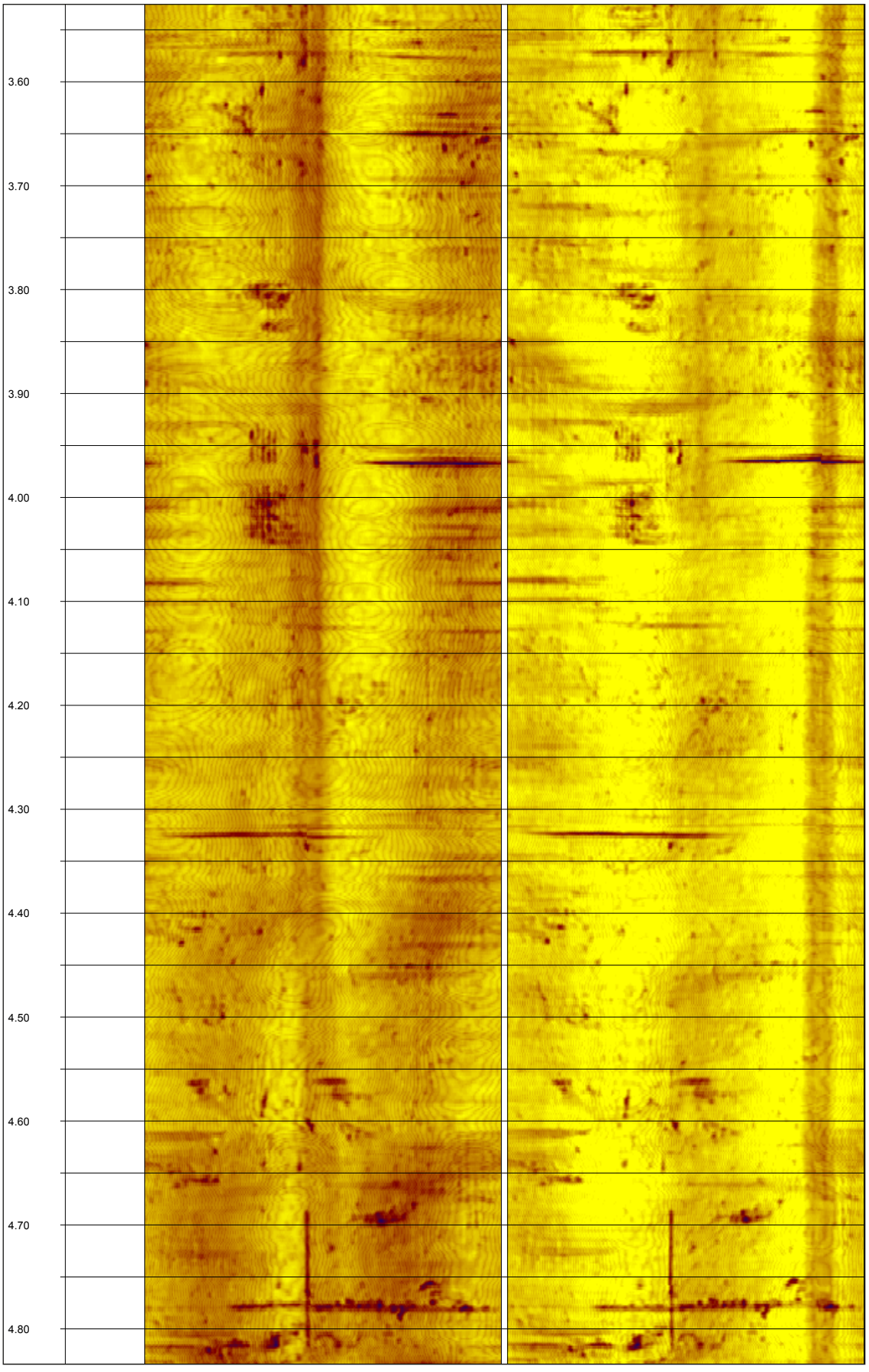
3.60
3.70
3.80
3.90
4.00
4.10
4.20
4.30
4.40
4.50
4.60
4.70
4.80

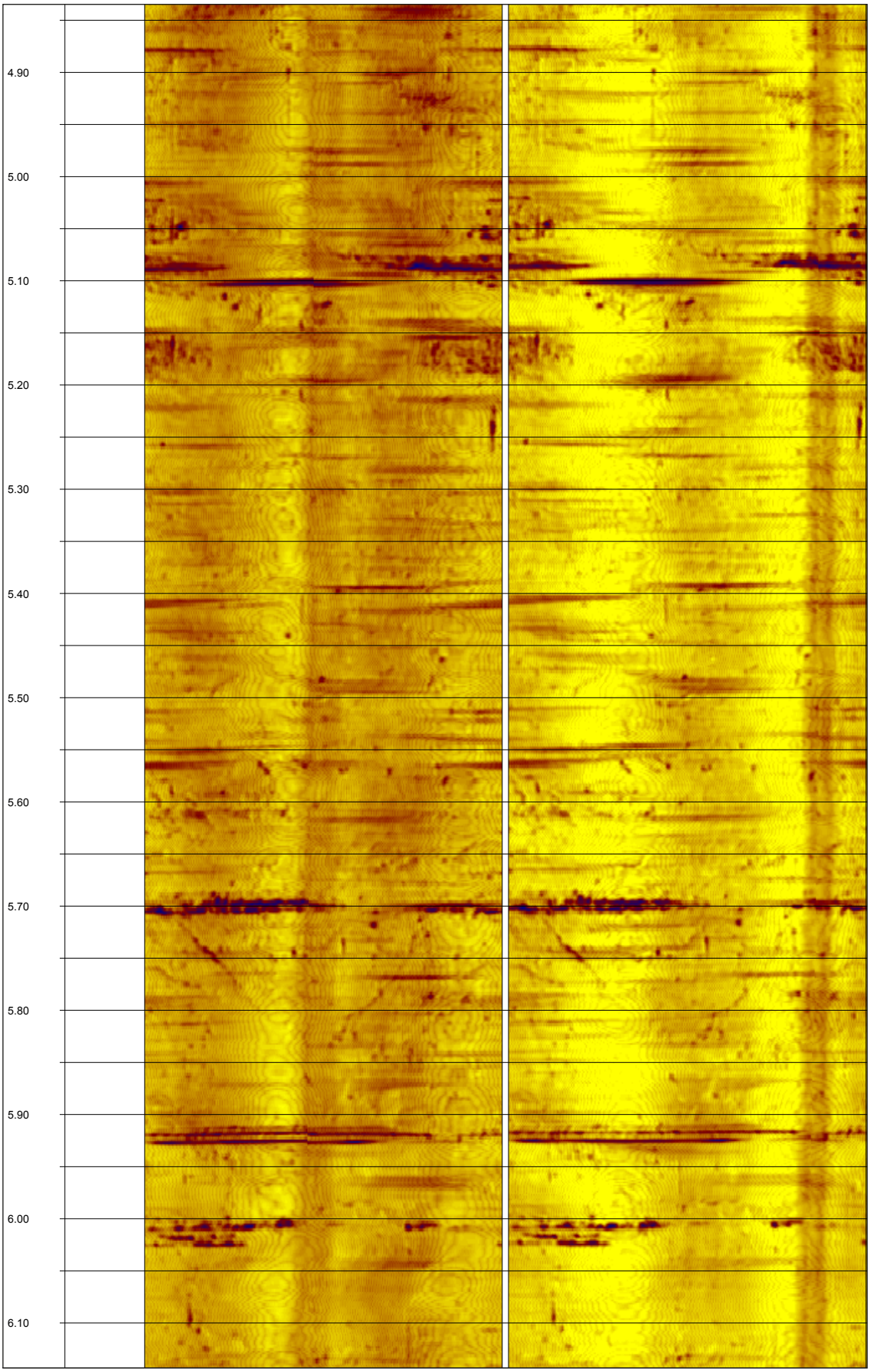
4.90
5.00
5.10
5.20
5.30
5.40
5.50
5.60
5.70
5.80
5.90
6.00
6.10

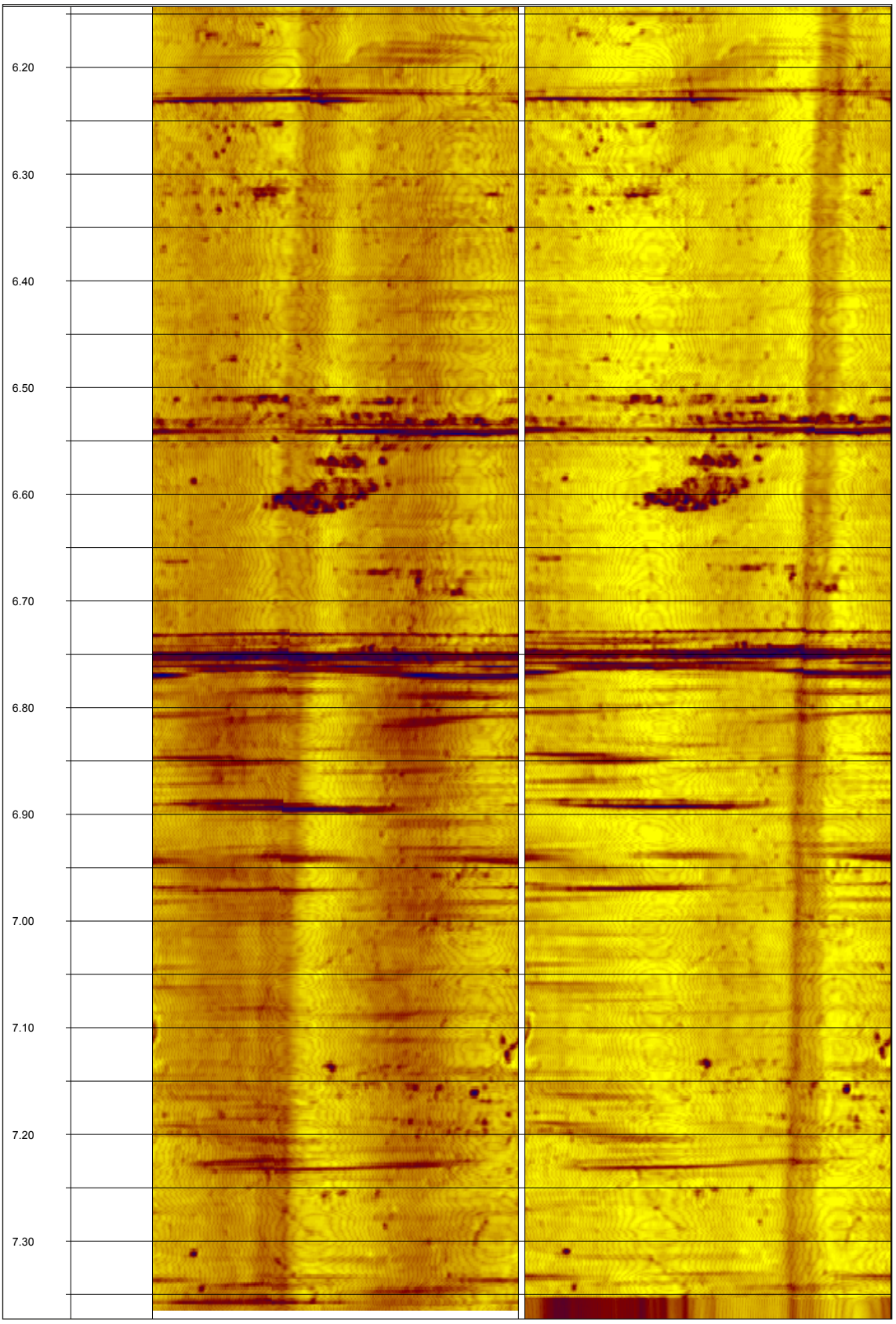
6.20
6.30
6.40
6.50
6.60
6.70
6.80
6.90
7.00
7.10
7.20
7.30